Universitat de Girona

ALTERED GLYCOSYLATION IN PANCREATIC CANCER: DEVELOPMENT OF NEW TUMOR MARKERS AND THERAPEUTIC STRATEGIES

Pedro Enrique Guerrero Barrado

Per citar o enllaçar aquest document:
Para citar o enlazar este documento:
Use this url to cite or link to this publication:
http://hdl.handle.net/10803/671007

ADVERTIMENT. L'accés als continguts d'aquesta tesi doctoral i la seva utilització ha de respectar els drets de la persona autora. Pot ser utilitzada per a consulta o estudi personal, així com en activitats o materials d'investigació i docència en els termes establerts a l'art. 32 del Text Refós de la Llei de Propietat Intel·lectual (RDL 1/1996). Per altres utilitzacions es requereix l'autorització prèvia i expressa de la persona autora. En qualsevol cas, en la utilització dels seus continguts caldrà indicar de forma clara el nom i cognoms de la persona autora i el títol de la tesi doctoral. No s'autoritza la seva reproducció o altres formes d'explotació efectuades amb finalitats de lucre ni la seva comunicació pública des d'un lloc aliè al servei TDX. Tampoc s'autoritza la presentació del seu contingut en una finestra o marc aliè a TDX (framing). Aquesta reserva de drets afecta tant als continguts de la tesi com als seus resums i índexs.

ADVERTENCIA. El acceso a los contenidos de esta tesis doctoral y su utilización debe respetar los derechos de la persona autora. Puede ser utilizada para consulta o estudio personal, así como en actividades o materiales de investigación y docencia en los términos establecidos en el art. 32 del Texto Refundido de la Ley de Propiedad Intelectual (RDL 1/1996). Para otros usos se requiere la autorización previa y expresa de la persona autora. En cualquier caso, en la utilización de sus contenidos se deberá indicar de forma clara el nombre y apellidos de la persona autora y el título de la tesis doctoral. No se autoriza su reproducción u otras formas de explotación efectuadas con fines lucrativos ni su comunicación pública desde un sitio ajeno al servicio TDR. Tampoco se autoriza la presentación de su contenido en una ventana o marco ajeno a TDR (framing). Esta reserva de derechos afecta tanto al contenido de la tesis como a sus resúmenes e índices.

WARNING. Access to the contents of this doctoral thesis and its use must respect the rights of the author. It can be used for reference or private study, as well as research and learning activities or materials in the terms established by the 32nd article of the Spanish Consolidated Copyright Act (RDL 1/1996). Express and previous authorization of the author is required for any other uses. In any case, when using its content, full name of the author and title of the thesis must be clearly indicated. Reproduction or other forms of for profit use or public communication from outside TDX service is not allowed. Presentation of its content in a window or frame external to TDX (framing) is not authorized either. These rights affect both the content of the thesis and its abstracts and indexes.

Universitat de Girona

DOCTORAL THESIS

Altered glycosylation in pancreatic cancer:
development of new tumor markers and therapeutic strategies

Pedro Enrique Guerrero Barrado

2020

Universitat de Girona

DOCTORAL THESIS

Altered glycosylation in pancreatic cancer:
development of new tumor markers and therapeutic strategies

Pedro Enrique Guerrero Barrado

2020

Doctoral Programme in Molecular Biology, Biomedicine and Health

Thesis supervisors:

Dr. Rosa Peracaula Miró
Dr. Esther Llop Escorihuela

Tutor:

Dr. Rosa Peracaula Miró

PhD thesis submitted in fulfilment of the requirement to for the title of doctor from the University of Girona

Certificate of thesis direction

Hereby, Dr. Rosa Peracaula Miró and Dr. Esther Llop Escorihuela from the University of Girona

DECLARE:

That the work entitled Altered glycosylation in pancreatic cancer: development of new tumor markers and therapeutic strategies, which presents Pedro Enrique Guerrero Barrado to obtain the title of doctor, has been carried out under our direction and that it meets the requirements to be eligible for an International Mention.

And for the record and have the appropriate effects, we sign this document.

For all intents and purposes, the following certification is signed:

Dr. Rosa Peracaula Miró Dr. Esther Llop Escorihuela

Girona, June 2020

Agradecimientos

En primer lugar, me gustaría dar las gracias a mis dos directoras de tesis Esther y Rosa que han hecho posible que hoy pueda estar escribiendo esta tesis. Por todo lo que me han enseñado desde ese primer contacto de prácticas de empresa con nuestras columnas de SNA. Gracias por vuestra paciencia, por todo el apoyo científico y personal recibido en los momentos buenos y en los de ofuscación con la tesis. Agradeceros por todo lo enseñado, por las oportunidades que me habéis dado para continuar aprendiendo cosas nuevas en sitios tan diferentes. Gracias por hacer que en estos años fuera de casa estando en el trabajo me sintiera como en casa y por ponerle ruedas a la tesis aunque hubiera unos cuantos kilómetros o una cuarentena por medio. ¡¡Lo de hacer frases más cortas todavía lo tengo que practicar más Esther!! Pero por lo demás, he aprendido mucho de vosotras.

Por supuesto agradecer a todos los miembros que forman o han formado parte de Bioquímica del cáncer (BQ-105 para los amigos) con l@s cuales he coincidido estos años. A Rafa, mil gracias por acabar siempre consiguiéndome las firmas antes del deadline por muy justos que fuéramos y por darme la oportunidad de poder ver como han ido creciendo cosas del TFG e involucrarme en ellas y la ilusión que me ha hecho! Que nada te quite tú buen humor y esas risas que se escuchaban desde el pasillo que animan a todos. A Mª Ángeles porque gracias a ella tuve la oportunidad de colaborar con el grupo, Silvia por esos consejillos con las 2D, Anna por la ayuda por cultivos y por supuesto especialmente dar gracias a Montse, por esa actitud y alegría que transmites, por todos esos consejos, por la de veces que me has ayudado, por todas las charlas y las horas de laboratorio mano a mano que he tenido la suerte de pasar como compi de poyata. Txell que no me olvido tampoco!!! por ser la alegría de la huerta, nuestro radiopatio y nuestra social manager de los congresos. Ni que decir de mis compis de despacho,,,,, que han tenido la paciencia de aguantar mis tonterías todos estos años, hasta el punto de colgar un ola k ase del techo incluso con outfit navideño, por dejarme llenar el despacho de telarañas en Halloween e ir colonizando la mesa a modo de vivero privado. Muchísimas Gracias Adrià, Anna y Laura por hacer tan ameno todos estos años,

por todas nuestras tonterías y el buen rollo que transmitís, por todos esos momentazos que solo recordar te sacan la risa tonta, como nuestra traicionera, nuestros paseos en unicornio XXL por la playa, las bromas saliendo de las cajas, nuestro cultivo *in vitro* de orquídeas y algún que otro petardo con hielo seco siempre en el momento mas inoportuno del mundo por supuesto. Gracias a nuestros vecinos Bioquímicos, Alex por el buen rollo que transmites, Jess, Santi, Imma por ese buen carácter y estar siempre ahí para echar una mano. Gracias a todo el granja team por hacer las comidas tan amenas, por todos esos escape rooms de los cuales hemos salido a tiempo y todas esas experiencias y cenitas de becarios, por ponerle banda sonora a la barca de rafting o nuestros ataques a la máquina de hielo para las escapadas playeras. Micro team, Elianita por ser siempre tan detallista y compartir las penas y estrés estos últimos meses con todos los papeleos de la tesis y la burocracia; ¡¡¡Qué por fin vemos la luz!!! Mireia, gracias por siempre estar dispuesta a echar una mano en lo que haga falta y ser el SOS de las dudas ya sean del sepe, protocolos, papeleo o lo que haga falta, ni Wikipedia puede competir,,,, Eli, Elena, Queralt, Sara, Nuria, Paola, Carla y Pau en el pack por ese buen rollo y risas que hemos compartido, Pau siempre tan sarcástico y sacándole punta a todo animando el cotarro. Siempre me acordare con cariño de ese san Juan tan especial en los tipis con Carla sufriendo con mi hoguera. Biocels y neuro, Irene y Sandra, daros las gracias por vuestra paciencia con mi nivel de catalán y las risas que me habéis sacado, por ir muchas más veces a la playa con cervezas con limón sin alcohol Sandrita. Iker y sus chupitos de licor de oso consiguiendo que te lo pases bien hasta encerrados en un ascensor y a las genéticas Judith y Melania y a todos los miembros del departamento que en algún momento u otro me han ayudado todos estos años.

Agradecer también a todo el equipo del IMIM, Carlos, Joan, Héctor, Mireia y con especial cariño a Pilar y Neus por todo lo que me habéis enseñado, las innumerables ayudas y las bases que me habéis brindado, Snails incluidos. Gemma, Aida por la ayuda siempre con los protocolos y las becas. Ni que decir de la mejor científica que ha pisado el IMIM y mi corresponsal de Barcelona, Mrs galectina la doctora Vinaixa, por la de veces que me ha tenido que ayudar de emergencia y mandar pantallazos de su libreta, por tu carácter, por ser la alegría de la huerta, por esas risas que siempre sacas a quien te

rodea, por ese apoyo en los momentos mas flojos, por las anécdotas, por esas invitaciones a valencia con Paella de verdad incluida y alguna que otra noche de fiesta. Muchas gracias es quedarse corto.

Mil gracias también al konstantopoulos lab: kostas por adoptarme esos tres meses en el laboratorio y enseñarme todo el mundillo de la microfluídica, especialmente a Panagiotis y Alexandros por vuestro buen carácter y enseñarme Baltimore y por supuesto gracias al resto del equipo, Bin, Tay, Christopher, Se Jong, Yuqi, Kaustav, Emily, Robert, Runchen y Cristina por cuidarme, enseñarme truquillos del lab y compartir culturas diferentes y recetas durante la estancia. Agradecer a mi familia española adoptiva en EEUU y Piloto favorito: Naiara y Paul (Monchici incluido), muchas gracias por hacerme esos meses llevaderos y toda la ayuda que me ofrecisteis. A Candela y su marido por ser tan detallistas e invitarme a celebrar la Navidad brindando con un Rioja a pesar de estar al otro lado del charco.

Por supuesto agradecer el apoyo a todos mis amigos de Zaragoza, Barcelona y Girona que han sido un punto de apoyo muy fuerte estos años, Especialmente a todos mis amigos/as de la carrera y sobre todo a las IreneS y Clara por todos esos momentos y experiencias vividos, nuestros viajes, excursiones a montaña, playa, fiestas universitarias con knebep y Rebecca siempre con la cuchara de azúcar de más, por los bautismos de buceo por la costa brava, las barracas, esos pasteles de cumpleaños que nos hace siempre Irene y que son la envidia de Instagram, las calçotadas, las excursiones Andorranas, las clases de Word de Clara y por la de veces que me ha hecho de Taxi siempre quejándose si bajaba 20 segundos tarde por supuesto. Por todas las incontables anécdotas de estos casi 10 años por Cataluña que mirando atrás han pasado muy rápidos. Dar las gracias al grupo M2BE de Zaragoza: Mª Jose, Mº Angeles, Nieves, Pilar, Yago, Sandra, Carlos y especialmente a Manu por esta simulación de Postdoc sin Doc estos meses raros mientras acabo la tesis en medio de una pandemia global.

Finalmente agradecer especialmente a toda mi familia por apoyarme siempre en todas las decisiones que he ido tomando personal y académicamente y animarme a seguir

investigando y poner mi grano de arena contra el cáncer. Y por supuesto a todas las diferentes fuentes de financiación y organismos que me han permitido obtener diferentes becas y contratos para mi formación todos estos años: Universidad de Girona, Ministerio Español de Educación y Cultura, Generalitat y fondo social europeo especialmente.

Abbreviations

Most common abbreviations are highlighted in **bold**

A

ACVR1B	Activin A Receptor Type 1B
ACVR2A	Activin A Receptor Type 2A
AFP	Alpha-Fetoprotein
AJCC	American Joint Committee on Cancer
AKT2	AKT Serine/Threonine Kinase 2
Amp	Ampicillin
ANOVA	Analysis Of Variance
Asn	Asparagine
ATCC	American Type Culture Collection
ATM	ATM Serine-Threonine Kinase
AUC	Area Under the ROC Curve

B

Bp	Base Pair
Brij-35	Polyethyleneglycol Lauryl Ether
BRPC	Borderline Resectable Pancreatic Cancer
BSA	Bovine Serum Albumin

C

CA 125	Cancer Antigen 125
CA 15-3	Cancer Antigen 15-3
CA 19-9	Carbohydrate Antigen 19-9
CA 72-4	Cancer Antigen 72-4
CAFs	Cancer-Associated Fibroblasts
CCND2	Cyclin D2
CDKN2A	Cyclin Dependent Kinase Inhibitor 2A or INK4A or P16
cDNA	Complementary DNA
CEA	Carcinoembryonic Antigen
CFTR	Cystic Fibrosis Transmembrane Conductance Regulator
CHO	Chinese Hamster Ovary
CMP	Cytidine Monophosphate
CP	Ceruloplasmin
CSC	Cancer Stem Cell
CT	Computed Tomography
CTRC	Chymotrypsin C
Ctrl	Control

D

DEPC	Diethyl Pyrocarbonate
DMEM	Dulbecco's modified Eagle's Medium
DNA	Deoxyribonucleic Acid
DTT	Dithiothreitol

E

ECM	Extracellular Matrix
EDTA	Ethylenediaminetetra-Acetic Acid
EGF	Epidermal Growth Factor
EGFR	Epidermal Growth Factor Receptor
EMEM	Eagle's Minimum Essential Medium
EMT	Epithelial to Mesenchymal Transition
EP300	E1A Binding Protein P300
ER	Endoplasmic Reticulum
ERBB2	Erb-B2 Receptor Tyrosine Kinase 2 or HER2
EUS	Endoscopic Ultrasonography

F

FAM	Fluorescein Amidites
FBS	Fetal Bovine Serum
FBXW7	F-Box and WD Repeat Domain Containing 7
Fc	Crystallisable Fragments
FC	Flow Cytometry
FDA	Food and Drug Administration
FGF	Fibroblast Growth Factor
FHIT	Fragile Histidine Triad Diadenosine Triphosphatase
FITC	Fluorescein Isothiocyanate
FReD	Fibrinogen-Related Domain
Fuc	Fucose
FucT-III to VII	Fucosyltransferase 3 to 7 (Enzymes)
FucTs	Fucosyltransferases (enzyme)
FUT1 to 7	Fucosyltransferase 1 to 7

G

Gal	Galactose
GalNAc	N-Acetylgalactosamine
Glc	Glucose
GlcNAc	N-Acetyl-D-glucosamine or N-Acetylglucosamine
GPCR	GTP-Protein Coupled Receptor

GPI	Glycosylphosphatidylinisotol

H

HC	Healthy Control
HE	Hematoxylin
HER2	Receptor tyrosine-protein kinase erbB-2
HER3	Receptor tyrosine-protein kinase erbB-3
HGF	Hepatocyte growth factor,
HGFR	Hepatocyte Growth Factor Receptor
HIFU	High-Intensity Focus Ultrasound
HRP	Horseradish Peroxidase
HUVEC	Human Umbilical Vein Endothelial Cells

I

IAA	Iodoacetamide
IEF	Isoelectric Focusing
IGF1	Insulin Like Growth Factor 1
IGF1R	Insulin Like Growth Factor 1 Receptor
IGFBP-2	Insulin Like Growth Factor Binding Protein 2
IGFBP-3	Insulin Like Growth Factor Binding Protein 3
IgG	Immunoglobulin G
IgM	Immunoglobulin M
IHC	Immunohistochemistry
IMILT	Immunostimulating Interstitial Laser Thermotherapy
IP	Immunoprecipitation
IPMNs	Intraductal Papillary-Mucinous Neoplasms
IRE	Irreversible Electroporation

K

KD	Knock-Down
KDa	Kilodaltons
KRAS	Kirsten rat sarcoma viral oncogene homolog

L

LacNAc	N-acetyllactosamine
LB	Lysogeny Broth
LeA	Lewis A
LeX	Lewis X
LKB1	Serine-Threonine Kinase 11 or STK11

M

MAA II	Maackia Amurensis II Lectin
mAb	Monoclonal Antibodies
MALDI	Matrix-assisted laser desorption/ionization
Man	Mannose
MAN2A1	Alpha-Mannosidase 2
MAN2A2	Alpha-Mannosidase 2x
MAP2K4	Mitogen-Activated Protein Kinase Kinase 4
MAPK	Mitogen-activated protein kinase
MCNs	Mucinous Cystic Neoplasms
MDCT	Multiple Detector Computed Tomography
MFAP2	Microfibril Associated Protein 2
MFAP4	Microfibril Associated Protein 4
MGAT1	Alpha-1,3-mannosyl-glycoprotein 2-beta-N-acetylglucosaminyltransferase
MGAT2	Alpha-1,6-mannosyl-glycoprotein 2-beta-N-acetylglucosaminyltransferase
MGAT5	Alpha-1,6-Mannosylglycoprotein 6-Beta-N-Acetylglucosaminyltransferase
Min	Minutes
miR	MicroRNA
MLH1	MutL Homolog 1
MRI	Magnetic Resonance Imaging
mRNA	Messenger RNA
MS	Mass spectrometry
MUC5AC	Mucin 5AC
MW	Molecular Weight
MWA	Microwave Ablation
MYB	MYB Proto-Oncogene Transcription Factor

N

ncRNAs	Non-Coding RNAs
Neu5Ac	5-N-Acetylneuraminic Acid
NOTCH	Notch Receptor 1
NP-40	Nonyl Phenoxypolyethoxylethanol
NT	Non-Tumor

O

O/N	Overnight
OST	Oligosaccharyltransferase

p	Statistical significance
PALB2	Partner and Localizer of BRCA2
PanIN	Pancreatic Intraepithelial Neoplasia
PanNETs	Pancreatic Neuroendocrine Tumors
PBS	Phosphate Buffered Saline
PCR	Polymerase Chain Reaction
PDA	Pancreatic Ductal Adenocarcinoma
PDMS	Polydimethylsiloxane
PEI	Polyethylenimine
PET	Positron Emission Tomography
PFA	Paraformaldehyde
PhoSL	Pholiota Squarrosa Lectin
pI	Isoelectric Point
PI3K	Phosphatidylinositol 3-Kinase
PMSF	Phenylmethylsulfonyl Fluoride
PNGase F	Flavobacterium meningosepticum N-glycosidase F
PP	Pancreatic polypeptide
ppGalNAcT	Polypeptide-N-Acetylgalactosaminyltransferases
Pro	Proline
PRSS1	Serine Protease 1
PRSS2	Serine Protease 2
PS	Performance Status
PSA	Prostate Specific Antigen
PTM	Post-Translational Modification
PURO	Puromycin
PVDF	Polyvinylidene Difluoride
PVP	Polyvinylpyrrolidone

REG1A	Regenerating Family Member 1 Alpha
REG1B	Regenerating Family Member 1 Beta
REG3A	Regenerating Family Member 3 Alpha
REG4	Regenerating Family Member 4
RELN	Reelin
RFA	Radiofrequency
RGD	Arginylglycylaspartic Acid
rh-E-selectin	Recombinant Human E-selectin
RIPA	Radioimmunoprecipitation Assay Buffer
RNA	Ribonucleic Acid

RPA1	Replication Protein A1
Rpm	Revolutions Per Minute
RPMI	Roswell Park Memorial Institute medium
RT-qPCR	Reverse Transcription Quantitative Polymerase Chain Reaction
RT	Room Temperature

S

S1-3	Spot 1-3
SA	Sialic Acid
SD	Standard Deviation Of The Mean
SDS-PAGE	Sodium Dodecyl Sulfate Polyacrylamide Gel Electrophoresis
SDS	Sodium Dodecyl Sulfate
SEM	Standard Error Of The Mean
Ser	Serine
SHH	Sonic Hedgehog Signaling Molecule
shRNA	Short Hairpin RNA
SLe	Sialyl Lewis
SLe^A	Sialyl Lewis A
SLe^X	Sialyl Lewis x
SMAD4 /DPC4	SMAD Family Member 4 or DPC4
SNA	Sambucus Nigra Lectin
SOCS-1	Suppressor Of Cytokine Signaling 1
SPINK1	Serine Peptidase Inhibitor Kazal Type 1
ST3Gal III	ST3 Beta-Galactoside Alpha-2,3-Sialyltransferase 1 (Enzyme)
ST3Gal IV	ST3 Beta-Galactoside Alpha-2,3-Sialyltransferase 4 (Enzyme)
ST3Gal VI	ST3 Beta-Galactoside Alpha-2,3-Sialyltransferase 6 (Enzyme)
ST3GAL1	ST3 Beta-Galactoside Alpha-2,3-Sialyltransferase 1
ST3GAL2	ST3 Beta-Galactoside Alpha-2,3-Sialyltransferase 2
ST3GAL3	ST3 Beta-Galactoside Alpha-2,3-Sialyltransferase 3
ST3GAL4	ST3 Beta-Galactoside Alpha-2,3-Sialyltransferase 4
ST3GAL5	ST3 Beta-Galactoside Alpha-2,3-Sialyltransferase 5
ST3GAL6	ST3 Beta-Galactoside Alpha-2,3-Sialyltransferase 6
ST6GAL1	ST6 Beta-Galactoside Alpha-2,6-Sialyltransferase 1
ST6GAL2	ST6 Beta-Galactoside Alpha-2,6-Sialyltransferase 2
ST6GALNAC1	ST6 N-Acetylgalactosaminide Alpha-2,6-Sialyltransferase 1
ST6GALNAC6	ST6 N-Acetylgalactosaminide Alpha-2,6-Sialyltransferase 6
STn	Sialyl Tn
STs	Sialyltransferases

T

TACA	Tumor Associated Carbohydrate Antigen
TB	Terrific Broth
TBP	TATA box binding protein
TBS	Tris Buffered Saline
TBST	Tris Buffered Saline Tween-20
TCGA	The Cancer Genome Atlas
TF	Thomsen-Friedenreich
TGF-β	Transforming Growth Factor Beta
TGFBR1	Transforming Growth Factor Beta Receptor 1
TGFBR2	Transforming Growth Factor Beta Receptor 2
Thr	Threonine
TIMP-1	TIMP Metallopeptidase Inhibitor 1
TMs	Tumor Markers
Tn	Thomsen-nouvelle antigen
TNF-α	Tumor Necrosis Factor Alpha
TNM	Tumor Node Metastasis
TOF	Time-Of-Flight
TP53	Tumor Protein P53
TRIS	Tris(hydroxymethyl)aminomethane
Type-1 chain	Galβ1,3GlcNAc
Type-2 chain	Galβ1,4GlcNAc

U

UDP	Uridine diphosphate
UICC	International Union Against Cancer
US	Ultrasonography

V

VCAMs	Vascular cell adhesion molecules
VSMC	Vascular smooth muscle cells

W

WB	Western Blot
WNT	Wnt Family Member 1

X

Xyl	Xylose

18-FDG	18-F-fluorodeoxyglucose
2D	Two-Dimensional
2DE	Two-Dimensional Electrophoresis
3D	Three-Dimensional

List of figures

List of tables

Summary

Pancreatic Ductal Adenocarcinoma (PDA) represents more than 90% of pancreatic cancers. PDA is an extremely aggressive solid tumor, with the direst prognosis among all carcinomas. This type of pancreatic cancer is characterized by the presence of a microenvironment formed by an abundant desmoplastic reaction. The fibrotic stroma of the PDA favors the survival of the tumor and contributes to its wide resistance against current antitumor therapies. For PDA patients, tumor resection surgery is currently one of the best curative options. However, this option remains only possible for a small group of patients, since it is usually detected on late and locally advanced stages of the disease, where patients already have metastases or vascular infiltration. Currently, only about 9% of patients survive 5-years after diagnosis, and recurrence of the disease is a common feature. This poor prognosis is also due to the lack of tumor markers with enough specificity and sensitivity for the diagnosis of this tumor before metastasis occurs.

During carcinogenesis, several alterations have been observed both in the genome and the cellular physiology. One of these transformations commonly found in oncogenic transformation is aberrant glycosylation that affects the carbohydrates from the cell surface and from secreted glycoconjugates. This phenomenon confers multiple advantages on tumor cells, ranging from evasion of the immune response to the promotion of migration and cell invasion events. One of the most common alterations is the expression of new carbohydrate antigens and the synthesis of truncated glycan structures, in which sialic acid residues usually play a key role. This work has been focused specially on the role of the carbohydrate antigen Sialyl Lewis X (SLe^X); a glycan structure that is only present in pancreatic cells during the development of pancreatic cancer. Previous studies of the group have shown that the overexpression of this carbohydrate antigen in PDA cells favors the aggressiveness of the tumor *in vitro* and *in vivo*, playing an important role in the metastasis process.

Under these premises, in this work we have proposed the identification of glycoproteins containing SLe^X in PDA tissues for their usefulness as biomarkers for this tumor. To accomplish this goal, glycoproteins carrying SLe^X present in tissues from PDA patients were separated by two-dimensional electrophoresis. The use of this technique allowed us to isolate SLe^X-positive bands and subsequently detect those glycoproteins of interest by mass spectrometry. This way,

the microfibril-4-associated protein (MFAP4) was identified as one of the SLe^X carrier glycoproteins in tissues from PDA patients. MFAP4 expression was subsequently analyzed in different pancreatic cancer cell lines, as well as in pancreatic tissues (tumor and non-tumor) using immunohistochemical and western blot techniques. MFAP4 levels in PDA tissues were higher than in non-tumor samples from PDA patients and healthy controls. Furthermore, the expression of MFAP4 in tissues was localized in their extracellular matrix and not in the pancreatic cells. No expression of MFAP4 was detected in the panel of PDA cell lines or in their corresponding conditioned media. Co-localization of SLe^X over MFAP4 in PDA tissue samples was confirmed in a panel of eight PDA tissues where all of them showed this sialylated glycoform, which was not detected in pancreatic tissue samples from healthy patients. Thus, the MFAP4-SLe^X glycoform is characteristic of PDA tissues and may be found in serum, opening a window of possibilities for its subsequent study as a possible PDA biomarker.

In this work, the effect of the inhibition of the expression of the main genes that code for the enzymes responsible for the final steps of SLe^X biosynthesis has been studied. The main objective has been to analyze whether their inhibition can reverse the invasive phenotype of PDA. This work has focused on the α2,3-sialyltransferases (α2,3-ST) ST3Gal III and ST3Gal IV, which add sialic acid with an α2,3 linkage to galactose of type-1 or 2 (Galβ1,3GlcNAc or Galβ1,4GlcNAc) glycan structures. To do this, firstly, the sialome of a panel from seven human PDA cell lines was characterized at the level of their cell surface glycoconjugates and their secreted glycoproteins. The level of expression of α2,3-STs and fucosyltransferases involved in the biosynthesis of antigens of the sialyl Lewis (SLe) family was also analyzed. All PDA cells showed sialic acid expression with different levels of sialylated determinants such as SLe^X or SLe^A as well as different degrees of α2,3-ST expression, reflecting the phenotypic heterogeneity of PDA. Capan-1 and BxPC3 cell lines that expressed both ST3GAL3 and ST3GAL4 as well as moderate-high levels of sialyl Lewis antigens were chosen as candidates for inhibition of ST3GAL3 and ST3GAL4 genes by shRNAs. Silencing of ST3GAL3 and ST3GAL4 in both cell lines led to a significant reduction in SLe^X and in most of them also led to a reduction in SLe^A levels, with slight increases in the α2,6-sialic acid content. To assess the effect of inhibition at the phenotypic level, different *in vitro* tests were carried out with transwells and microfluidic devices. These showed a significant decrease in migratory (reduction between 42 and 57%) and

invasive capacities (33-67%) of the cells silenced for each of both genes. We also proved that this reduction was associated, at least in part, with the decrease in SLe^X expression levels. The silenced cells of both cell lines also showed a significant decrease in adhesion and rolling to E-selectin, key protein in the extravasation process that takes place during metastasis. Taken together, all of these results indicate that the ST3GAL3 and ST3GAL4 genes play an important role in these migratory, invasive and E-selectin binding processes and therefore could be considered potential therapeutic targets against PDA.

In conclusion, the results obtained from this work highlight the importance of the sialyl Lewis X antigen and the sialyltransferases involved in its biosynthesis in PDA. On one hand, this work has shown the potential of identifying glycoproteins with sialyl Lewis X as possible biomarkers of PDA. On the other hand, it has pointed to α2,3-STs as potential targets to reduce PDA migration and invasion in future *in vivo* tests.

Resumen

El adenocarcinoma ductal pancreático (PDA) representa más del 90% de los cánceres de páncreas. El PDA es un tumor sólido muy agresivo, asociado a uno de los peores prognosticos. Este tipo de cáncer de páncreas, se caracteriza por la presencia de un microambiente formado por una gran reacción desmoplásica. El estroma fibrótico del PDA favorece la supervivencia del tumor y contribuye a la amplia resistencia del mismo frente a las terapias antitumorales actuales. Para los pacientes con PDA, la resección del tumor mediante cirugía es actualmente una de las mejores opciones curativas. No obstante, está opción solo es viable en un reducido grupo de pacientes, debido a que la enfermedad suele detectarse en etapas tardías, localmente avanzadas donde los pacientes ya presentan metástasis o infiltración vascular. Actualmente, aproximadamente sólo un 9% de los pacientes sobreviven 5 años después del diagnóstico y la recurrencia de la enfermedad es muy frecuente. Esta mala prognosis se debe también a la falta de marcadores tumorales con suficiente especificidad y sensibilidad para el diagnóstico de este tipo de tumor antes de que ocurra la metástasis.

Durante el desarrollo del cáncer se han observado múltiples alteraciones tanto en el genoma como en la fisiología celular. Una de estas transformaciones comúnmente encontrada en células cancerígenas es la glicosilación aberrante que afecta a los carbohidratos de la superficie celular y de los glicoconjugados secretados por la célula tumoral. Este fenómeno confiere una serie de ventajas a las células tumorales que incluyen desde la evasión de la respuesta inmunológica hasta la promoción de fenómenos de migración e invasión celular. Una de las alteraciones más comunes es la aparición de nuevos antígenos carbohidratos de membrana o estructuras glucídicas incompletas, en las cuales los residuos de ácido siálico suelen tener un papel muy relevante. Este trabajo, se ha centrado específicamente en el rol del antígeno carbohidrato sialil Lewis X (SLe^X); que es una estructura glucídica que sólo está presente en las células del tumor pancreático. Estudios previos del grupo han demostrado que la sobre-expresión de este antígeno carbohidrato en células de PDA favorece la agresividad del tumor *in vitro* e *in vivo* jugando un importante rol en el proceso de metástasis.

Bajo estas premisas, en este trabajo se planteó la identificación de proteínas portadoras de SLe^X en tejidos de PDA, por su potencial utilidad como biomarcadores de este tipo de tumor.

Para ello, se separaron mediante electroforesis bidimensional las glicoproteínas portadoras de SLe^X presentes en tejidos de pacientes con PDA. La utilización de esta técnica permitió aislar las bandas positivas para SLe^x y posteriormente detectar aquellas glicoproteínas de interés por medio de espectrometría de masas. De esta forma se identificó la proteína asociada a microfibrillas-4 (MFAP4) como una de las glicoproteínas portadoras de SLe^X en tejidos de pacientes con PDA. La expresión de MFAP4 fue posteriormente analizada en diferentes líneas celulares de cáncer de páncreas, así como en tejidos pancreáticos (tumorales y no tumorales) mediante técnicas de inmunohistoquímica y western blot. Los niveles de MFAP4 en tejidos de PDA fueron superiores a los de las muestras no tumorales de pacientes con PDA y controles sanos. Además, la expresión de MFAP4 en tejidos, se localizó en la matriz extracelular de los mismos y no en las células pancreáticas. No se detectó expresión de MFAP4 en el panel de líneas celulares de PDA ni en sus correspondientes medios condicionados. La colocalización de SLe^X sobre MFAP4 en muestras de tejidos de PDA se confirmó en un panel de ocho tejidos de PDA donde todos ellos presentaron esta glicoforma sialilada, que no se detectó en las muestras de tejidos de pacientes sanos. La glicoforma MFAP4- SLe^X es propia de los tejidos de PDA y podría encontrarse en suero, abriendo una ventana de oportunidades para su posterior estudio como posible biomarcador de PDA.

En este trabajo también se ha estudiado el efecto de la inhibición de la expresión de los principales genes que codifican para las enzimas responsables de la síntesis del SLe^X en sus etapas finales. El principal objetivo es estudiar si su inhibición puede revertir el fenotipo invasivo del PDA. Estas enzimas son las α2,3-sialiltransferasas (α2,3-ST) ST3Gal III y ST3Gal IV, que adicionan ácido siálico con un enlace α2,3 sobre galactosas de estructuras glucídicas tipo-1 o 2 (Galβ1,3GlcNAc o Galβ1,4GlcNAc). Para ello, en primer lugar, se caracterizó el sialoma de un panel de siete líneas celulares de PDA a nivel de sus glicoconjugados de superficie celular y de sus glicoproteínas secretadas. También se estudió el nivel de expresión de las α2,3-ST y fucosiltransferasas involucradas en la biosíntesis de antígenos de la familia sialil Lewis (SLe). Todas las células de PDA mostraron expresión de ácido siálico con diferentes niveles de determinantes sialilados como SLe^X o SLe^A así como con diferentes grados de expresión de las α2,3-STs, reflejando la heterogeneidad fenotípica del PDA. Las líneas celulares Capan-1 y BxPC3, que expresaban tanto ST3GAL3 como ST3GAL4, así como niveles moderados-altos

de antígenos sialil Lewis, fueron elegidas como candidatas para la inhibición génica de ST3GAL3 y ST3GAL4 mediante shRNAs. El silenciamiento de los genes ST3GAL3 y ST3GAL4 en ambas líneas celulares indujo una reducción significativa en los niveles de SLe^X y en la mayoría de ellas en los niveles de SLe^A, con ligeros aumentos en los niveles de ácido α2,6-siálico. Para valorar el efecto de la inhibición a nivel fenotípico, se realizaron diferentes ensayos *in vitro* con transwells y en dispositivos de microfluídica que mostraron una disminución significativa en las capacidades migratorias (reducción entre el 42 y 57%) e invasivas (33-67%) de las células silenciadas para cada uno de ambos genes. También se demostró que esta reducción está asociada al menos en parte, a la bajada en los niveles de expresión de SLe^X. Las células silenciadas de ambas líneas celulares, mostraron también una disminución significativa en la adhesión y rodamiento con la proteína E-selectina, clave en fenómenos de extravasación tumoral durante la metástasis. En conjunto, todos estos resultados indican que los genes ST3GAL3 y ST3GAL4 juegan un papel importante en estos procesos migratorios, invasivos y de unión a E-selectina y por lo tanto, podrían considerarse potenciales dianas terapéuticas contra el PDA.

En conclusión, los resultados obtenidos de este trabajo ponen de manifiesto la importancia del antígeno sialil Lewis X en el PDA y de las sialiltransferasas involucradas en su biosíntesis. Por un lado, se destaca el potencial de identificar glicoproteínas con sialil Lewis X como posibles biomarcadores del PDA. Por otro, señala a las α2,3-STs como potenciales dianas para reducir la migración e invasión en futuros ensayos *in vivo*.

Resum

L'adenocarcinoma ductal pancreàtic (PDA) representa més del 90% dels càncers de pàncrees. El PDA és un tumor sòlid molt agressiu, associat a una de les pitjors prognosis. Aquest tipus de càncer de pàncrees es caracteritza per la presència d'un microambient format per una gran reacció desmoplàsica. L'estroma fibròtic del PDA afavoreix la supervivència del tumor i contribueix a l'àmplia resistència del mateix enfront de les teràpies antitumorals actuals. Per als pacients amb PDA, la resecció del tumor mitjançant cirurgia és actualment una de les millors opcions curatives. No obstant això, aquesta opció només és viable per a un grup reduït de pacients, degut a que la malaltia sol detectar-se en etapes tardanes, localment avançades, on els pacients ja presenten metàstasis o infiltració vascular. En l'actualitat, aproximadament només un 9% dels pacients sobreviuen cinc anys després del diagnòstic, i la recurrència de la malaltia és molt freqüent. Aquesta mala prognosi es deu també a la falta de marcadors tumorals amb suficient especificitat i sensibilitat per al diagnòstic d'aquest tumor abans que ocorri la metàstasi.

Durant el desenvolupament del càncer s'han observat múltiples alteracions tant en el genoma com en la fisiologia cel·lular. Una d'aquestes transformacions trobades habitualment en cèl·lules canceroses és la glicosilació aberrant que afecta els carbohidrats de la superfície cel·lular i dels glicoconjugats secretats. Aquest fenomen confereix una sèrie d'avantatges a les cèl·lules tumorals que inclouen des de l'evasió de la resposta immunològica fins a la promoció de fenòmens de migració i invasió cel·lular. Una de les alteracions més comunes és l'aparició de nous antígens carbohidrats de membrana o estructures glucídiques incompletes, en les quals els residus d'àcid siàlic solen tenir un paper molt rellevant. Aquest treball s'ha centrat específicament en el rol de l'antigen carbohidrat sialil Lewis X (SLe^X); que és una estructura glucídica que només està present a les cèl·lules pancreàtiques durant el desenvolupament del càncer de pàncrees. Estudis previs del grup han demostrat que la sobre-expressió d'aquest antigen carbohidrat en cèl·lules de PDA afavoreix l'agressivitat del tumor *in vitro* i *in vivo* jugant un rol important en el procés de metàstasi.

Sota aquestes premisses, en aquest treball es va plantejar la identificació de proteïnes portadores de SLe^X en teixits de PDA, per la seva possible utilitat com a biomarcadors d'aquest tumor. Per a això, es van separar mitjançant electroforesi bidimensional les glicoproteïnes portadores de SLe^X presents en teixits de pacients amb PDA. La utilització d'aquesta tècnica va permetre aïllar les bandes positives per a SLe^X i posteriorment detectar aquelles glicoproteïnes d'interès per mitjà d'espectrometria de masses. D'aquesta forma es va identificar la proteïna associada a microfibrilles-4 (MFAP4) com una de les glicoproteïnes portadores de SLe^X en teixits de pacients amb PDA. L'expressió de MFAP4 va ser posteriorment analitzada en diferents línies cel·lulars de càncer de pàncrees, així com en teixits pancreàtics (tumorals i no tumorals) mitjançant tècniques d'immunohistoquímica i western blot. Els nivells de MFAP4 en teixits de PDA van ser superiors als de les mostres no tumorals de pacients amb PDA i controls sans. A més, l'expressió de MFAP4 en teixits es va localitzar a la matriu extracel·lular dels mateixos i no a les cèl·lules pancreàtiques. No es va detectar expressió de MFAP4 al panell de línies cel·lulars de PDA ni als seus corresponents medis condicionats. La colocalització de SLe^X sobre MFAP4 en mostres de teixits de PDA es va confirmar en un panell de vuit teixits de PDA on tots ells van presentar aquesta glicoforma sialilada, que no es va detectar en les mostres de teixits de pacients sans. La glicoforma MFAP4- SLe^X és pròpia dels teixits de PDA i podria trobar-se al sèrum, obrint una finestra d'oportunitat al seu posterior estudi com a possible biomarcador de PDA.

En aquest treball també s'ha estudiat l'efecte de la inhibició de l'expressió dels principals gens que codifiquen per als enzims responsables de les últimes etapes de la biosíntesi del SLe^X. El principal objectiu és estudiar si la seva inhibició pot revertir el fenotip invasiu del PDA. Aquests enzims són les α2,3-sialiltransferases (α2,3-ST) ST3Gal III i ST3Gal IV, que addicionen àcid siàlic amb un enllaç α2,3 sobre galactoses d'estructures glucídiques tipus-1 o 2 (Galβ1,3GlcNAc o Galβ1,4GlcNAc). Per a això, en primer lloc, es va caracteritzar el sialoma d'un panell de set línies cel·lulars de PDA a nivell dels seus glicoconjugats de superfície cel·lular i de les seves glicoproteïnes secretades. També es va estudiar el nivell d'expressió de les α2,3-ST i fucosiltransferases involucrades en la biosíntesi d'antígens de la família sialil Lewis (SLe). Totes les cèl·lules de PDA van mostrar expressió d'àcid siàlic amb diferents nivells de determinants sialilats com SLe^X o SLe^A així com amb diferents graus d'expressió de α2,3-STs, reflectint

l'heterogeneïtat fenotípica del PDA. Les línies cel·lulars Capan-1 i BxPC3, que expressaven tant ST3GAL3 com ST3GAL4, així com nivells moderats-alts d'antígens sialil Lewis, van ser escollides com a candidates per a la inhibició gènica de ST3GAL3 i ST3GAL4 mitjançant shRNAs. El silenciament dels gens ST3GAL3 i ST3GAL4 en totes dues línies cel·lulars va induir una reducció significativa en els nivells de SLe^X i a la majoria d'elles en els nivells de SLe^A, amb lleugers augments en els nivells d'àcid α2,6-siàlic. Per a valorar l'efecte de la inhibició a nivell fenotípic, es van realitzar diferents assajos *in vitro* amb *transwells* i en dispositius de microfluídica que van mostrar una disminució significativa en les capacitats migratòries (reducció entre el 42 i 57%) i invasives (33-67%) de les cèl·lules silenciades per cadascun dels dos gens. També es va demostrar que aquesta reducció està associada, almenys en part, a la baixada en els nivells d'expressió de SLe^X. Les cèl·lules silenciades de ambdues línies cel·lulars van disminuir significativament la seva adhesió i rodament amb la proteïna E-selectina, clau en fenòmens d'extravasació durant la metàstasi. En conjunt, tots aquests resultats indiquen que els gens ST3GAL3 i ST3GAL4 juguen un paper important en aquests processos migratoris, invasius i d'unió a E-selectina i, per tant, podrien considerar-se potencials dianes terapèutiques contra el PDA.

En conclusió, els resultats obtinguts d'aquest treball posen de manifest la importància en PDA de l'antigen sialil Lewis X i de les sialiltransferases involucrades en la seva biosíntesi. D'una banda, es destaca el potencial d'identificar glicoproteïnes amb sialil Lewis X com a possibles biomarcadors del PDA. D'altra banda, s'assenyala a les α2,3-STs com a potencials dianes per a reduir la migració i invasió en futurs assajos *in vivo*.

Table of Contents

I. Introduction

1. The pancreas

1.1. Anatomy of the pancreas

The pancreas is a retroperitoneal organ located at a height between the second and third lumbar vertebra, in a transverse arrangement from the duodenal frame to the splenic hilum. Anatomically the pancreas can be divided into three distinct parts: the head, the neck or body and the tail [1].

The head corresponds to the wide part of the pancreas located between the stomach and the intestine and placed behind the liver, the head of the pancreas partially surrounds the duodenum. The neck or the body of the pancreas is located in the central section, behind the liver and the small intestine. Lastly, we found the narrowest part, named as the tail. The tail of the pancreas is found at the end of the pancreas and extends to the left side of the abdomen, next to the spleen.

The pancreas is a highly vascularized organ and is surrounded by major blood vessels that provide upper and lower irrigation to the organ, such as the superior mesenteric artery and vein, the celiac axis and the portal vein. Also, for its location, the pancreas is in contact with a large number of lymphatic vessels on it, but also with the surrounding organs [1] (**figure 1A**).

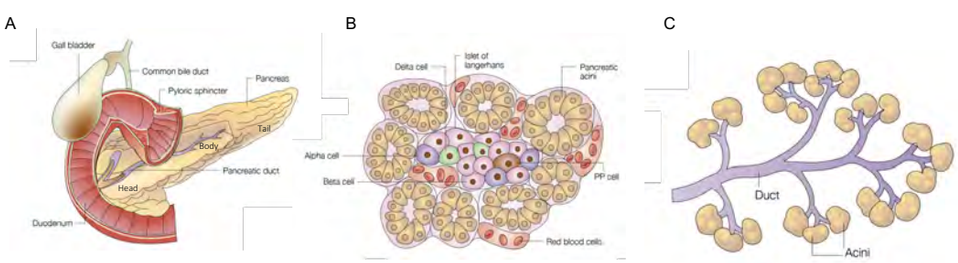

Figure 1 | Anatomy of the Pancreas. A) Gross anatomy of the pancreas. B) The endocrine pancreas: pancreatic islet embedded in exocrine tissue. C) The exocrine pancreas. Extracted and modified from: [2].

Both histologically and functionally, we found two distinct components in this gland: the endocrine and the exocrine pancreas.

The endocrine pancreas shown in **figure 1B** is composed of clusters of endocrine cells (the islets of Langerhans) and represents a small portion of the total pancreas. Inside the islets of Langerhans, we found a variety of different endocrine hormone-producing cells involved in the synthesis, store and secretion into the blood stream of several hormones. Beta cells of the islets are the most abundant cells in the islets. They are responsible of insulin synthesis and storage into secretory granules until its release after sensing elevated glucose levels and other secretagogues. Alpha cells produce the hormone glucagon. Delta cells mainly secrete the peptide hormone somatostatin and finally the pancreatic polypeptide cells (PP cells), which produce pancreatic polypeptides [3].

The exocrine pancreas comprises about the ninety-five percent of the pancreatic mass and is composed of a complex tubular network associated with connective tissue, vessels, and nerves that includes two major cell types: acinar and ductal cells (**figure 1C**). Exocrine pancreas produces and secretes digestive enzymes for nutrient digestion. Acinar cells are polarized pyramidal-shaped cells involved in the production and secretion of digestive enzymes. Due to its high secretory activity, these cells have numerous mitochondria, bigger Golgi and endoplasmic reticulum organelles and are surrounded by numerous acidophilic granules or zymogen granules [4]. Enzymes such as amylases, lipases and proteases are secreted and flow from the acini and acinar tubules until the centroacinar cells. These cells drain the enzymes to the highly branched network of duct cells, which channel the pancreatic juice into the duodenum for hydrolysis. Duct cells are ciliated, polarized epithelial cells with clear cytoplasm, oval nucleus and a poorly developed Golgi and endoplasmic reticulum. They secrete bicarbonate and mucins and form extensive networks of tubules. The ductal network starts with the intercalary ducts (ducts of Boll), that concur to form the intralobular ducts (simple squamous epithelia), which come together to form the interlobular ducts (stratified squamous epithelia). Finally, these will converge to form the main pancreatic ducts (formed by columnar epithelia), the accessory duct of Santorini and the duct of Wirsung [4–6].

1.2.Pancreatic cancer

In 2018, cancer was the second cause of death in Spain after circulatory system diseases. According to the last report of death statistics published by the Spanish Statistics National Institute in 2019, 112714 individuals died from cancer and from theses, 7120 died from pancreatic cancer a 3.7 percent more than the previous year. Pancreatic cancer is one of the cancers with the worst prognosis representing a big challenge for the medical and scientific community. Pancreatic cancer is a heterogeneous group of pancreatic malignancies due to the cellular diversity of this organ. However, most pancreatic cancers are developed in the exocrine tissue of the pancreas, among them, pancreatic ductal adenocarcinoma (PDA) and its histological variants are by far the most common group of malignant neoplasm of the pancreas, accounting for greater of 90% of pancreatic neoplasms [7]. Other exocrine tumors include acinar carcinomas, intraductal papillary-mucinous neoplasms (IPMNs) and Mucinous cystic neoplasms (MCNs). Pancreatic neuroendocrine tumors (PanNETs) represent about 7 percent of pancreatic tumors. However, the prognosis of PanNETs is much better than PDA, with approximately 40% of survival after 10-years diagnosis [8,9]. Other rare pancreatic neoplasms include, colloid carcinomas, pancreatoblastomas and solid-pseudopapillary neoplasms among others [10,11].

2. Pancreatic ductal adenocarcinoma

2.1. Epidemiology, problematic and risk factors

Pancreatic ductal adenocarcinoma (PDA), the most frequent pancreatic tumor is considered one with the direst prognosis among all cancers. PDA dismal outcome and aggressiveness is shown by the fact that PDA mortality and incidence ratio has not experienced significant revision over the last few decades. Moreover, PDA has the lowest five-year survival rate for all stages combined, that remains just around 9% [12] with 80% of diagnosed patients dying within a year [13,14]. Notwithstanding the efforts and advances in PDA research, death rates continue rising. Despite PDA has a low incidence, (around 3% of the new cancer cases each year), PDA is however the fourth most common cause of cancer mortality [15]. To be aware of the impact that PDA is projected to have in the society compared to other cancers, is interesting to point out that PDA is estimated to surpass from the fourth leading cause of cancer-related death and will become the second by 2030 in the United States [16,17].

PDA is associated with poor prognosis for several reasons, one of them is the generalized lack of effective therapies for the treatment of the disease. PDA is a high chemo-resistance tumor, where the systemic delivery of chemotherapy drugs has severe side effects in patients but does not significantly improve the overall survival rate with poor responses [18] (as explained later in section 2.5. PDA treatment). One of the reasons of its chemo-resistance is the nature of the tumor for itself. PDA is an abnormal tumor with chaotic vascular morphology. This morphology, results in a hypoxic microenvironment that impairs appropriate delivery of chemotherapy agents [19]. Furthermore, hypoxia promotes the invasiveness and metastatic potential of PDA via inducing epithelial-to-mesenchymal transition EMT and cancer stem cell (CSC) pathways [20]. Besides tumor heterogeneity and plasticity, another critical promoter of the resistance to treatment is the stroma that surrounds the tumor. Due to the dense stroma reaction, anti-tumor drugs are inefficiently delivered to the tumor site contributing to its resistance and aggressiveness (see section 2.2. PDA stroma).

Another reason for PDA grim outcome is its delayed diagnosis. Most PDAs are in advanced stages at diagnosis. This scenario is mainly caused by a lack of visible and distinctive symptoms in the early stage of the disease [21] and the absence of reliable tumor markers for early diagnosis as will be discussed in depth later on. Since PDA is a very aggressive pathology the result is a high rate of unresectable tumors or spread metastasis when the disease is diagnosed. Furthermore, for the small percentage of patients that have potentially resectable tumors, many of them present recurrence of disease after surgery [22]. Finally, the biology features of the tumor, like the broad heterogeneity of genetic mutations contribute also to its poor outcome.

Among the risk factors of PDA, age is one of the major determinants of the disease. PDA is associated with advancing age [2], most patients are diagnosed at an age older than 50 years old with most cases occurring between 60 and 80 [23]. There is also a positive correlation between PDA and common risk factors that include tobacco smoking, obesity, low physical activity, environmental factors, heavy alcohol consumption, nonhereditary and chronic pancreatitis, long-standing diabetes mellitus, hereditary pancreatitis (due to mutations in any of PRSS1, SPINK1, PRSS2 and CTRC genes) and family history of PDA (about 5 to 10% of cases have familial basis due to inherited predisposition) [23,24]. Established genetic syndromes such as Peutz-Jeghers and Lynch syndrome and germline mutations in CDKN2A, BRCA2, LKB1, CFTR and MLH1 among others have also been associated with PDA [10,23–25].

2.2.PDA stroma

Desmoplasia in PDA is a key factor to understand the disease. It represents a source of new therapeutically targets and contains several potential molecules that could serve as biomarkers. In PDA, the characteristic highly dense fibrotic stromal reaction (known as desmoplasia or desmoplastic reaction) can constitute up to 90% of the tumor volume being one of the most prominent histological features of PDA [26,27]. The stroma in PDA is heterogeneous and it is composed of abundant distinct cell types as well as acellular components, which all together actively contribute to tumor progression, invasion and

provide an immunosuppressive microenvironment. This takes place thanks to a complex crosstalk between its components and tumor cells [13,28,29]. Those tumor-stroma interactions generate a very complicated signaling network where signaling pathways such as TGF-β and Hedgehog are implicated [27,30].

The cellular components of PDA stroma include fibroblasts, stellate cells, immune cells from myeloid and lymphoid lineages, neuronal cells, endothelial cells and pericytes, which give rise to blood vessels [31]. Regarding the stromal cells, activated pancreatic stellate cells have been shown to be a source of extracellular matrix (ECM) and are considered the most important source of cancer-associated fibroblasts (CAFs) [32]. However, CAFs can be originated through different sources such as: the recruitment and activation of pre-existing stromal cells to a “myofibroblastic” state; the trans-differentiation from quiescent precursors like mesenchymal stem cells; via epithelial-to-mesenchymal transition and through derivation from cancer stem cells [27]. Pancreatic tumor stroma is also characterized by an immunosuppressive niche reached by immune tolerance to tumor associated antigens [33] and through immune suppression by T-cell exhaustion and infiltration of tumor-associated macrophages [30,34].

The acellular portion of the stroma is comprised of abundant extracellular matrices containing fibrous proteins such as collagens, polysaccharides like hyaluronan and glycoproteins such as fibrinogen, fibronectin, and fibrins as well as variety of further proteins, cytokines, enzymes, and growth factors [35].

Different components of pancreatic stroma ECM have been shown to have pro-tumorigenic properties [35–40]. This mesh of fibroinflammatory reaction generates high interstitial fluid pressures in the tissue that leads to vascular collapse, while presents substantial barriers to perfusion, diffusion and convection of therapeutics. Hence, molecules such as hyaluronan (highly expressed in PDA stroma) have been identified as primary determinants and targeted, aiming to reduce intra-tumoral pressure that may result in improved tumor perfusion and better therapeutic response, being nowadays this approach tested in clinical trials [39,40].

2.3.PDA transformation and precursor lesions

PDA evolves through non-invasive precursor lesions. The most common is the microscopic precursor lesion entitled pancreatic intraepithelial neoplasia (PanIN). PanINs are graded from PanIN-1A to high-grade PanIN-3 before arising to invasive PDA [41]. Despite its lower incidence, PDA tumors can also arise from larger cystic precursor lesions such as intraductal papillary-mucinous neoplasms and mucinous cystic neoplasms [11,41–43]. In **figure 2** the most common features affecting each PanIN stage and their characteristic mutations that drive to pancreatic tumorigenesis and dysplasia from each stage are shown.

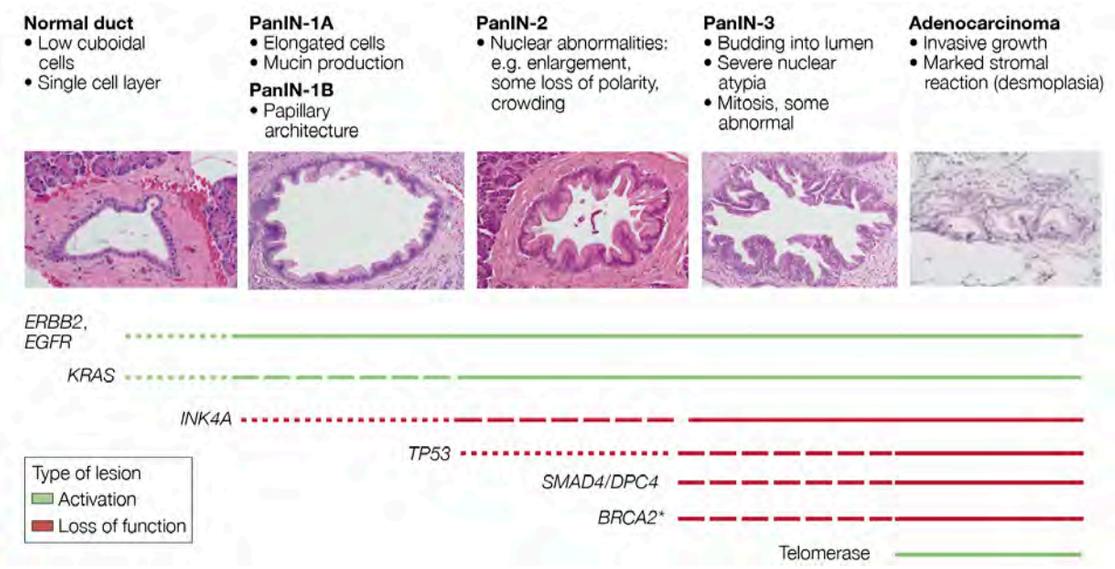

Figure 2 | Precursor lesions of PDA: pancreatic intraepithelial neoplasia (PanINs). Genetic activations in green lines and loss of function in red lines, upon PanINs progressive stages of neoplastic growth that precede the onset of the invasive adenocarcinoma. Extracted and modified from: [2]. Images reproduced and modified from: [42].

The multiple genetic changes upon PDA transformation are complex and include gene amplifications, DNA changes that involve activation of oncogenes, inactivation of tumor suppressors, widespread chromosomal losses, telomere length alterations (shortening) and epigenetic modifications, which include alterations in DNA methylation, histone modifications and non-coding RNAs (ncRNAs) [7,11,42].

Sequencing studies of invasive PDA have showed that activation mutation in Kirsten-RAS (KRAS) oncogene is the most frequent genetic mutation. It is even found in low-grade pancreatic intraepithelial neoplasias but the proportion of cells with KRAS mutation increases with PanIN grade [44]. KRAS activation is present in more than 90% of PDA

tumors [45,46]. KRAS encodes for a GTPase, its activation due to mutations involves the triggering of downstream pathways affecting to cell proliferation, differentiation and cell survival, being determinant for PDA progression [47–49].

Mutations on tumor-suppressor genes are also common in PDA, the most frequent (between 50-80% of PDAs) included inactivation of CDKN2A/p16, TP53, and SMAD4/DPC4 [10,50], being inactivation of CDKN2A the most common (95% of PDAs) [51]. Since CDKN2A plays a crucial role in cell cycle control, its inactivation promotes unrestrained proliferation of the neoplastic cells. CDKN2A encodes for two tumor suppressor proteins INK4A and ARF and many pancreatic cancers sustain loss of both transcripts [2]. The tumor suppressor gene TP53 is involved in the prevention of neoplastic transformation through DNA checkpoint in the repair mechanism against DNA damage or within different forms of cellular stress, leading to cell cycle arrest or apoptosis [7,52]. It is inactivated in approximately 75 up to 85% of PDAs [44] but such mutations do not occur until late [53]. Finally, SMAD4 is found inactivated in 55% of PDAs. Regarding its molecular function, SMAD4 is a co-transcription factor implicated in mediating the transforming growth factor-β (TGFβ) pathway, involved in cellular growth among others and has been associated with shorted survival and metastasis [11,54,55].

Other less common mutations include activating mutations in MAP2K4, STK11, TGFBR1, TGFBR2, ACVR1B, ACVR2A, FBXW7, EP300 [42] HER2, AKT2 and MYB genes [51]. And mutations in oncogenes and DNA repair genes such as BRCA2 (up to 10% of cases), BRCA1, PALB2, RPA1, ATM, [48,55] BRAF, MYB, AKT2, and EGFR, [42] FHIT and STK11 [51]. PDA also exhibits other alterations like aberrant autocrine and paracrine signaling, activation of anti-apoptotic pathways and molecules implicated in signaling cascades such us: TGFβ, EGF, IGF1, HGF, FGFs and their tyrosine kinase receptors: EGFR, HGFR, HER2, HER3, IGF1R, MET [51,56] and GTP-protein coupled receptors (GPCRs) [57] or genes active during development: SHH, WNT, NOTCH [58]. Overall all these mutations enhance its malignancy, self-replication, migratory and invasive features [10,48,59]. Since PDA is also an epigenetic disease, genes like RELN [60], Cyclin D2 [61], and SOCS-1 [62] among others, are commonly methylated in PDA while they rarely show methylation in non-neoplastic pancreatic tissues [53].

As showed in **figure 2** PDA is characterized by the accumulation of multiple genetic alterations during disease progression. Emerging strategies to treat PDA include the characterization of these genetic alterations and the molecular interactions that lead to carcinogenesis. In the last decade, advances in nucleic acid sequencing have allowed to define molecular PDA subgroups that seemed morphologically indistinguishable but presented distinct biology. The identification of different PDA subtypes with recurrently mutated genes (beyond the predominant mutations in KRAS, TP53, SMAD4 and CDKN2A), with specific clinical features and prognosis, represents a source of different therapeutic approaches for specific PDA subtypes [63,64] and a fruitful opportunity to better understand the disease and improve overall outcomes [44]. Typically, several subtypes have been identified based on gene expression and this classification is actively changing [64–67] (**figure 3**).

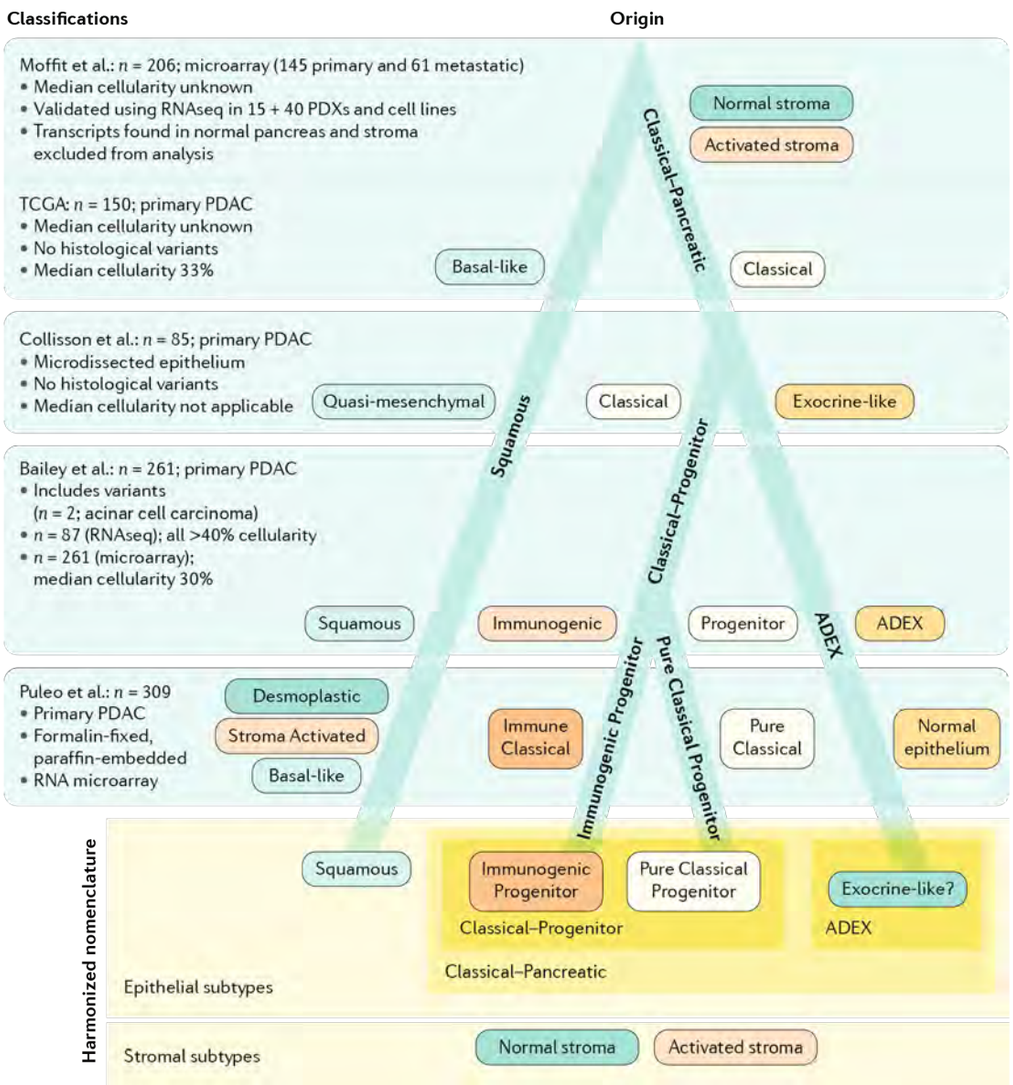

Figure 3 | Phylotranscriptomic tree of pancreatic cancer. Extracted from [63].

PDA tumors include at least two groups distinguished by markers of epithelial differentiation state, with the more poorly differentiated subtype (squamous) exhibiting reduced overall survival and worst outcome [66] relative to well-differentiated subtypes (classical-pancreatic) (**figure 3**). The actual classification distinguishes between epithelial and stromal subtypes. The latter includes normal and activated [67], evidencing that stroma-targeted therapies might need to be subtype directed.

In addition, integrative genomics characterization of PDAs has proven that PDA subtypes also rely on diverse molecular findings such as gene expression via miRNA and DNA methylation [68], that can be integrated to more conventional approaches. Novel approaches have also arisen from the study of metabolic circulating proteins by mass spectrometry to try to improve subtype classification [69]. The inclusion of OMICS such as the genome, proteome, transcriptome, or metabolome, will definitely facilitate a better classification of PDA subtypes in future years.

2.4.PDA diagnosis

PDA diagnosis has hardly improved in recent years despite intense research focused on finding new tools for early diagnosis in patients with high risk. [48] As we will see later, available biomarkers for PDA despite their clinical usefulness, lack of diagnostic and prognostic potential, particularly in the early steps of the disease (see 3.1. Tumor markers in pancreatic cancer). Symptoms of PDA are quite nonspecific delaying its diagnosis since they become apparent in late-stages, (where the tumor has grown large enough to interfere with the function of the pancreas or other nearby organs), or after the invasion, allowing the silent progression of the disease [21]. The most common symptoms associated with PDA included upper abdominal or mid-back pain, nausea and digestive difficulties, obstructive jaundice, diarrhea, weight loss and new-onset diabetes mellitus, [10,42,70], however patients with PDA are frequently asymptomatic. Particularly, tumors located in the head of the pancreas are more likely to be diagnosed at a less advance stage in comparison with body and tail tumors, since they are frequently related to obstruction of the common bile duct and/or pancreatic duct [71].

Regarding the diagnostic tools currently available, imaging techniques remain as the main tool to detect asymptomatic PDA, staging of the disease, assessment of the treatment response and detection of metastatic lesions [72,73]. After the suspicion of the disease, multiple detector computed tomography (MDCT) is usually the best initial staging and diagnostic test for PDA [42,74–76]. Computed tomography (CT) has shown to be also effective for the evaluation of vascular structures invasion [77] and can be used to evaluate spread of the disease and to biopsy [22]. Other useful image techniques include several modalities like magnetic resonance imaging (MRI) [76] 18-F-fluorodeoxyglucose (18-FDG) radiotracer with positron emission tomography (PET) [78,79], and ultrasonography (US) and its variant endoscopic ultrasonography (EUS) that allows not only PDA detection, but also staging and sampling [80]. Ultimately, most patients will undergo histological and cytological diagnosis.

Other methodologies for PDA diagnosis include biochemical tests. Those tests can detect signs of cancer located in the head of pancreas, since rising serum levels of total bilirubin, alkaline phosphatase, gamma glutamyl transferase and transaminases are produced.

However, elevated values usually appear after the obstruction of surrounding organs. Another limitation of serum biochemical markers reside in their poor specificity, since the increase of serum proteins that are commonly significantly higher in other pathologies of the pancreas including biliary pancreatitis [81].

Concerning available tumor markers for PDA detection, there is still no reliable biomarker with enough specificity. Carbohydrate antigen 19-9 (CA 19-9) the only FDA approved tumor marker for PDA is a tumor marker without enough accuracy for screening asymptomatic population [53] being restricted its use predominantly for PDA follow-up [82] (as explained in section 3.1. Tumor markers in pancreatic cancer).

2.5.PDA treatment

PDA treatment varies in relation to the staging of the cancer and patient's general health [83]. Clinical stage of PDA describes the extent or spread of cancer at the time of diagnosis and includes tumor extension, staging and vascular involvement. The stage of a pancreatic cancer is one of the most critical factors in choosing treatment options and predicting a patient's outcome. PDA patients are organized into different categories inside the clinical classification for surgical intervention: resectable, bordeline resectable pancreatic cancer (BRPC) and unresectable (locally advanced or metastatic) [23,84]. The classification of resectability in pancreatic neoplasms is based on international consensus and its determined by several criteria such as size and location of the primary tumor, the involvement of extra-pancreatic spreading to distant lymph nodes and blood vessels and visceral metastasis [53,85,86].

The most common treatments of PDA patients are shown in **figure 4** and include: neoadjuvant chemotherapy, surgery, adjuvant chemotherapy (once the tumor is surgically removed), systemic chemotherapy, radiation and palliative care [23,83].

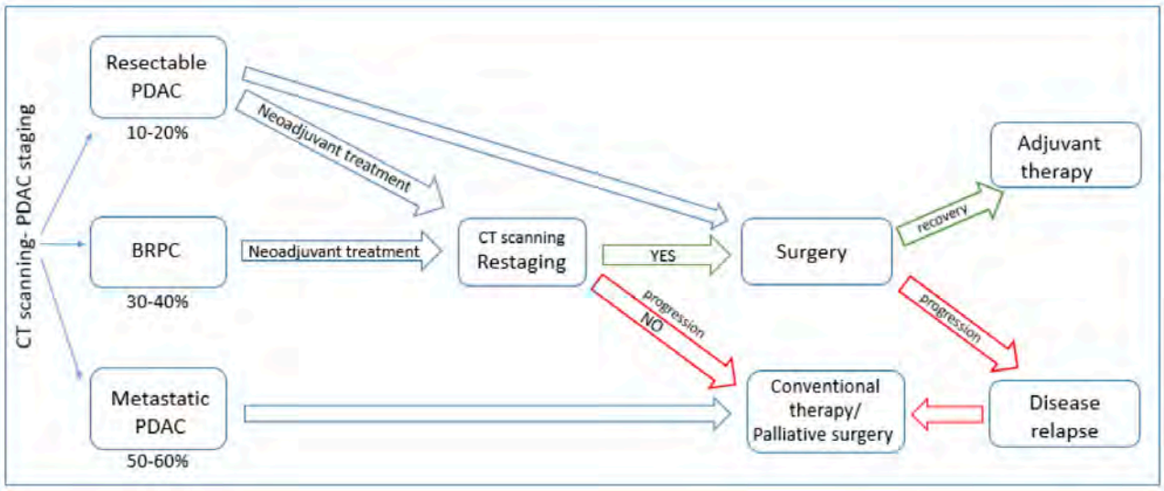

Figure 4 | PDA treatment: A schematic model of treatment strategies against PDA. In green are represented successful procedure, in red failed one. Extracted from [13].

Nowadays complete surgical resection in combination with systemic chemotherapy or chemoradiation offers the only curative treatment for this disease, that can result in improved survival. Nevertheless, this option remains impossible for the 75-80% of patients since at the moment of the diagnostic most patients already have metastases at sites such as the liver, lymph nodes, peritoneum or lung too disseminated to be surgically removed [13,22,87] and even for resectable patients, only 15% of them have earliest-stage cancers, representing only a 2-3% of all PDA patients. However, complete resection leads to increasing the 5-year survival rate up to 20-25%. But the overall survival remains only 25 months, because the 80% will relapse and ultimately will die of their disease [10,13,23,51,53,88,89].

For those eligible patients, surgery to remove the tumor offers the best chance for long-term control and survival for all pancreatic cancer types [88]. Since head and body tumors grow close to visceral vessels, infiltration of the portomeseteric vein and superior mesenteric artery or coeliac axis is commonly found in locally advanced cancer, therefore they often cannot be removed completely by surgery due to its complexity. Different surgery procedures are performed depending in the location of the tumor within the organ. For PDA tumors located in the head of the pancreas, the Whipple procedure, or pancreaticoduodenectomy is the most common procedure [85]. For tumors in the body or tail section of the pancreas, distal pancreatectomy with splenectomy (spleen removal) is one of the current most common procedure. A total pancreatectomy, despite being rarely required, is executed when there are multiple tumors spread throughout the pancreas

and it implicates the total removal of the pancreas resulting in exocrine and endocrine insufficiency [10]. Other ablation techniques for PDA treatment include: radiofrequency (RFA), irreversible electroporation (IRE), microwave ablation (MWA), cryoablation, high-intensity focus ultrasound (HIFU) and immune stimulating interstitial laser Thermotherapy (IMILT).

Neoadjuvant therapy is the one administered before the surgical procedure with the aim of reducing tumor size minimizing tumor burden, it generally involves chemotherapy, radiotherapy or both. In PDA it only represents modest benefits to unresectable patients [90,91] and its use for localized resectable cases is controversial since may delay the operation. Surgical complete resection is followed by adjuvant chemotherapy (given after surgery to kill cells that may have remained in the tissue once removed the tumor) in order to reduce recurrence of the cancer since surgery alone is not enough to accomplish long-term survival [10]. There are currently several chemotherapy treatments approved by the Food and Drug Administration (FDA) for PDA treatment such as: ABRAXANE® (albumin-bound paclitaxel), Gemzar® (gemcitabine), 5-FU (fluorouracil) ONIVYDE® (irinotecan in nanoliposomes), Capecitabine (Xeloda), Erlotinib (Tarceva), Irinotecan (Camptosar), Leucovorin (Wellcovorin), Oxaliplatin (Eloxatin) and some combinations of them.

Despite little survival benefit, Gemcitabine and 5-FU-based chemotherapies or chemoradiotherapies are the most common treatments in adjuvant therapy to reduce the risk of relapse when the patient can tolerate chemotherapy [13,23]. Luckily, many clinical trials are still being carried on to improve the grim prognosis of PDA and improve patient survival that involves new cytotoxic agents, Ras or PI3K inhibitors or cancer vaccines among others [92,93].

Once metastasis has occurred, a poorly prognosis is expected and chemotherapy represents the principal option despite a mildly increased survival rate. Chemoradiation in these patients other than palliation is controversial since the benefit is unclear despite its wide use in the USA [88,92,94]. In patients with advanced and metastatic cancer gemcitabine-based therapy, which can be combined with capecitabine [95–97]. or FOLFIRINOX (a multidrug combination of irinotecan, fluorouracil, leucovorin and

oxaliplatin) are the standards of care. FOLFIRINOX showed recently better results in terms of response, possible down-staging followed by curative resection, progression-free survival and overall survival of patients. Therefore, it is considered as first option for patients with advanced PDA or metastasis under 75 and with good performance status (PS) due to its relative high toxicity [94,98–101]. However, combination chemotherapy, (associated with slightly better outcomes) is often limited since the final treatment chosen will depend on the PS of the patient as each treatment has different potential adverse events.

Palliative care also is important to alleviate and improve patients' symptoms, since in this stage they will probably suffer symptoms of jaundice, pain, nausea and vomiting that are caused by gastric outlet obstruction, duodenum obstruction and obstructive jaundice and an intervention will be needed. The most common palliative procedures for pancreatic cancer are biliary bypass surgery, gastric bypass surgery and biliary or duodenal stent insertion among others such as nutritional support, with the aim of preserve patients' quality of life [23,102].

2.6. Clinical classifications for staging PDA

Accurate evaluation of tumor stage is a prerequisite for further treatment and prognostic prediction. The AJCC/UICC TNM staging system has been widely applied worldwide as the most authorized tool for tumor staging assessment [103]. In **table 1** the PDA definitions for TNM stage classification of PDA patients are described.

Table 1 | The definitions of the 8th edition of TNM staging system of PDA.

Definition of Primary Tumor (T)	
Tx	Primary tumor cannot be assessed
T0	No evidence of primary tumor
Tis	Carcinoma *in situ*. This includes high-grade pancreatic intraepithelial neoplasia (PanIn-3), intraductal papillary mucinous neoplasm with high-grade dysplasia, intraductal tubulopapillary neoplasm with high-grade dysplasia, and mucinous cystic neoplasm with high-grade dysplasia.
T1	Maximum tumor diameter ≤2 cm
T2	Maximum tumor diameter >2, ≤4 cm
T3	Maximum tumor diameter >4 cm
T4	Tumor involves the celiac axis, common hepatic artery or the superior mesenteric artery regardless of size

Definition of Regional Lymph Node (N)	
Nx	Regional lymph nodes cannot be assessed
N0	No regional lymph node metastasis
N1	Metastasis in 1–3 regional lymph nodes
N2	Metastasis in ≥ 4 regional lymph nodes

Definition of Distant Metastasis (M)	
M0	No distant metastasis
M1	Distant metastasis

Stage classification			
	T	**N**	**M**
IA	T1	N0	M0
IB	T2	N0	M0
IIA	T3	N0	M0
IIB	T1-T3	N1	M0
III	T4	any N	M0
III	any T	N2	M0
IV	any T	Any N	M1

3. Tumor markers

The term cancer biomarker or tumor markers (TMs), usually refers to molecules o biochemical indicators, produced or released by tumor cells (like cell surface antigens, cytoplasmic proteins, hormones, enzymes, oncofetal antigens, receptors, oncogenes and their products) or produced by host in response to a tumor, which can be found in the circulation (blood, serum or plasma) or in other body fluids either excretions or secretions [104–106].

Nowadays, tumor markers are playing an increasingly important role in cancer detection and management [107]. Clinical uses of tumor markers can be classified into four groups [104]. Thus, the ideal tumor marker should be able to screen early-stage disease (detect disease in persons without symptoms for improve the curative potential), allow tumor characterization, diagnostic confirmation and determine the prognosis, (confirm tumor presence, stratify and predict the malignancy of the disease). Tumor markers should also identify therapeutic response of the patients and detect recurrences after treatment [104,108]. Ideally, tumor markers should be easily assessed by non-invasive techniques, be of low risk and cost and have reasonable/high predictive value, specificity and sensitivity.

The specificity of a tumor marker is defined as the percentage of patients without a malignant tumor or with benign conditions, for whom a negative result is obtained within the range established as non-pathologic. Briefly, the greater the specificity, the fewer the false-positives should be detected in benign cases. On the other hand, it is considered sensitivity as the ability to detect the disease when it is present and it corresponds to the percentage of patients with a certain tumor, which are correctly positively diagnosed for having values outside the normal reference range. The greater is the sensitivity of a tumor marker, the fewer the false-negatives will be detected in malignant cases [106,109].

Limited sensitivity and specificity in tumor markers generate a big limitation in screening, especially when combined with low incidence in the general population because it can trigger two different consequences. The first one is a low positive predictive value in screening asymptomatic populations, decreasing the possibility of detecting an early-

stage tumor before metastases has occurred and limiting potential curative treatments. The second consequence is the diagnosis of false positives which would result in expensive and probably invasive examinations [107].

In some benign conditions, tumor markers may result in increased levels of the marker, such as the tumor marker prostate specific antigen (PSA) used for prostate cancer, which is also increased under prostatitis or benign prostatic hyperplasia, or CA 125, the tumor marker used for ovarian cancer, which is also increased in peritoneal irritation, endometriosis, pelvic inflammatory disease or hepatitis [104]. Furthermore, TMs alone often cannot differentiate between aggressive cancer from indolent variants of the disease and thus has led to overdiagnosis and overtreatment of patients [110]. As direct consequence, tumor markers for itself are not considered a reliable diagnostic tool and often are accompanied with additional diagnostic tests as physical exams, laboratory and imaging test, biopsies and cytological diagnosis [106]. Disorders in the liver or kidneys functions could also accumulate small quantities of some tumor markers increasing false positive results [111].

Cellular glycoproteins play an important role in malignant transformation and cancer progression. Many of the currently used biomarkers are glycoproteins and mucins such as CA 125, CA 15-3, CA 19-9, CA 72-4, or PSA [112,113]. Taking into account that glycosylation is altered during cancer development, there is a growing tendency to study changes in the glycosylation of such proteins to improve the sensitivity and specificity of tumor markers overcoming their limitations. Investigation of glycoprotein glycoforms using high-throughput glycan structural analysis [114], and lectins and antibodies against carbohydrate antigens [115–117] is becoming a tool to discover novel candidates.

As will be explained later in section 4.7. (Altered glycosylation in cancer) the glycan moieties of glycoproteins could be aberrantly expressed in many diseases including cancer. Glycan aberrations become more marked as the tumor acquires a more aggressive phenotype during malignant transformation, so we can use the ability to study those changes in the glycosylation profile to detect, define cancer development and provide insights into disease stages [113,118,119]. The overexpression of these altered glycosylated structures (found in secreted proteins or expressed on the cell surface) and

the loss of polarity of the carcinoma cells, lead to the shedding of the above-mentioned aberrant glycosylated proteins into the blood stream [120], where they could be detected and targeted for promising novel tumor markers. Under these premises, a part of this thesis consists in exploiting these changes in glycosylation for the discovery of new tumor markers in PDA.

3.1. Tumor markers in pancreatic cancer

The measure of serum levels of carbohydrate antigen 19-9 (CA 19-9) also known as sialyl Lewis A (SLe^A) blood group antigen is currently the most widely used biomarker for PDA after carcinoembryonic antigen (CEA) [10,82,121].

However, neither CA 19-9 nor CEA biomarkers meet the performance standards required for being reliable diagnostic markers or have the accuracy for screening asymptomatic populations [122]. In healthy individuals, CA 19-9 concentrations in serum are below 37 U/mL [123]. The principal CA 19-9 limitations include its low positive predictive value (0.5-0.9%), due to the relatively low incidence of PDA in the general population, which translates CA 19-9 in an insufficient tool for the diagnosis or screening of PDA [122,124]. CA 19-9 sensitivity and specificity in symptomatic patients remains moderate about (79-81% and 82-90% respectively) [74,122,125] and its AUC, 0.88 [126]. Thus, these drawbacks strongly limit the effectiveness CA 19-9, which is not useful for the diagnosis of PDA [127]. Nevertheless CA 19-9 levels provide helpful information in the prognosis and monitoring of the disease progression and the tumor response in the assessment of neoadjuvant therapy [10,128]. For example, CA 19-9 serum levels <100 U/mL help to predict resectability of the tumor, whereas that >1000 U/mL usually predict unresectability and plausible metastatic spread [74]. However lower cut-offs (ranging from 130 to 400 U/mL) have been proposed for considering staging laparoscopy in order to detect small metastases tumors. Also, preoperative levels higher than 500 U/mL has been associated with worse prognosis and decreased survival after surgery [82,127]. Monitoring of CA 19-9 levels have also proven useful in the therapeutic follow-up of patients, where decreasing changes in CA 19-9 levels during and after chemotherapy are predictive of a patient's

response to therapy and increased overall survival [74,82]. Similarly, lower postoperative CA 19-9 levels correlate with increased survival, being CA 19-9 levels a useful prognostic tool to predict outcome of PDA patients [75,129].

Another major disadvantages of CA 19-9 in its clinical use involve the elevation of its serum levels in other benign pathologies. Since the biomarker is expressed in a small proportion of non-malignant epithelial cells, CA 19-9 is secreted in mucins, pancreatic juice, bile, and saliva. Thus, those cells under occlusion or inflammatory processes of non-malignant disorders or in chronic inflammation lead to CA 19-9 accumulation and backflow to the circulation, increasing serum levels of the protein that can conclude false-positive results. Those pathologies include obstructive jaundice, liver cirrhosis, pancreatitis, cystic diseases of salivary gland or kidney peritoneal pseudomyxoma [130]. Furthermore, elevated CA 19-9 levels have been also observed in other advanced gastrointestinal, breast and small cell lung cancers [122,130–132]. The Lewis phenotype is determined by FUT3 and FUT2 genes [129]. Between five to seven percent of population (up to 10% for Caucasians) lack a functional FUT3 allele, (termed Lewis genotype negative Le $^{a-b-}$), being the synthesis of CA 19-9 from the precursor carbohydrate antigen not possible in those patients and consequently it generates false-negative results [74,82,123,133–136]. Since up to 40% of patients with chronic pancreatitis have elevated CA 19-9 levels [126], our group has developed a combinational algorithm of clinical markers routinely used for improving the classification of patients with pancreatic cancer from those with chronic pancreatitis. The combination includes factors produced by the tumor and from the systemic response to the growing tumor, including inflammatory molecules. Thus, combination of CA 19-9, albumin and IGF-1 levels resulted in an AUC of 0.96 with 93.6% sensitivity and 95% specificity [137]. Other multimarker panels that can increase sensitivity or specificity have been described in the last decade [138–142]. Several other candidates such as hormones, apoptotic factors, cytokines, apolipoproteins [139] have been studied as biomarkers. Research in novel candidates for PDA biomarkers, has exploited different strategies including autoantibodies, circulating free DNA released upon cellular death encoding PDA mutations [143,144], differences in DNA methylation in PDA cases [145] which includes higher methylation at CpG sites in tumor suppressor genes [146] or MicroRNAs (miR)

whose expression is altered in numerous cancers and can be detected in blood or plasma such as miR-223 [147–149]. In **table 2**, a few more examples of potential PDA target biomarkers published in recent years are shown.

Table 2 | Overview of biomarkers for pancreatic cancer. Modified from [139,150,151].

Traditional biomarkers	CA 19-9, CEA
Proteomics	CEMIP, C4BPA, IGFBP2/3, ICAM-1, OPG, MUC1/2
Metabolites	M2-pyruvate kinase, palmitic acid, glucitol, xylitol, inositol, histidine, proline, sphingomyelin, phosphatidyl choline, isocitrate, ceramide
Antibodies	immunoglobulin G4 (IgG4)
Cytokines	interleukin-1β, interleukin-6, interleukin-8, interleukin-10, vascular endothelial growth factor and transforming growth factor (macrophage inhibitory cytokine-1 [MIC-1])
Noncoding RNAs	microRNAs (miRNAs), small ncRNAs (sncRNAs), long ncRNAs (lncRNAs)
Liquid biopsy	circulating tumor cells (CTCs), circulation tumor DNA (ctDNA) and exosomes
Body fluids	detecting biomarkers from saliva, urine, stool or pancreatic juice

However, most of these biomarkers despite generate promising results in the onset of the discovery phases fail in the subsequent validation for clinical usefulness. As a result, no marker for PDA has been approved for use in clinical practice by the FDA in the past two decades [71,133]. Therefore, despite the vast efforts made in investment of novel biomarkers there is still an urgent need for discovering new biomarkers that could overcome CA 19-9 limitations. The low incidence of PDA demands a biomarker with higher predictive value sensitive and specific enough to detect early stage disease and improve PDA diagnosis. Luckily, in recent years it has been described that there is a period of about a decade between the occurrence of the initial mutation and the appearance of the initial precursor neoplastic clone, and estimated seven more years before the acquisition of metastatic ability and the death of the patient [152]. Nevertheless, other studies point out that some pancreatic tumors can drive from non-invasive to metastatic within a short period between screening intervals [153,154]. Although these estimates reflect a range of tumor behavior in diverse patients, they also indicate that a primary cancer can reside in the pancreas for many years before metastasis occurs. This fact provides opportunities for screening [42] and detection of PDA at early stages when surgical resection is still possible. It could favor a significantly change in PDA statistics since early detection is one of the best ways to improve PDA prognosis [53].

4. Glycobiology

4.1. Introduction to glycosylation: monosaccharides and glycoconjugates

Glycosylation is defined as the enzymatic process that produces glycosidic linkages of saccharides to other saccharides, proteins or lipids [155]. Glycosylation among others like phosphorylation, methylation and ubiquitination is a post-translational modification (PTM). Those modifications in proteins play a very wide-ranging role in cell biology and their functions may include protein localization, activity state and interactions, among others [156]. Glycosylation is not only the most complex post-translational mechanism, but is also the most common and abundant PTM with more than half of all proteins being glycosylated [157–159].

The monosaccharide is the simplest unit that form carbohydrates. Carbohydrates can be expressed either as free reducing sugars or as glycoconjugates [160], as presented later. Monosaccharides are traditionally presented using the Fisher projection or the Haworth representation. However, in order to simplify its representation, they are usually shown with a consensus simplified symbol. In **figure 5** the most common monosaccharides of vertebrate glycans and their linkages are shown.

The monosaccharides are typically bond between them or with other molecules through covalent glycosidic bond, that is formed usually between the hydroxyl group of the anomeric center of one monosaccharide unit and the hydroxyl of the second molecule, generating α-linkages or β-linkages.

The term glycoconjugate includes compounds with one or more monosaccharide or oligosaccharide units (the glycon) that are covalently linked to a non glucidic part (the aglycon). Glycoconjugates play an indispensable role in many biological events and are widely distributed. They are defined according to the nature of the linkage of the aglycone (protein or lipid).

The most common eukaryotic examples are shown in **figure 5** and include: (GPI)-anchored glycoproteins, proteoglycans, glycosphingolipid and glycoproteins [161].

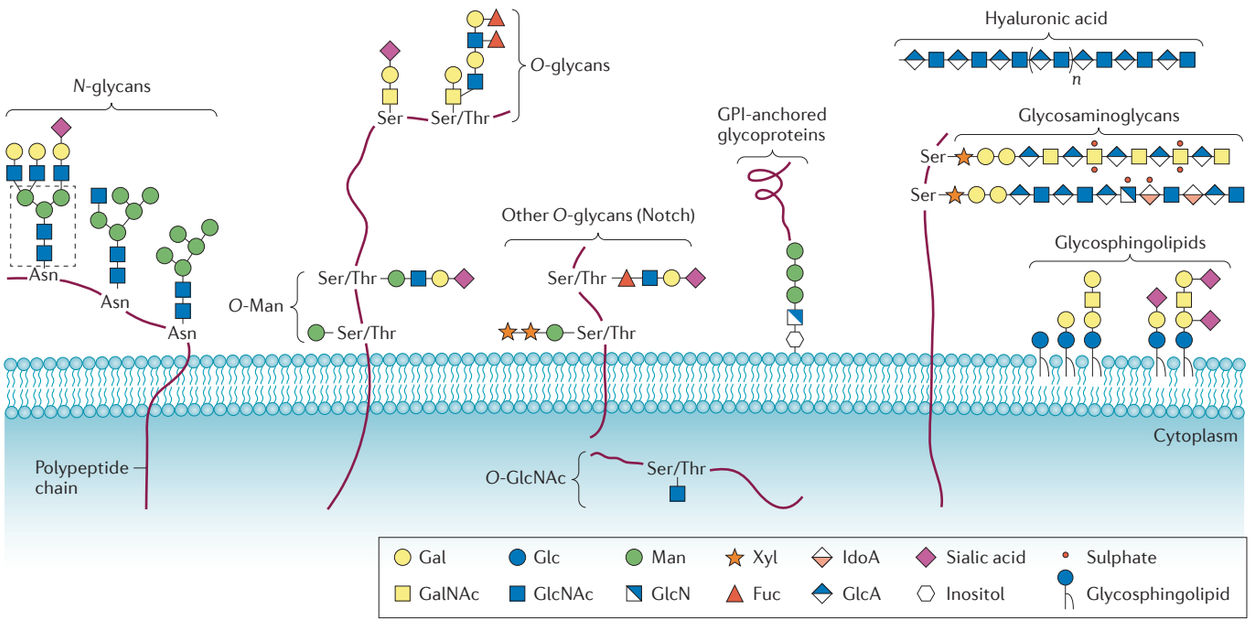

Figure 5 | Common major classes of glycan structures on animal cells. Representation on the most common glycoconjugates on animal cells and Monosaccharides consensus symbols. Extracted from: [155].

The glycon of the glycoconjugates is particularly complex, since its formation is not template-driven, varies between cell types and is difficult to predict; as an example, three hexose monosaccharides can theoretically produce up to 1056 possible glycans, and multiple glycan isomers could share the same monosaccharide composition but they differ in sequences and linkages, a finding commonly referred to as site-specific oligosaccharide heterogeneity or microheterogeneity. Furthermore, there is also a variable occupancy of glycosylation sites, known as macroheterogeneity [162].

The contribution of carrying glycans in many cases can significant vary the overall molecular mass of the aglycon, being its contribution up to 50% of the overall mass as occurs in some mucins [113]. Glycoconjugates have imperative roles and effects upon the biosynthesis, folding, solubility, stability, adhesion and signal modulation subcellular trafficking, turnover, and half-life of the molecules to which they are attached [162]. Furthermore, they are a powerful machinery that contributes to biological diversity and complexity due to the variable and dynamic nature of glycosylation.

In glycoproteins, glycans are classified in two major groups with differing biosynthetic pathways, according to their covalent attachment to the polypeptide backbone, usually via N-glycosidic linkage (N-glycans) or O-glycosidic linkage (O-glycans).

4.2. O-Glycosylation

The term O-glycan includes among others the O-fucose (O-Fuc), O-galactose (O-Gal), O-mannose (O-Man), O-Xylose (O-Xyl), nucleocytoplasmic O-linked β-N-acetylglucosamine (O-GlcNAc) [163,164] and finally the most common type of protein O-glycosylation in animals: The O-GalNAc glycan or also called mucin-type O-glycan [165].

GalNAc O-glycosylation is an evolutionarily conserved protein PTM present on membrane-bound and secreted proteins that is initiated in the Golgi, after most protein folding events have already happen [165,166]. O-GalNAc glycans are formed between the hydroxyl group of a serine or threonine residue of the polypeptide chain and an N-acetylgalactosamine (GalNAc) from a UDP-GalNAc donnor. The catalysis is performed by a large family of enzymes named polypeptide-N-acetylgalactosaminyltransferases (ppGalNAcT) from ppGalNAcT -1 to -21 [161,165,167]. This process is ruled by the sequence context of putative O-glycosylation sites but also regulated by enzymatic competition and epigenetic mechanisms [168].

O-GalNAc glycans include three different regions. The core region, proximal to the peptide that is comprised by the innermost monosaccharides of the glycan. The backbone, where the different chains are elongated and finally the peripheral region that add higher diversity and complexity to the glycan [168].

The first GalNAcα-Ser/Thr common structure is named Thomsen-nouvelle antigen or Tn-antigen, which acts as a substrate to be extended by glycosyltransferases that may further extend to core 1 and core 3 structures from which most O-GalNAc glycans are ultimately derived [169] as shown in **figure 6**. At least eight different types of core structures without including Tn-antigen and Sialyl Tn antigen have been reported so far [168].

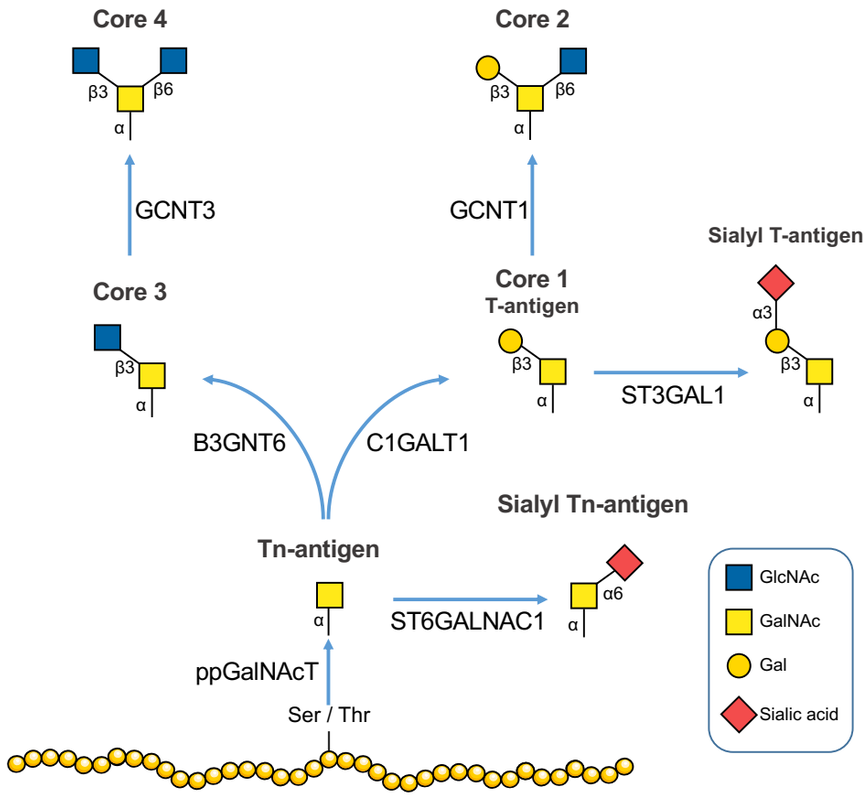

Figure 6 | Biosynthesis of different cores of O-GalNAc glycans. Representation of the most common mucin-type O-glycosylation core 1–4 biosynthetic pathways in mammals. Monosaccharide legend is shown on the right. Protein chain drawing was extracted from Servier medical art website and later modified. Data for the figure portrayal was extracted from: [161,165,166].

O-GalNAc glycans are highly expressed on mucins since they contain multiple Ser/Thr residues. O-GalNAc glycans are of special relevance thus in mucous sites, since their presence in mucins prevents disruption of the homeostasis and provide protection to the epithelia from environmental threats. Mucins are especially important lubricating epithelia in the airways, urogenital and gastrointestinal tracts and influence the secretion and composition of the extracellular matrix in a number of systems, thereby affecting cell adhesion [166,169,170]. Importantly, altered glycosylation in mucins enhances tumorigenicity, invasiveness, metastasis and drug resistance [171].

4.3.N-Glycosylation

N-linked glycans in glycoproteins have a common structure, where N-acetylglucosamine (GlcNAc) is attached through β-glycosylamine (N-glycosidic) linkage between the hydroxyl group of the anomeric carbon from GlcNAc and the amide nitrogen of the asparagine side chain, (abbreviated as GlcNAc-N-Asn). The asparagine (Asn) amino acid should be present as a part of the most representative consensus sequence: Asn-X-Ser/Thr, in which X may be any amino acid except proline (Pro). Although this sequence is frequently found in proteins, its occurrence does not always indicate the presence of N-glycosylation since it has to be considered the effect of conformational factors and other constraints during glycoprotein folding [161].

In humans all N-glycans have a common penta-saccharide region or core sequence consisting of three mannose (Man) residues and two N-acetylglucosamine (GlcNAc) linked to the asparagine (Manα1,3(Manα1,6)Manβ1,4GlcNAcβ1,4GlcNAcβ1–Asn-X-Ser/Thr). N-glycans can be divided in three main types: high mannose or oligomannose, hybrid N-glycans and finally the complex type (the most common extracellular N-glycans in vertebrates) [161,172]. In **figure 7**, the three types of N-glycan are shown.

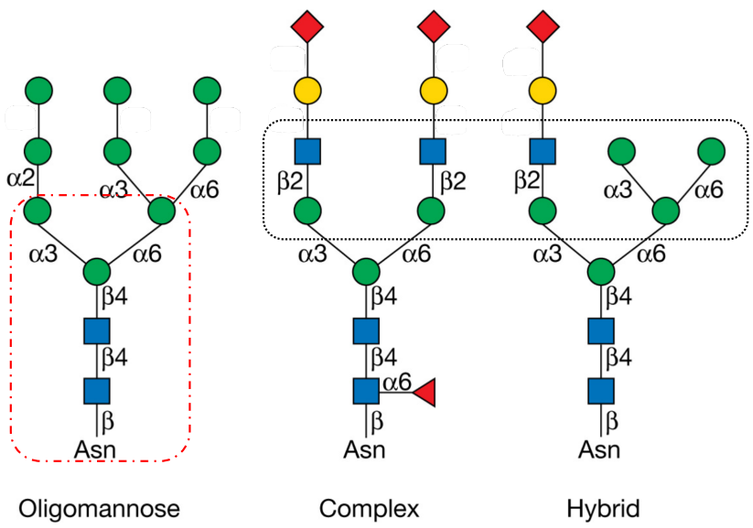

Figure 7 | Three main types of N-glycans. Representative scheme of main N-glycans types: oligomannose, complex and hybrid. The dashed box with lines and dots in red color represents the common penta-saccharide region that all three types of N-glycans share. On the right in a box of dashed black dots are depicted the differences between complex and hybrid structures. Complex N-glycans refers to those in which both the two terminal mannose residues of the penta-saccharide region are substituted with GlcNAc, while in the hybrid structures only one of the terminal Man residue is substituted with GlcNAc linkage. Extracted and modified from [161].

The assembly of N-linked glycans occurs in three major steps. The first one is the synthesis of a lipid-linked precursor oligosaccharide, followed by *in bloc* transfer of the oligosaccharide to an available asparagine residue in nascent or newly completed polypeptide chain and finally the processing and elongation of the oligosaccharide [173].

Despite the huge diversity, N-glycans' biosynthesis starts in the endoplasmic reticulum (ER) through a common pathway since they have conserved the earliest biosynthetic steps. In eukaryotes, the first step yields to the synthesis of a dolichol lipid linked to the precursor Glc3Man9GlcNAc2. This oligosaccharide precursor consists of 14 monosaccharides including 3 glucoses (Glc), 9 Manoses (Man) and 2 N-acetylglucosamines (GlcNAc) (**figure 8**).

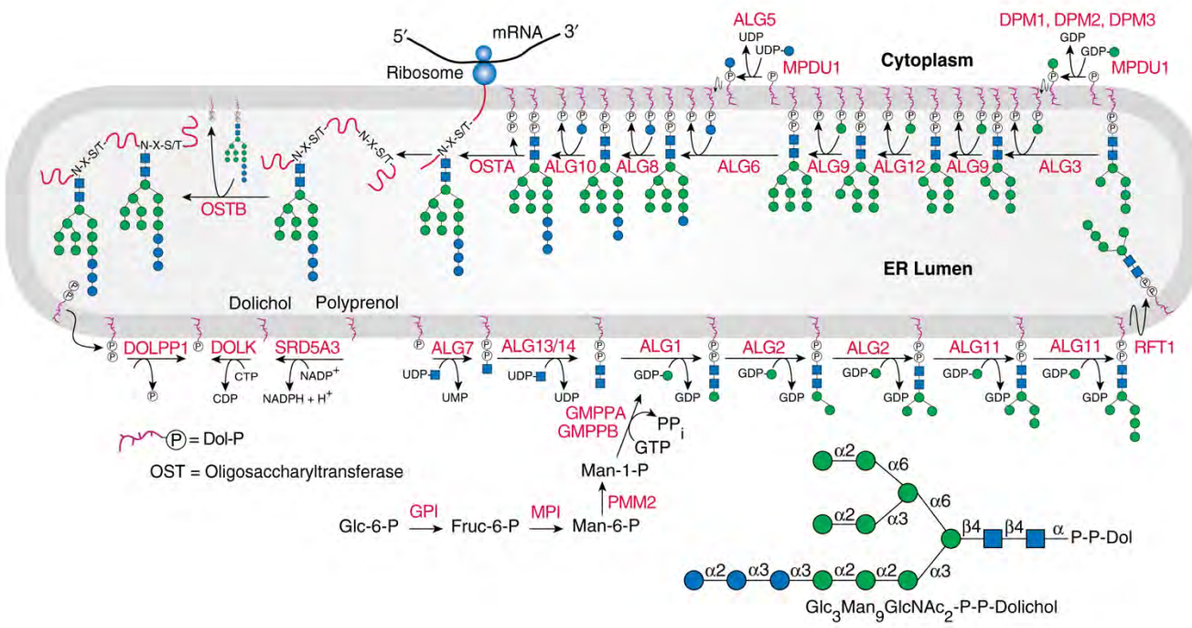

Figure 8 | N-glycans biosynthesis: Synthesis of a lipid-linked precursor oligosaccharide, followed by *in bloc* transfer to an asparagine residue. Extracted from [161].

This whole process occurs in two separated steps. Initially, in the cytoplasmic side of the endoplasmic reticulum, two GlcNAc residues followed by five Man residues are attached through a pyrophosphate linkage to the dolichol located in the membrane of the ER, via to nucleotide sugar donors. Once Dolichol-GlcNAc2-Man5 is formed, it happens the translocation from the cytoplasmic to the luminal side of the ER where the subsequent monosaccharides are added until the completion of the lipid-linked oligosaccharide precursor that is ready for being transferred to nascent polypeptides chains. This transference of the 14-sugar oligosaccharide is completed by oligosaccharyltransferase (OST) at the consensus Asn residue in the polypeptide chain, which has been

translocated into the ER lumen. The rate of glycosylation depends on the availability of active glycosyltransferases and of lipid-linked precursor among others. After the transfer of the precursor oligosaccharide by OST and through the action of glycosidases begins the glycan early processing in the ER lumen (**figure 9**). Sequential Glc residues are removed by glucosidases and a linked mannose residue is detached by mannosidases in the ER. Then the partially processed and folded high-mannose glycoprotein is transferred to the cis-Golgi cisternae. In cis-Golgi, high-mannose glycoproteins destined to lysosomes are phosphorylated, while in the other glycoproteins three mannose residues are sequentially removed [161,173].

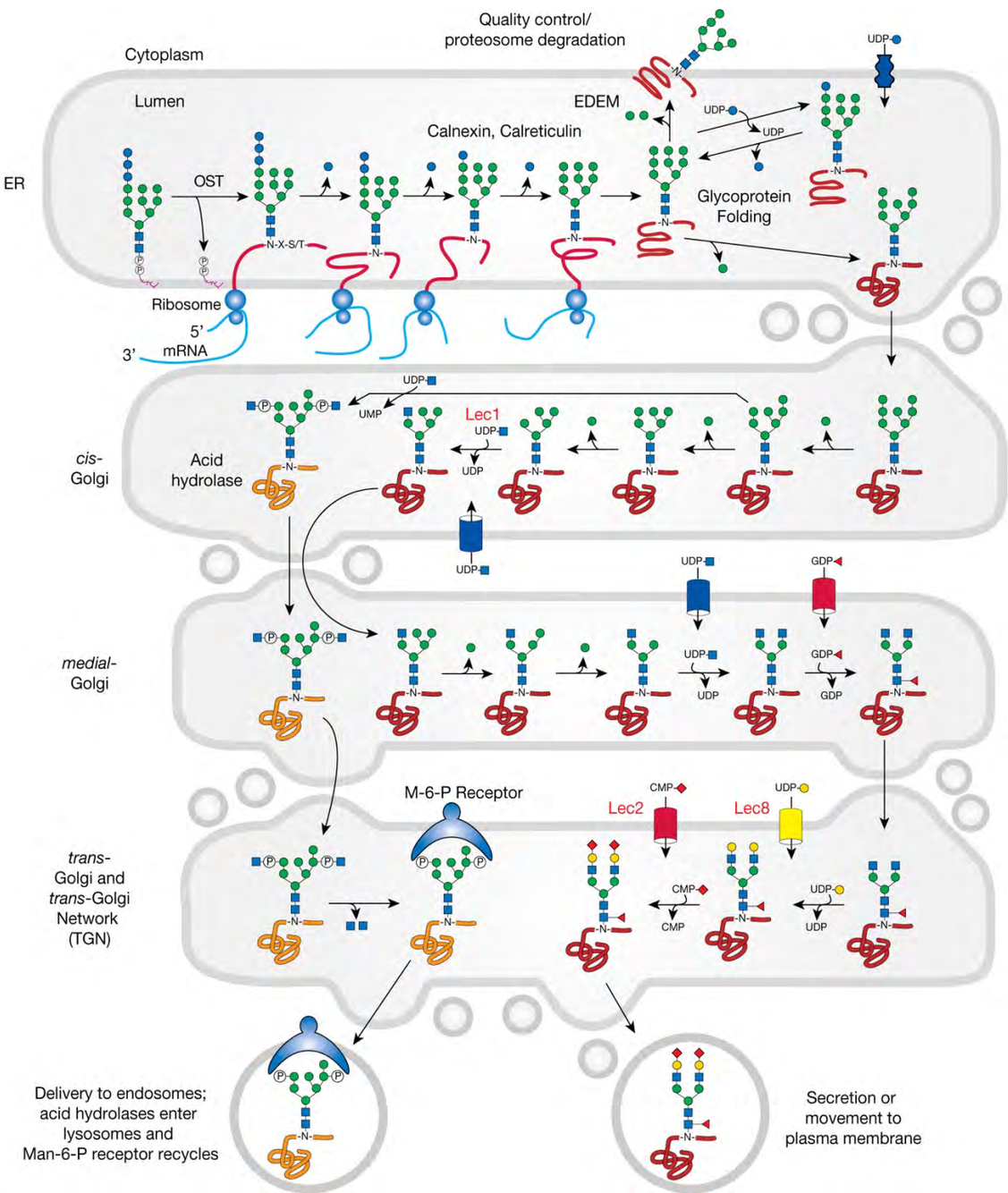

Figure 9 | N-glycans processing and maturation: Diagram of N-glycan formation. Extracted from: [161].

After the removal of the three mannose residues a structure with 5 Man and 2 GlcNAc remains. The first step of biosynthesis of hybrid and complex N-glycans begins with the addition of GlcNAc to the core α1,3-mannose by the N-acetylglucosaminyltransferase MGAT1 upon the aforementioned structure, as shown in **figure 10**.

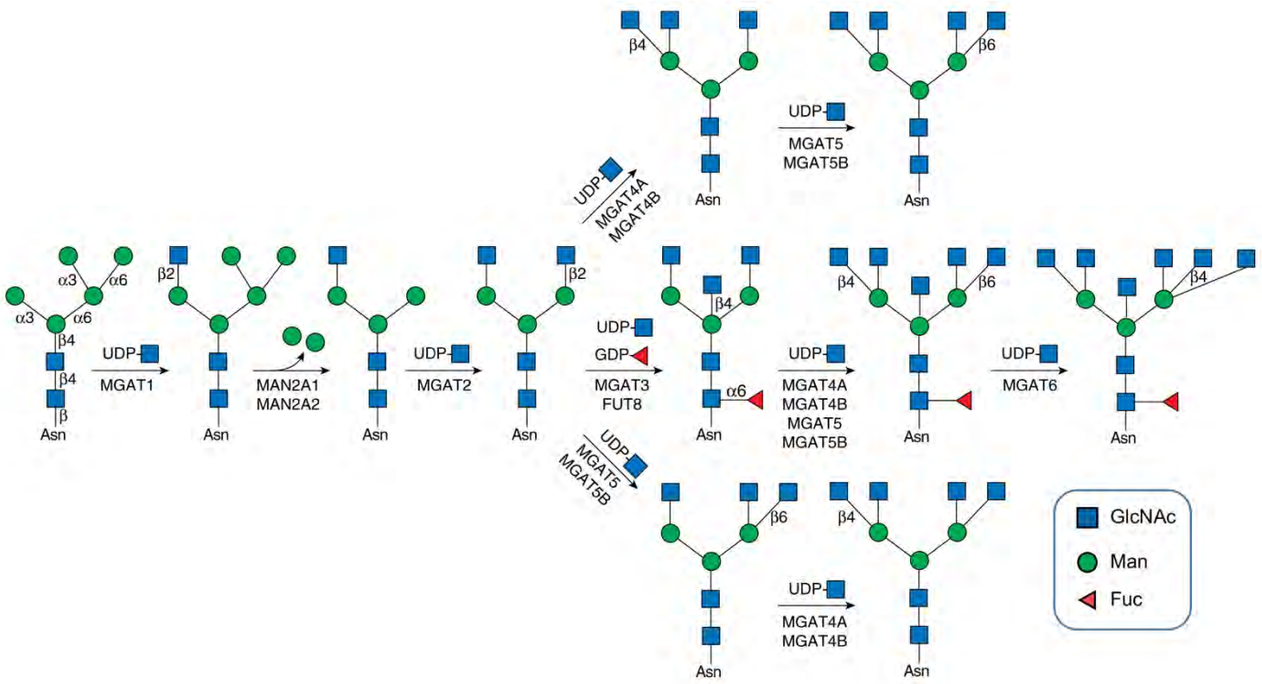

Figure 10 | Branching and core modification of complex N-glycans. Extracted from: [161].

Then, the glycan is transferred to medial-Golgi. Subsequently, if mannose residues are not trimmed by the α-mannosidase-II enzymes MAN2A1 or MAN2A2, a hybrid N-glycan results. If MAN2A1 or MAN2A2 remove the terminal α1,3-Man and α1,6-Man, MGAT2 can act adding a second GlcNAc residue to the α1,6-mannose core, generating a biantennary N-glycan (each GlcNAc constitute one antennae or branch). However, complex N-glycans may contain more branches because of GlcNAc-transferases in the Golgi that act after MGAT2. Consequently, biantennary chains may accept additional branches by the addition of GlcNAc to α1,3-Man or α1,6-Man to yield tri- and tetra-antennary N-glycans. Complex and hybrid types can also carry a bisecting GlcNAc.

The last steps of N-glycans synthesis include further elongation and maturation in the medial-Golgi and trans-Golgi regions. In this last step “capping” sugars may be added to the N-glycan core and branches can be elongated with Gal and GlcNAc. Those peripheral sugars will form a mature complex-type oligosaccharide. The most imperative capping residues formation involves addition of sialic acids, fucoses, galactoses, GlcNAc and

sulfate to complex N-glycan antennas. Those capping sugars such as sialic acids and fucoses are commonly α-linked to facilitate its presentation to antibodies and lectins. The final glycan product will depend on the availability of monosaccharide donors and the accessibility to the different glycosyltransferases present within the medial and trans Golgi.

4.4. The type-1 and type-2 glycan chains

In N-Glycans, most hybrid and complex structures have extended branches made by the addition of Gal to the initiating GlcNAc to produce the starting (Gal-GlcNAc) junction. This external terminal structure is shared by N-glycans, O-glycans of glycoproteins and glycolipids. The addition of galactose to GlcNAc could be in β1,3 or β1,4 linkage, which generate the type-1 and type-2 structures respectively (**figure 11**).

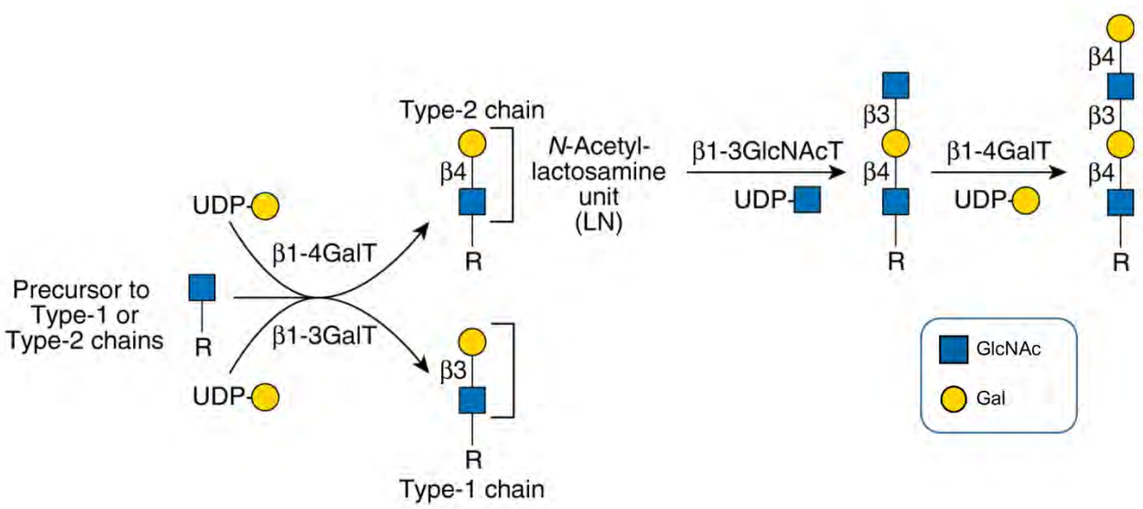

Figure 11 | Type-1 and type-2 glycan chains: Elongation of GlcNAc branches with Gal residues in different linkages will form type-1 and type-2 structures on N-glycans. Modified from [161].

Type-1 structures are composed by Galβ1,3GlcNAc also known as neo-N-acetyllactosamine or LacNAc type-1. They are highly abundant in glycolipids and O-glycans of glycoproteins in the gastrointestinal or reproductive tracts epithelia. Those structures constitute a motif for galectin binding.

Type-2 unit constituted by Galβ1,4GlcNAc, also known as N-acetyllactosamine (LacNAc) or LacNAc type-2, can generate Poly-LacNAc chains by the addition of β1,3GlcNAc, which in turn can receive a β1,4Gal leading to LacNAc chains.

Those poly-LacNAc chains and type-1 structures, can serve as acceptors for subsequent modifications by glycosyltransferases that transfer sugars to terminal Gal or subterminal GlcNAc, generating sialylated, fucosylated (by sialyltransferases or fucosyltransferases) or sulfated structures. Those structures constitute precursors of several important blood group and Lewis epitopes such as sialyl Lewis X and A, which play important roles in tumor metastasis and are considered as markers for diagnosis and prognosis of cancer metastasis [174–178].

4.5.Sialylation and sialyltransferases

Sialylation is one of the most common capping reactions in the formation of complex glycans. They are commonly added onto either N- or O-linked glycans of glycoproteins and glycolipids [179]. The incorporation of a sialic acid (SA) is performed by a family of glycosyltransferase enzymes known as sialyltransferases (STs). In vertebrates STs are type II transmembrane glycoproteins located in the *trans*-Golgi, which transfer sialic acid in different linkages using the nucleotide sugar CMP-SA as a donor [180]. Animal STs share similar peptide conserved motifs (sialylmotifs) that include shared sites for CMP-SA recognition [181]. In humans the most common sialic acid is 5-N-acetylneuraminic acid also known as Neu5Ac, an acid monosaccharide (pKa of 2.6) that confers a negative charge to the glycan [161].

Based on the type of glycosidic linkage formed, STs have been classified into four major subfamilies ST3Gal, ST6Gal, ST6GalNAc, and ST8Sia [182]. STs can transfer the sialic acid in α-linkage via the anomeric carbon (C-2) of the sialic residue to the galactose carbon 3 or 6, by α2,3-STs and α2,6-STs respectively. Additionally, sialic acids can be also attached to N-acetylgalactosamine in α2,6 linkage. When several sialic acid residues are linked between them via α2,8 linkage, a linear homopolymer of Sias referred as polysialic acid structure is formed [161,167].

In humans there are six genes coding for α2,3-STs that bind sialic acid into the galactose of type-1, 2 or type-3 (Galβ1,3GalNAc) structures in glycoproteins or glycolipids in α2,3 linkage (ST3GAL1, ST3GAL2, ST3GAL3, ST3GAL4, ST3GAL5 and ST3GAL6). In N-glycans α2,3-sialylation is catalyzed by the enzymes ST3Gal III, ST3Gal IV and ST3Gal

VI [183] being ST3GAL3 and 4 genes broadly expressed in mammals. The addition of α2,3 sialic acid to Gal inhibits the action of other enzymes, including α1,2-FucTs, α1,3-GalT, GlcNAcTs, and GalNAcTs, which compete with terminal α2,3-sialyltransferases [161].

There are two α2,6-STs genes (ST6GAL1 and ST6GAL2) that codify for the sialyltransferases that transfer sialic acid to Gal in α2,6 linkage. Their products are typically found on N-glycoproteins and to a lesser extent, on O-glycoproteins, glycolipids and free oligosaccharides. Furthermore, other 6 STs genes that link sialic acid in α2,6 to GalNAc (from ST6GALNAC1 to ST6GALNAC6) have been described [161].

The overall sialic acid content on glycoconjugates depends on sialyltransferases' activity, but also on enzymes that regulate the synthesis of the sialic acid nucleotide sugar donor, the adequate substrate colocalization in Golgi and lastly through the enzymatic activity of sialidases or neuraminidases that cleave sialic acid residues [179,184].

Sialylation of glycans occurs during the late stages of glycan maturation and capping. As terminal event, sialylated caps usually result in exposed locations conferring negative charge at physiological pH values and hydrophilicity to the glycan [120,185]. Those exposed terminal sialic acids upon glycans, also contribute to the half-life of circulating plasma glycoproteins by covering terminal galactose residues preventing in this way a faster clearing from serum through hepatocyte asialoglycoprotein receptors [161,167,186]. Sialylation has many other roles, including the modulation of cellular recognition, cell signaling, cell adhesion, neural signaling and plasticity, glomerular filtration or blood cell charge repulsion and constitutes a binding site for several human pathogens and toxins [167,187–193]. On chapter 4.8. (The role of sialylated determinants pumping cancer) the role of sialic acid in cancer malignancy will be reviewed.

4.6. The Lewis blood group family

Type-1 and 2 structures act as a substrate for further glcosyltransferases' modifications, such as the addition of fucose residues by fucosyltransferases (FucT) and the transfer of sialic acid by sialytransferases (STs). The sialic acid transfer in α2,3 linkage over galactose, over Gal-GlcNAc junction structures, and the addition of fucose residues in α1,3/α1,4 linkage to GlcNAc will yield to terminal glycan chains known as Lewis determinants.

Type-1 and type-2 Lewis determinants are generated from type-1 and type-2 glycans correspondingly and have a fucose in α1,4 or in α1,3 linkage to the internal GlcNAc, giving rise to Le^A and Le^X determinants, respectively. They can be found both in N-glycans, O-glycans or glycosphingolipids [194]. Some members of the Lewis blood group antigens accomplish essential functions as selectin ligands on glycoproteins [195] which promotes extravasation and tumor-cell metastasis. Thus, their biosynthesis and implication in malignancy will be reviewed in the present work. Specifically, we are focused on the sialyl Lewis A (SLe^A) Neu5Acα2,3Galβ1,3(Fucα1,4)GlcNAc and sialyl Lewis X (SLe^X) Neu5Acα2,3Galβ1,4(Fucα1,3)GlcNAc antigens for their potential role in tumorigenesis in gastric cancers.

The sialyl Lewis A biosynthetic pathway, shown in **figure 12**, starts upon precursor type-1 chains, where ST3Gal-sialyltransferases ST3Gal III and with lower catalytic efficiency ST3Gal IV (since it prefers type-2 chains), may transfer sialic acid in α2,3 linkage to galactose to form the structure known as Dupan-2 antigen. Then, the subsequent addition of α1,4 fucose to GlcNAc by fucosyltransferases FucT-III and FucT-V will form the sialyl Lewis A antigen [196].

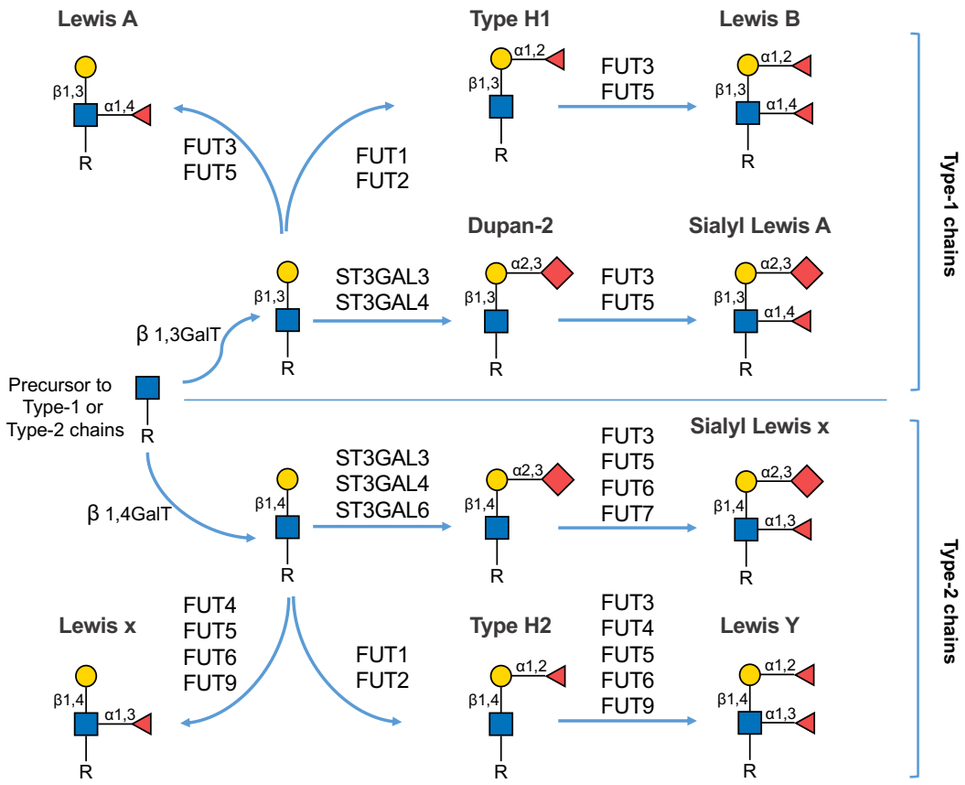

Figure 12 | Synthesis of Sialyl Lewis antigens: Different Lewis biosynthesis paths on type-1 and type-2 glycan chains and genes implicated. Data for the figure was extracted from: [161,197].

Alternatively, on type-2 chains, three α2,3-sialyltransferases enzymes (ST3Gal III, ST3Gal IV and ST3Gal VI) are capable of transferring α2,3 sialic acid to terminal galactose [198–200]. In humans, it has been reported that ST3Gal IV but not ST3Gal III or ST3Gal VI, is the major sialyltransferase regulating the biosynthesis of E-, P- and L-selectin ligands in leukocytes [201]. In other tissues like colon it was postulated that ST3Gal IV was the main responsible for sialyl Lewis antigens owing to the very low expression of ST3GAL3 [202] and that ST3GAL III preferentially acts on type-1 chain and has lower catalytic efficiency on type-2 chains [183]. However, our group demonstrated that in pancreatic cancer cell lines, both ST3GAL3 and ST3GAL4 genes are able to participate in SLe^X biosynthesis [203,204]. In the synthesis of the SLe^X antigen, the subsequent step after sialic acid linkage includes the sequential transfer by α1,3-fucosyltransferases (mainly, FucT-III [205], FucT-V [206], FucT-VI [207] and FucT-VII [208] that will fucosylate GlcNAc in α1,3 linkage.

Lately, it has been shown that FucT-VI and FucT-VII have the highest potency in the SLe^X biosynthesis [198,209]. Regarding FucT-IV it has been reported that yields to SLe^X

synthesis in PC-3 prostate cancer cells [210], but its contribution seems to be very limited and does not generate SLe^X on glycolipids in human mesenchymal stem cells [198]. Also, it is important to point out that there is no alternative route for SLe^X biosynthesis from Le^X since any mammalian sialyltransferase is able to link sialic acid in α2,3 in Le^X to synthetize SLe^X [198].

4.7. Altered glycosylation in cancer

In recent years, anomalous glycosylation remains in the scientific spotlight since it is a frequent hallmark of cancer. Glycans expressed in several types of glycoconjugates are known to change during cellular transformation and progression. The main modifications involve changes in core structures in O-GalNAc and N-glycans, and those changes represent key steps during cancer cell signaling and tumor formation, progression and tumor cell disassociation and metastasis [211,212]. Glycan alterations in cancer cells display a wide range of alterations both in tumor cell surface, secreted glycoproteins and host elements [213]. **Figure 13** portrays the changes that are commonly associated with cancer transformation, which are also present in PDA.

Among those changes, alterations in branching of N-glycans are common. Usually they are attributed to MGAT5 increased activity, whose expression is regulated by RAS-MAPK signaling. Along with altered branching, during carcinogenesis the expression of certain glycans, with overexpression of sialylation and fucosylation is frequently altered. These changes produce an increase in selectin ligands and blood antigens groups. In Gastric cancer truncated O-GalNAc glycans or incomplete glycans are commonly found [155,161,212,214–216].

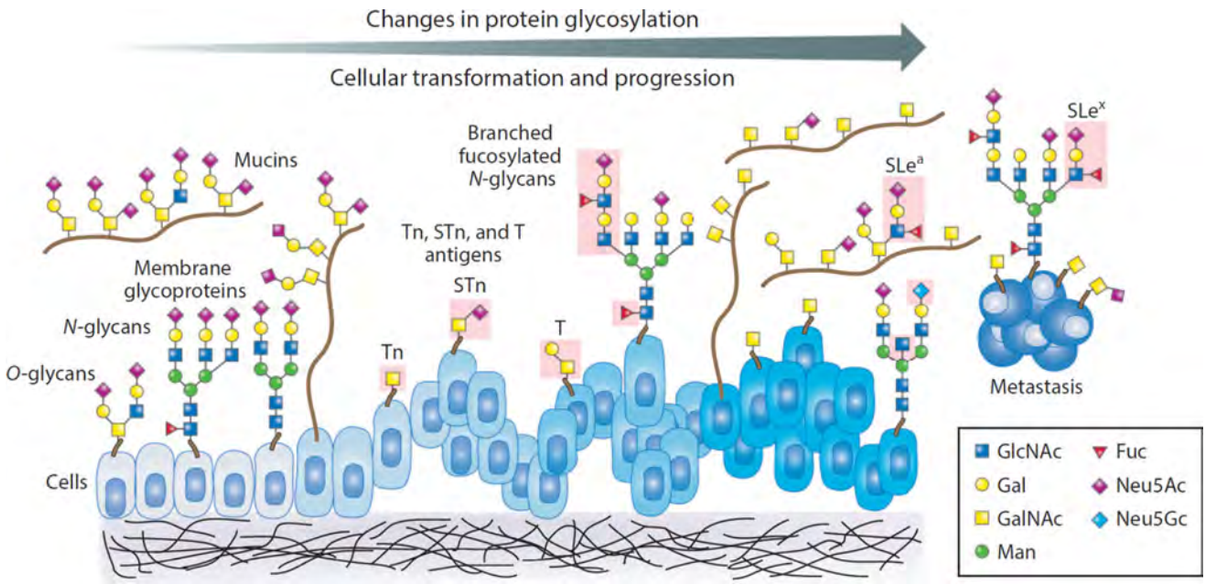

Figure 13 | Altered glycosylation during cellular transformation. Different types of changes in glycosylation commonly associated to carcinoma transformation and progression are shown in pink-boxed areas. Extracted from: [212].

Those frequent modifications in cancer are labeled as TACAs (tumor-associated carbohydrate antigens). TACAs are distinctly overexpressed in large number of tumors and are considered biomarkers for cancer detection since they are useful to discriminate between tumor cells from normal ones. The presence or TACAs is the result from the combined action of glycosyltransferases and glycosidases which are abnormally expressed in tumor cells [217]. Since TACAs are expressed on glycoproteins and glycolipids that regulate key steps and main pathways in cellular biology, their expression can mediate important signaling effects, enhancing several tumor features like cell migration or metastasis [218].

TACAs antigens in PDA include the mucin related Thomsen-nouvelle antigen (Tn) that is detected in up to 90% of PDAs but it is not expressed in normal pancreas [219,220]. Another TACAs antigens include its sialylated epitope, sialyl Tn (STn), Thomsen-Friedenreich (TF) antigens and blood group determinants such as Lewis-related Lewis Y and Lewis X and its sialylated derivative sialyl Lewis X (SLe^X), Globo H, gangliosides, and polysialic acid among others [211,214,217,221]. TACAs nowadays constitute an attractive target for immunotherapy to fight against cancer [92,217,222] directly by using antibodies [223] or with antitumor vaccines [221].

Nevertheless, the role of glycans in cancer often remains insufficiently understood since the mechanisms that produce altered glycosylation are complex and the field of glycobiology is relatively young. However, recent studies in the field have correlated epigenetic changes, gene mutations, altered expression of glycosyltransferase and chaperone genes and mislocation of glycosyltransferases or glycosidases with altered glycosylation [211,212,224–227]. Additionally, changes in glycans have been associated with the promotion of the different hallmarks of cancer proposed by Douglas Hanahan [228] (**figure 14**).

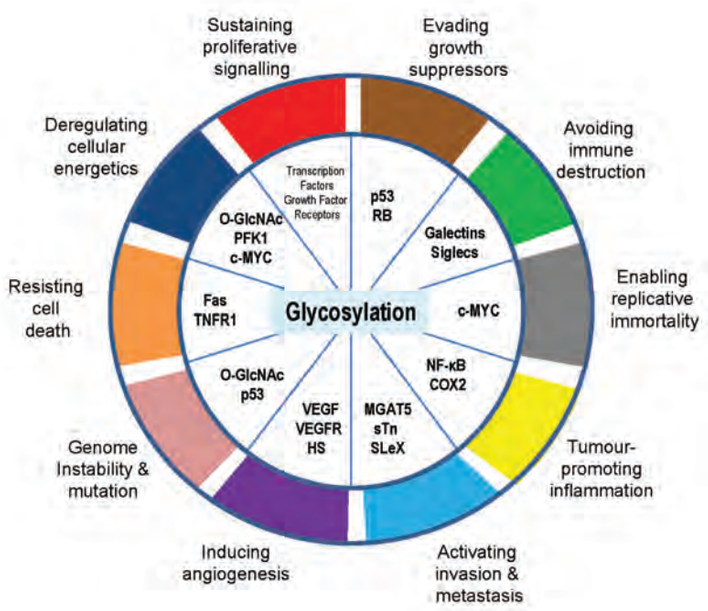

Figure 14 | Hallmarks of glycosylation in cancer. Altered glycosylation is involved in the acquisition of all cancer hallmark capabilities. Extracted from: [211].

Importantly, those changes in glycosylation could be exploited as novel diagnostic tumor markers for its common presence upon cancer development as well as new targets to fight against it.

Specifically, the next last chapter of glycosylation will be focused on the altered sialylation and sialylated Lewis antigens since they are key in invasion and metastasis as shown in blue upon **figure 14**.

4.8. The role of sialylated determinants pumping cancer

Cancer cells often enhance sialylation in glycans on their surface generating many tumor-associated oligosaccharide antigens, which correlate with malignancy, invasion and cell survival in cancer. [229–231]. The increased expression of sialic acid on the glycoconjugates imparts a negative charge to the glycan chain. This altered negative charge on the cancer cells might enhance cell-cell detachment, and cell-extracellular matrix detachment through charge repulsion promoting the invasion to other tissues and metastasis [120,213,232–237].

The increase in α2,6 and α2,3 linked SA resulting from the altered expression of the sialyltransferases ST6Gal and ST3Gal respectively and from the aberrant activity of sialidases is a hallmark of cancer [179,199,211,238–240]. Levels of sialyltransferases in cancer patients are often increased and can be found even in plasma and they usually correlate with poor prognosis. For this reason, altered sialylation has been targeted, both in murine models and *in vitro*, as therapeutic target to fight against tumor growth and metastasis by inhibition of sialyltransferases activity with pharmacologic compounds experiments [241–246].

Probably the most common example of how upregulation of STs can modulate pathways intrinsic to tumor cell biology in many cancer variants is the upregulation of ST6GAL1 gene. ST6GAL1 increases α2,6 linked sialic acid, which blocks galectin proapoptotic binding enhancing tumor survival [231], but also can promote tumor growth and metastases [247]. Other common examples of the role of altered sialic acid expression in cancer, includes polysialylation expression that can enhance the spread of invasion and correlates with poor prognosis in several cancer types [213].

α2,6 linked sialic acid expression and both ST3GAL3 and ST3GAL4 sialyltransferases genes are often deregulated in many kinds of cancer [248–250] such as in gastric carcinomas [251–254] and PDA [204]. In the gastric cancer cell line MKN45, the over expression of α2,3-STs, ST3GAL3 and ST3GAL4, a led to de novo synthesis of SLe^X antigen [253], and the overexpression of ST3GAL4, enhanced the invasive phenotype through SLe^X synthesis, c-Met pathway activation [254] and activation of RON receptor

tyrosine kinase [255]. Previous work from our research group revealed that both ST3GAL3 and ST3GAL4 mRNA levels were increased in pancreatic adenocarcinoma tissues when compared to pancreatic control tissues in about four and two-fold for ST3GAL4 and ST3GAL3 respectively [204,256]. Additional research proved that ST3GAL3 and 4 overexpressing PDA cell lines showed a heterogeneous increase in SLe^X, enhanced E-selectin adhesion and there was a correlation between higher α2,3-SA with increased migration capability. Furthermore, when injected into athymic nude mice, the α2,3-ST overexpressing PDA cell lines showed increased metastasis formation and a decreased mice survival, compared with their corresponding controls, implying the potential role of α2,3-STs in malignant behavior of PDA cells [203,204,257,258].

4.9.SLe^X expression in cancer

As previously presented, upregulation of glycosyltransferases and expression of SLe^A and SLe^X is present in most cancers. The main relevance of sialyl Lewis antigens in cancer resides in its ability to bind selectins.

Selectins are vascular cell adhesion molecules (VCAMs) that belong to the C-type lectins family, expressed by endothelial cells and bone-marrow-derived cells [167,259]. There are three main different selectins: L-selectin that is expressed mainly on leukocytes, P-selectin expressed on platelets and endothelial cells and E-selectin that is expressed on activated endothelia but also in quiescent, non-inflamed, skin micro vessels and in parts of the bone marrow microvasculature [167,260–262].

The main physiological role of E-selectin is to recruit leukocytes to activated endothelium, promoting the transmigration or extravasation of leukocytes through the inflammation sites. However, the overexpression of selectin ligand expression (SLe^X and SLe^A) upon tumor cell membrane glycoconjugates is used by those tumor cells, to enable the binding between their Lewis antigens and the E-selectin expressed in activated endothelia in presence of Ca^{2+}. As a result, a deceleration in the flowing cells onto the endothelial surface happens, and tumor cells may then create stronger interactions with molecules

such as integrins and hyaluronic acid, promoting cell arrestment and intravasation [198,263]. In circulating cancer cells, SLe^X interaction with selectin also plays a main role in forming tumor emboli of platelets or immune cells with cancer cells propagating metastases [155,231,264].

Consequently, overexpression of those glycoconjugates leads to shorter survival rates of cancer patients and plays an important role in tumor cell invasion in blood microvessels, extravasation and metastatic dissemination [197,265–268] in pancreas, breast, colon, stomach, kidney and lung cancers [194,214,235,264,269–273]. For this reason, targeting SLe^X through inhibition approaches have been validated as a tool to reduce metastases to lung in murine models of colon cancer for example [274] and to reduce proliferation in hepatocarcinoma cells [275]. Lastly, in adenocarcinoma cells, expression of sialylated Lewis antigens confers higher metastatic potential than the same cells where their expression have been inhibited [276,277].

5. Microfluidics and its applications in biomedical research

The term microfluidics refers to those techniques that allow investigators the handling of small volume of liquids for the miniaturization of biomedical science and fundamental research. A microfluidic chip is a set of micrometer-sized channels, molded into diverse materials that allow the formation of microstructures connected together in order to achieve the desired features [278].

Microfluidics offers much potential since this science has an interdisciplinary nature that can combine diverse fields of biology, chemistry, physics, and engineering [279]. Thus, microfluidics devices and their great flexibility in terms of design and application, have the ability to replace and improve traditional macroscale approaches. Furthermore, microfluidics technologies have several advantages and unique properties that have made them a noticeable area of science to study new forms of *in vitro* experiments in systems that allow for greater control and versatility in the design and performance of the experiment, mimicking better *in vivo* approaches. Among those advantages several properties standout such as the improving in the precision of experiments thanks to accurate control of fluids and microstructures patterning formation. Others advantages include the rapid sample processing, the ability to generate spatio-temporal gradients and the reduction in instrument and reagent usage that allows the running of multiple analyses simultaneously because of this small size that also facilitates its monitoring in real time.

The simplest microfluidic device consists in micro-channels molded in a polymer that is bonded to a flat surface (such as a glass slide). Nowadays, polydimethylsiloxane (PDMS) is the most widely adopted polymer used for molding and fabrication of microfluidic devices. The use of PDMS have lots of advantages; it is a biocompatible and optically transparent material, which also allows the gas exchange. Additionally, PDMS is a deformable and inexpensive elastomer that can be easily bond to glass and plastic surfaces [278].

Microfluidics technology has found many applications in the biomedical research field in the last decade, encompassing a wide range of biomedical applications such as biomedical diagnostics, nucleic acid detection, immunodiagnostics, organoid and

spheroid culture on chips, and drug screening of tissue biopsy samples among others. [280,281].

In cell mechanobiology, research upon microfluidic devices and its versatility, has allowed the design of micro-channels with desired measures (closer to those found in physiological conditions) for better understanding the mechanisms behind cell migrationand how cancer cells migrate *in vivo* within three-dimension extracellular matrices.

In vivo, metastasizing cells have to migrate to spread to tissues and organs beyond the primary tumor. Those metastasizing cells will migrate through different extratumor microenvironments but often they have to migrate through pores of the extracellular matrix and 3D longitudinal tracks originated by ECM degradation (with secreted metalloproteinases) or channels formed between the connective tissue and the basement membrane of muscle, epithelium, nerves and along blood vessels or ECM fibrils [282,283] (**figure 15**).

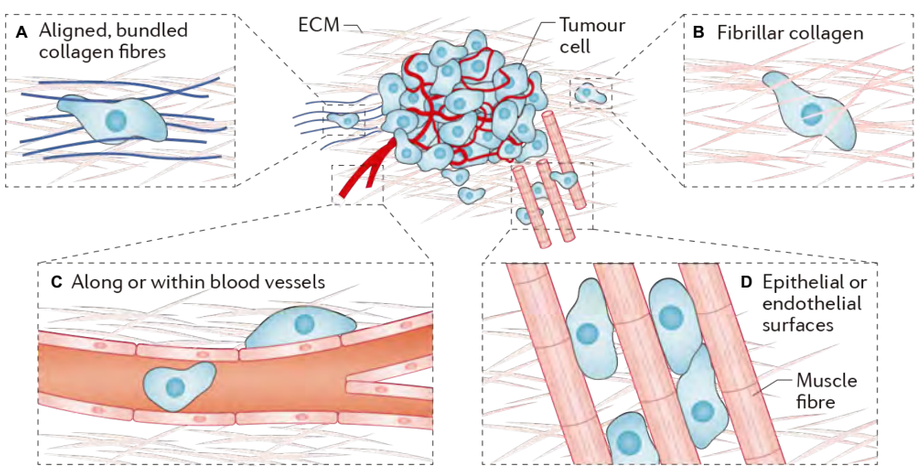

Figure 15 | Extratumor microenvironments for confined migration *in vivo*. A) Alignment and bundling of collagen fibers at the tumor periphery provide cues for directed migration. B) Cells may also migrate through unbundled extracellular matrices (ECMs), such as fibrillar collagen, which present pore-like migration spaces. C) Microtracks also occur both intravascularly and perivascularly. D) Cells can also migrate between epithelial or endothelial surfaces, such as those found between muscle and nerve fibers. Extracted from: [284].

The cross-sectional area of these *in vivo* paths ranges from 10 to 300 μm^2 [285]. Consequently, metastasizing cancer cells *in vivo* experience varying degrees of physical confinement. Microfluidics devices based on different size microchannels integrated in

only one chip, such as the one describer later on (see material and methods 23. PDMS-based microchannel migration assay) will allow us to study cell migration through cell-tracking in diverse degrees of confinement: from unconfined migration, similar to conventional 2D migration (when the channel width is larger than the cell diameter), to confined migration (when the channel width, is smaller than the cell diameter).

II. Objectives

This thesis has been dedicated to the study of aberrant glycosylation in pancreatic ductal adenocarcinoma cell lines and tissue samples from PDA patients. Specifically, it is focused on the tumor associated carbohydrate structure sialyl Lewis X (SLe^X), which is found in PDA. SLe^X expression is relevant not only in cancer migration events and metastases but also as a potential tool to find novel tumor biomarkers. Under these premises, this work has two different main objectives:

1. **Identification of glycoproteins carrying SLe^X from PDA tissues by glycoproteomic techniques, followed by the analysis of their expression in PDA samples to decipher their role in PDA and their potential use as novel PDA biomarkers.**

   .

2. **Assessment of the reduction of α2,3-sialyltransferases ST3GAL3 and ST3GAL4 expression in the decrease of cell SLe^X content and evaluation of its impact in the migratory and invasive phenotype of PDA cells.**

   For that, the following subobjectives will be pursued:

   To knock-down ST3GAL3 and ST3GAL4 genes in PDA cell lines by using short hairpin RNAs (shRNAs).

   To characterize the silenced cells and their changes in cell glycoconjugates to define the impact of those glycosylation changes in cell migration, invasion and adhesion to E-selectin by using *in vitro* and microfluidic assays.

III. Material and methods

1. Cell lines

Human pancreatic cancer cell lines Capan-1, Capan-2, HPAF-II, Panc 10.05 and SW 1990 were purchased from the American Type Culture Collection (ATCC). AsPC-1 and BxPC-3 were obtained from the cancer cell repository at Hospital del Mar Medical Research Institute (IMIM) Barcelona, Spain. Cells were cultured at 37°C in a humidified atmosphere of 5% CO_2. HPAF-II were cultured in Eagle's Minimum Essential Medium (EMEM) from Lonza, supplemented with 10% heat-inactivated fetal bovine serum (FBS, Gibco), 100 U/mL penicillin, 100 U/mL streptomycin and 2 mM L-glutamine (Gibco). Panc 10.05 cells were grown in Roswell Park Memorial Institute Medium (RPMI-1640) from Lonza, with FBS to a final concentration of 15% and 10 U/mL of human recombinant insulin. AsPC-1, BxPC-3, Capan-1, Capan-2 and SW1990 cells were routinely grown in Dulbecco's modified Eagle's Medium (DMEM) from Gibco, supplemented with 10% FBS, (20% FBS for Capan-1 cells), 100 U/mL penicillin, 100 U/mL streptomycin and 2 mM L-glutamine. Cells were propagated in adherent culture according to conventional protocols. Routine tests were performed to confirm the absence of mycoplasma. For the selection of the cells that contained the vector pLKO.1-puro, a dose response curve for antibiotic selection (kill curve) was performed. Resistant cells were selected by adding puromycin dihydrochloride (Sigma) at a final concentration of 1.5 µg/mL for BxPC-3 and 1 µg/mL for Capan-1 cells.

2. Pancreatic tissue samples

Pancreatic tissues from patients undergoing surgical resection or paraffined archived pancreatic tissues, were provided by Hospital Dr. Josep Trueta (Girona, Spain) following the standard operating procedures of its Ethics Committee. The histopathologic features of the resected specimens were confirmed by biopsy or image examination by the digestive and pathology units and classified according to the Tumour Node Metastasis Classification of Malignant Tumours of the International Union Against Cancer (UICC) 8th edition.

A small piece of the resected pancreatic tissues was immediately frozen in liquid nitrogen and kept at -80ºC until their use for protein extraction. Pancreatic tissue samples are portrayed in **Table 3**.

Table 3 | Pancreatic tissue samples.

Healthy Control (HC) from donors with non-pancreatic disorders.

Sample	Stage	Gender	Age	Age average	±SD	Range
HC1	-	Female	68	65.33	14.19	50-78
HC2	-	Male	50			
HC3	-	Female	78			

Non-Tumor (NT) from PDA patients

Sample	Stage	Gender	Age	Age average	±SD	Range
NT1	-	Male	64	68.33	7.51	64-77
NT2	-	Female	64			
NT3	-	Male	77			

PDA patients

Sample	Stage	Gender	Age	Age average	±SD	Range
T1	IIB	Male	72	67.04	8.04	51-79
T2	IIB	Female	64			
T3	III	Male	64			
T4	III	Male	52			
T5	IIB	Female	68			
T6	IIB	Female	69			
T7	IIB	Male	61			
T8	IIB	Male	79			
T9	IIA	Male	70			
T10	IIA	Female	64			
T11	IIA	Female	78			
T12	IV	Male	76			
T13	IIB	Male	58			
T14	IIA	Male	70			
T15	IV	Female	59			
T16	IIB	Male	76			
T17	IIB	Female	63			
T18	IIB	Male	77			
T19	IIA	Female	75			
T20	IIB	Female	51			
T21	III	Female	77			
T22	IIA	Male	65			
T23	IIB	Female	66			
T24	T3Nx	Male	65			
T25	IIB	Male	57			

Samples corresponded to: three control patients with non-pancreatic-related disorders (two females and one male, age range 50-78), three non-tumor pancreas from three PDA patients (1 female and 2 males age range 64-77) and twenty-five pancreatic ductal adenocarcinoma samples (11 females and 14 males; age range 51–79). The twenty-five PDA patients included nineteen of non-advanced stages, stage IB (T2N0M0), stage IIA (T3N0M0) and stage IIB (T1-2-3N1M0), five advanced stages, stage III (T4NxM0 and TxN2M0) and stage IV (TxNxM1) and one T3Nx.

3. **Cell and tissue protein lysates**

3.1. Cell lysates

Pancreatic cells were seeded in 6-well plates until they reached a confluence of about 75%. Then, cells were washed thoroughly 3 times with cold phosphate buffered saline (PBS, Lonza) and total protein extracts were obtained by lysing the cells after 10 minutes incubation on ice with cold RIPA buffer (50 mM Tris-HCl pH 7.4, 0.1% NP-40 (v/v), 0.5% sodium deoxycholate (w/v), 0.1% SDS (w/v), 150 mM NaCl, 2 mM EDTA, 50 mM sodium fluoride, 1 mM PMSF, 0.2 mM sodium orthovanadate and complete™ ULTRA tablets protease inhibitors cocktail (Roche)). Cells were then removed by using a cell scraper, and then the cell suspension was mechanically lysed with a 25-gauge needle. Cell lysates were centrifuged at 14000 g for 10 min at 4ºC, and supernatants were collected for their subsequent quantification and storage at -20ºC (see methods section 5. Protein quantification).

3.2. Tissue lysates

Frozen tissue samples were cut into small pieces under an aluminum foil surface. The surface was previously cleaned with diethyl pyrocarbonate (DEPC)-Treated water and RNaseZap a RNase Decontamination Solution (Thermo Fisher Scientific) in order to preserve RNA integrity of the sample. Tissue pieces were then inserted in 2 mL tubes of Lysing Matrix D (MP Biomedicals). This matrix supports a maximum amount of sample of

400 mg and it is composed of 1.4 mm ceramic beads. 700 µL of lysis buffer were added to the lysing tube. Lysis buffer is composed of 7 M urea, 2 M thiourea, 500 mM Tris-HCl pH 8.5, 4% CHAPS (w/v) and complete™ ULTRA tablets protease inhibitors cocktail (Roche). For N-deglycosylation experiments (see methods section 11.) tissue samples were lysed in modified RIPA buffer (50 mM Tris-HCl pH 7.4, 0.1% NP-40 (v/v), 150 mM NaCl, 2 mM EDTA, 50 mM sodium fluoride, 1 mM PMSF, 0.2 mM sodium orthovanadate and complete™ ULTRA tablets protease inhibitors cocktail). Lysing tubes were loaded in a FastPrep24 homogenizer (MP Biomedicals) and tissues were lysed three times for 40 seconds at 6 m/s velocity, leaving the sample on ice 5 min between pulses. After homogenizing the samples, tubes were centrifuged at 14000 g for 5 min at 4ºC. and the supernatant was then transferred to a 1.5 mL microtube. Samples were centrifuged twice for 15 min at 14000 g at 4ºC and supernatant was then aliquoted for its subsequent quantification and storage at -20ºC.

4. Cell conditioned media

Human pancreatic cancer cells: AsPC-1, BxPC-3, Capan-1, Capan-2, HPAF-II, Panc 10.05 and SW 1990 were cultured in 125 cm^2 flasks with their corresponding complete media. Once cells reached 80% confluence, they were thoroughly washed 3 times with 20 mL of PBS and left with 20-30 mL of serum-free media. After 48 hours, media were collected on ice in 50 mL centrifuge tubes. The media were then filtered with a 25 mm diameter sterile syringe filter of polyethersulfone membrane with a 0.22 µm pore size (Pall). Filtered conditioned media were transferred and concentrated by centrifugation with Amicon® Ultra-15 centrifugal filters (10K). Previous to media concentration, centrifugal filters were passivated with 5% Brij-35 overnight and then, they were washed by rinsing with water 3-4 times and by centrifugation with 10 mL of water for 10 min at 6500 rpm. After washing the filters, conditioned media were concentrated 40 min at 4ºC until a final volume between 300 and 400 µL. Finally, total protein concentration was determined.

5. Protein quantification

The protein concentration of cell, tissue lysates and conditioned media was quantified by using the QuickStartTM Bradford Protein Assay (Bio-Rad) in 96 well plates (Corning), using bovine serum albumin (BSA) standard (Bio-Rad) following the manufacturer's protocol. The standard curve was diluted with the same buffer concentration present in the diluted samples. Triplicates of each sample were performed. Finally, absorbance was read at 595 nm in an automated microplate reader Synergy 4 (BioTek).

6. Two-dimensional electrophoresis (2DE)

Active in-gel rehydration was performed with Immobiline® dry strips pH: 3–10 L, 18 cm (GE Healthcare) at 50 V overnight at 20ºC, using 200 µg of tissue lysates diluted in 340 µL of 2DE rehydration buffer containing: 7 M urea, 2 M thiourea, 4% CHAPS (w/v), 65 mM DTT, 1.5% IPG Buffer pH: 3-10 (v/v) and 0.005% bromophenol blue (v/v). First dimension was carried out on a Protean isoelectric focusing (IEF) cell system (Bio-Rad) with a default current limited to 50 µA to prevent overheating of the IPG strips and a temperature established at 20ºC. (see detailed method setup below in **table 4**).

Table 4 | Program method for Protean IEF cell (Bio-Rad).

STEP	VOLTAGE	VOLTAGE SLOPE	TIME (HRS:MIN) or V.HOURS
1	0-500	LINEAR RAMP	00:30
2	500	RAPID RAMP	01:00
3	500-2000	LINEAR RAMP	00:30
4	2000	RAPID RAMP	01:00
5	2000-5000	LINEAR RAMP	00:30
6	5000	RAPID RAMP	01:00
7	5000-8000	LINEAR RAMP	00:30
8	8000	RAPID RAMP	VH: 85.000
9	500	RAPID RAMP	∞

After IEF, strips were cut to appropriate size and incubated for 15 min in equilibration buffer 1: 6 M urea, 2% SDS (w/v), 30% glycerol (v/v), 50 mM Tris-HCl pH 8.8 and 65 mM DTT, and additionally in 15 min in equilibration buffer 2: 6M urea, 2% SDS (w/v), 30% glycerol (v/v), 50mM Tris-HCl pH 8.8 and 135 mM IAA. Second-dimension was carried out on polyacrylamide gels (4–15% Criterion™ Tris-HCl Protein gel for 11.8 cm strips (Bio-Rad) or 10% Mini-Protean® polyacrylamide homemade Gel for 7.7 cm strips). Following electrophoresis, 2DE gels were stained by Coomassie blue, silver staining or transferred onto a PVDF membrane (Millipore) for its subsequent immunodetection (see methods section 8. Western blot). The isoelectric point (pI) assignment of each individual strip was calculated by transforming distance into a pI value according to the relation supplied by the manufacturer.

7. SDS-PAGE

Before electrophoresis, concentrated 4x Laemmli Buffer within 2-mercaptoethanol (5% v/v) was added to samples (diluted ¼). Then, samples were heated to 95ºC for 5 min. For carbohydrate antigens analysis: 50 µg for cell line lysates and conditioned media and 20 µg for tissue lysates were electrophoresed into acrylamide gels (5% for staking and 8% for resolving). For MFAP4 analysis: 10 µg for tissue lysates were loaded into acrylamide gels (5% for staking and 12% for resolving). PageRuler prestained protein ladder (Thermo Fisher Scientific) was added to one of the sample lanes. Samples were electrophoresed in Mini-Protean Tetra Cell (Bio-Rad) at 120 V and then transferred onto a PVDF membrane or Coomassie or silver stained.

8. Western blot

Western blot (WB) analysis was performed as previously described [286]. Briefly, polyacrylamide gels were transferred into a PVDF membranes (Immobilon-P® membrane 0.45 µm, Millipore) at 30 V at 4ºC overnight in transfer buffer (10 mM $NaHCO_3$, 3 mM Na_2CO_3, and 20% methanol) or at 100 V for 4 hours at 4ºC in Tris-glycine transfer buffer (191 mM glycine, 24 mM Tris and 20% methanol). Transferred proteins on the

membranes were then washed with Tris Buffered Saline (10 mM Tris-HCl pH 7.5, 100 mM NaCl) with 0.1% Tween-20 (TBST) and blocked with their corresponding blocking solution. After incubation, membranes were washed and incubated with their respectively primary antibody or lectin listed below in **table 5**. Lectin Buffer composition: 100 mM Tris-HCl pH 7.4, 150 mM NaCl, 1 mM $CaCl_2$, 1 mM $MgCl_2$.

Table 5 | Primary antibodies or lectins used for immunoblotting and usage conditions.

Antibody - Lectin	Host	Dilution	Supplier	Blocking solution
Sialyl Lewis X (Anti-Human CD15s) clone CSLEX1	Mouse	1/70 in TBST, 1% BSA	BD biosciences	TBST, 3% BSA
Sialyl Lewis A (57/27 Anti-CA 19-9)	Mouse	1/2	De Bolós 1995 [287]	TBST, 1% BSA
MFAP4 (A-9)	Mouse	1/500 in TBST, 3% milk	Santa Cruz Biotechnology	TBST, 5% milk
MFAP4	Rabbit	1/1000 in TBST, 3% milk	Invitrogen	TBST, 5% milk
α-Tubulin (B-7)	Mouse	1/500 in TBST, 3% BSA	Santa Cruz Biotechnology	TBST, 5% BSA
Biotinylated *Sambucus Nigra Agglutinin* (SNA)	-	1/1000 in lectin buffer	Vector Laboratories	Lectin Buffer, 2% PVP
Biotinylated Maackia Amurensis *Agglutinin* II (MAA II)	-	1/500 in lectin buffer	Vector Laboratories	Lectin Buffer, 2% PVP

Membranes were washed and incubated for 1 hour at room temperature (RT) with the following peroxidase-conjugated secondary antibodies or biotin-binding detection reagent (**Table 6**).

Table 6 | peroxidase-conjugated detection reagents and usage conditions.

Secondary reagent	Host	Dilution	Supplier
Peroxidase-Conjugated Anti-mouse (IgG+IgM)	Goat	1/40000 in TBST, 0.5% BSA	Jackson immune Research
Peroxidase-Conjugate Anti-mouse IgG	Goat	1/10000 in TBST, 3% milk	Merck-Millipore

Peroxidase-Conjugate Anti-rabbit IgG	Goat	1/40000 in TBST, 3% milk	Dako
Streptavidin-HRP Conjugate	-	1/100000 in TBST, 1% BSA	GE Healthcare

For protein band detection: After washing, membranes were incubated with tempered immobilon western horseradish peroxidase (HRP) substrate (Millipore) and images were captured using the imaging system Fluorochem SP (AlphaInnotech) under non-saturating conditions.

9. Stripping

In order to corroborate the presence of SLe^X over MFAP4, selected membranes were treated with Restore™ Western Blot Stripping Buffer (Thermo Fisher Scientific) previously to MFAP4 immunodetection. Stripping protocol was also used to reblot the membranes with an antibody against a constitutive protein, which was used as a protein loading control. Briefly: For dry PVDF membranes, they were submerged in methanol for 5 sec and after that, membranes were washed thoroughly with distilled water and two more washes with TBS solution for 5 min were performed. 20 mL of Restore™ western blot stripping buffer for 2D membranes and 10 mL for regular ones was added with shacking for 10 min at RT and then for 20 more min at 37ºC. Before blocking again, membranes were washed twice for 10 min with TBS and twice for 5 min with TBST.

10. Mass spectrometry analysis

Specific proteins from PDA patients that contained SLe^X positive spots from immunodetection were identified in their corresponding Coomassie-blue stained gel (run in parallel) by mass spectrometry (MS). Different gel-spots of interest were then excised and in-gel digested with trypsin. Digested peptides were extracted and analyzed in MALDI-TOF UltrafleXtreme (Bruker Daltonics) mass spectrometer. Mass spectrometry analyses were carried out in SePBioEs, the Proteomics facility from Universitat Autònoma de Barcelona (UAB).

11. N-deglycosylation

10 µg of total protein from RIPA tissue lysates were denatured by incubation in presence of 1% SDS (v/v) for 10 min at 70ºC. After denaturation, 1% NP-40 (v/v), 2 units of N-glycosidase F (recombinant N-glycosidase F from Roche. Ref: 11365185001) and 10 mU of sialidase (Neuraminidase from *Arthrobacter ureafaciens*, Roche Ref: 10269611001) were added on phosphate buffer 20 mM pH 7.2 and incubated overnight at 37ºC.

12. Bacterial culturing and purification of pLKO.1-puro vectors

Five different short hairpin RNAs (shRNAs) for each of the gene of interest were purchased from the Broad Institute MISSION® shRNA library (Sigma) against annotated human genes as shRNA bacterial glycerol stock (**Table 7**).

Table 7 | List of shRNA sequences screened for human ST3GAL4 and ST3GAL3 genes.

ST3GAL4	Sequence
shRNA 1	CCGGCCAGCACCAAGAGATTATTTACTCGAGTAAATAATCTCTTGGTGCTGGTTTTT
shRNA 2	CCGGGCCACGGAAGATTAAGCAGAACTCGAGTTCTGCTTAATCTTCCGTGGCTTTTTG
shRNA 3	CCGGCCTGGTAGCTTTCAAGGCAATCTCGAGATTGCCTTGAAAGCTACCAGGTTTTTG
shRNA 4	CCGGGCAATGGACTTCCACTGGATTCTCGAGAATCCAGTGGAAGTCCATTGCTTTTTG
shRNA 5	CCGGCCTGCGGCTTGAGGATTATTTCTCGAGAAATAATCCTCAAGCCGCAGGTTTTTG

ST3GAL3	Sequence
shRNA 6	CCGGTTTCGCAAGTGGGCTAGAATCCTCGAGGATTCTAGCCCACTTGCGAAATTTTTG
shRNA 7	CCGGTCGAATCCTCAACCCATATTTCTCGAGAAATATGGGTTGAGGATTCGATTTTTG
shRNA 8	CCGGGAATTGACGACTATGACATTGCTCGAGCAATGTCATAGTCGTCAATTCTTTTTG
shRNA 9	CCGGCGCAGGATTTGGCTATGACATCTCGAGATGTCATAGCCAAATCCTGCGTTTTTG
shRNA 10	CCGGGCCATCTTGTCAGTCACCAAACTCGAGTTTGGTGACTGACAAGATGGCTTTTTG

Bacterial cultures of *E. coli* (Genotype: F- Φ80lacZΔM15 Δ(lacZYA-argF)U169 endA1 recA1 relA1 gyrA96 hsdR17 (rk-, mk+) phoA supE44 thi-1 tonA) within different lentivirus plasmid vectors, pLKO.1-puro were amplified from the glycerol stock for the posterior purification of the shRNAs (DNA plasmids) using the following instructions given by the manufacturer with minor modifications:

75 µL were removed from the glycerol stock under sterile conditions and were placed into a culture tube containing 0.5 mL of Terrific Broth (TB). The culture was incubated for 25 min at 37ºC with shaking (250 rpm). Afterwards incubation, plate streaking was performed using a sterile loop onto a plate containing LB agar with ampicillin (Amp) (100 µg/mL). Plates were incubated in a humidified atmosphere for 15-20 hours at 37ºC. Isolation of a single colony from the plate was performed and it was used as a source of inoculum for downstream applications.

Plasmid purification was performed using a QIAGEN® Plasmid Midi Kit following the manufacturer's protocol with minor modifications. Briefly: Sterile culture tubes containing 4 mL of TB (starter culture) were inoculated from single colonies for 10 hours at 37ºC at 250 rpm. After the incubation, an overnight culture was performed inoculating 200 µL of the started culture in a new fresh Erlenmeyer flask containing 100 mL of TB with Amp at 37ºC and vigorous shaking. After 12-16 hours, bacterial cells were harvested by centrifugation at 6000 g for 15 min at 4ºC. Since we are using a low copy number plasmid, double of the recommend volumes of resuspension, lysis and neutralization buffers were used. Finally, DNA pellet was dissolved in 100 µL of TE buffer and the concentration and purity (ratios 260/280 and 260/230) were analyzed using a Nanodrop™ instrument (ND-1000, Thermo Fisher Scientific). Main features of the pLKO.1-puro vector are represented in **figure 16**. Note that the length of the vector with an shRNA sequence insert is 7086bp.

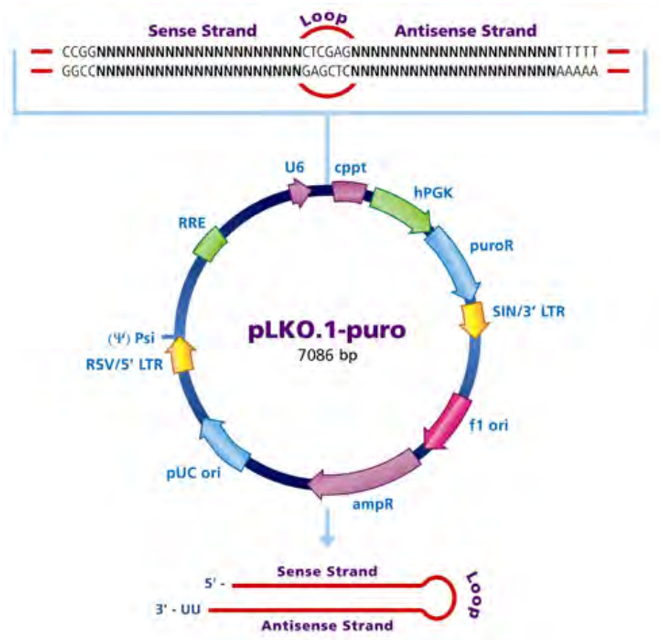

Figure 16 | Representative structure of the pLKO.1-puro plasmid. Extracted from sigma Mission.

13. Lentiviral generation, viral transduction and gene silencing by short hairpin RNA.

For ST3GAL3 and ST3GAL4 downregulation in both BxPC-3 and Capan-1 cell lines, five short hairpin RNA (shRNA) vectors (pLKO.1-puro) for each of the ST3GALs of interest were transduced by lentiviral infection (see sequences in **table 7** in section 12). A scramble vector, which does not target any known mammalian genes (scraRNA) was used as a control (Sigma, SHC002).

13.1. Lentiviral generation and transduction.

Lentivirus generation was performed in biosafety level 2 room: highly confluent HEK-293T/17 cells were transfected in 6-well plates. For transfection, 3 vectors for lentivirus generation (0.6 µg of pMDLg/pRRE, 0.2 µg of pRSV-Rev and 0.2 µg of pVSV-G vector) were mixed with 1 µg of the correspondent ST3GALs pLKO.1-puro vector or a vector which does not target any known mammalian genes (Sigma, SHC002) composed of a scramble non-targeting RNA sequence (shScramble). Vectors were then mixed with 190 µL of sterile 150 mM NaCl and 10 µL of polyethylenimine (PEI) concentrated at 1 mg/mL and incubated 30 min at RT. Then, the mixtures were diluted with 2 mL of DMEM 10% FBS. Media from HEK-293T/17 cells were removed and then, the transfection mixture was added to the cells and incubated at 37ºC, 5% CO_2 overnight. 24 hours after transfection HEK-293T/17 medium was replaced by 2.5 mL of fresh complete media. 48 hours post-transfection the HEK-293T/17 supernatant (with the lentiviral particles on it) was recollected and filtered through 0.45 µm low binding syringe filters (Millipore).

13.2. Viral infection and cell silencing.

Polybrene (final concentration of 8 µg/mL) and complete media until a final volume of 4 mL were added to the filtered media from transfected HEK-293T/17 with the lentiviral particles on it. Then, 2 mL of the mixture were added to each pancreatic cancer cell lines (BxPC-3 and Capan-1) seeded in a 6-well plate at 50% of confluence. 8 hours post-infection, cells were washed and medium lacking virus was added. These steps were performed twice to improve infection efficiency. 48 hours after the first lentivirus infection, selection was done adding puromycin dihydrochloride (Sigma) to the correspondent

complete media. (See cell lines for dose-response curve and antibiotic concentration for the selection). Downregulation of genes of interest 10 days post-infection was confirmed by RT-qPCR.

14. RNA isolation and cDNA synthesis by reverse transcription

Cell RNA extraction was performed using the RNeasy® Mini kit (Qiagen). Cells were seeded in 6-well plates until reach a confluence of about 75%. Then cells were washed thoroughly 3 times with cold PBS (Lonza) and treated on ice with RLT buffer within 2-mercaptoethanol (1:1000) for cell lysis. Afterwards, cells were removed by using a cell scraper, and then the suspension was mechanical lysed with a 25-gauge needle. RNA columns were treated with RNAse-Free DNase I, diluted in RNase-free Buffer RDD (Quiagen) for 15 min at 20–30°C according to the manufacturer's instructions. Concentration and quality assessment (ratios 260/280 and 260/230) of total eluted RNA yield were determined using a Nanodrop™ instrument (ND-1000, Thermo Fisher Scientific). 2 µg of total RNA were reverse transcribed to single-stranded cDNA using a high-capacity cDNA reverse transcription kit (Applied Biosystems) which includes MultiScribe™ Reverse Transcriptase. Conditions were selected according to manufacturer's instruction.

15. Reverse Transcription quantitative PCR (RT-qPCR) analysis

Quantification of gene expression was performed with TaqMan Pre-Designed Gene Expression AssaysTM (Applied Biosystems). Primers used for the evaluation of each glycosyltransferase gene and the housekeeping control references are listed below: ST3GAL3 (Hs00544033_m1), ST3GAL4 (Hs00920871_m1), ST3GAL6 (Hs00196085_m1), FUT3 (Hs01868572_s1), FUT5 (Hs00704908_s1), FUT7 (Hs00237083_m1) and TATA box binding protein (TBP) as housekeeping gene, TBP (Hs99999910_m1). For the PCR mix 1 µL of primer solution per reaction and 10 µL of TaqMan 2X Universal PCR Master Mix (Applied Biosystems) were added. Finally, 90 ng of cDNA template in a final volume of 9 µL (diluted in RNase-DNase-free water) were added to the PCR mix solution. All RT-qPCRs were performed in triplicate, following universal thermocycling parameters recommended by Applied Biosystems. Briefly: FAM

reporter, stage 1: 95ºC for 10 min (1 cycle) and stage 2: 95ºC for 15 s and 60ºC for 1 min (40 clycles). For data collection a 7500 real-time PCR system (Applied Biosystems) was used. Data were collected and analyzed using the 7500 SDS system software version 1.4 (Applied Biosystems). The results were analyzed by the delta-delta Ct method and using the TBP gene as a reference for calculation.

16. Flow cytometry analysis

The characterization of carbohydrate determinants in the cell membranes was performed by indirect immunofluorescence. Cells were trypsinized and counted. Then, $1x10^5$ viable cells were harvested and washed with cold PBS by centrifugation at 2600 rpm for 8 min at 4ºC. The pellet containing washed cells was resuspended in 100 µL of PBS 1% BSA and incubated for 30 min at 4ºC in the presence (or absence, for negative controls) of the corresponding primary antibodies or biotinylated lectins. After the incubation, cells were washed with PBS and incubated for an additional 30 min at 4ºC in the dark with its corresponding diluted secondary antibody. After this time, cells were washed and resuspended in 300 µL of cold PBS 1% BSA and cell fluorescence was acquired by Flow Cytometry. A minimum of $1x10^4$ cells within the gated region were analyzed on a FACSCalibur flow cytometer (BD biosciences). At least three independent assays for each sample were undertaken. No aggregation or loss of viability of the cells was detected after antibody or lectin incubations. All the antibodies and biotinylated lectins for surface labeling were diluted in PBS 1% BSA and are listed below in **table 8** and **9**.

Table 8 | Antibodies and biotinylated lectins for flow cytometry:

Antibody	Host	Dilution	Supplier
Sialyl Lewis X (Anti-Human CD15s)	Mouse	1/10	BD biosciences
Sialyl Lewis A (57/27 Anti-CA 19-9)	Mouse	1/2	De Bolós 1995 [287]
Alexa Fluor™ 488 anti-Mouse IgG (H+L)	Goat	1/200	Invitrogen

Table 9 | Lectins and streptavidin conjugated fluorescent dyes used for flow cytometry:

Lectin / Conjugated Fluorophore	Dilution	Supplier
Biotinylated *Sambucus Nigra Agglutinin* (SNA)	1/100	Vector Laboratories
Biotinylated Maackia Amurensis Agglutinin II (MAA II)	1/100	Vector Laboratories
Alexa Fluor™ 488 conjugated streptavidin	1/200	Invitrogen

17. E-selectin binding assay

Prior to experiment, 96-well maxisorp microplates (Thermo Fisher Scientific) were coated with 100 µL of PBS containing 5 µg/mL of human recombinant E-selectin (rh-E-Selectin) (R&D Systems) or with a solution of PBS 1% BSA sterile filtered for control wells. After 24h at 4ºC, wells were aspirated and then blocked with PBS, 1% BSA 1 hour at RT and then $1x10^5$ BxPC-3 or Capan-1 cells were added and allowed to settle for 1 hour at 37ºC in the incubator. In selected experiments, cells were previously incubated 20 minutes with anti-sialyl Lewis X (Clone CSLEX1) mouse monoclonal antibody (BD biosciences, 1:10). Plates were then gentle washed twice with PBS and the remained adherent cells were estimated following the manufacturer's instruction with CellTiter 96R Aqueous One Solution Cell Proliferation Assay based colorimetric method (MTS, Promega). Briefly, cells were incubated for 1 hour minimum in the dark with fresh culture medium (100 µL) containing MTS (20 µL). Then, plates were agitated at RT for 2 min and the absorbance of each well was determined reading at 490 nm, using a 96-well plate spectrophotometer Synergy 4 (BioTek). All the experiments were carried out in quintuplicate, and three independent assays were undertaken. For each experiment, the cell adhesion was determined as a percentage of the scrambled cells, by dividing the mean absorbance of each treatment by the mean absorbance of the scrambled shRNA cells.

18. Transwell migration assay

Cell migration was evaluated using modified Boyden chambers in 24-well plates. Cells were grown in absence of FBS for 24 hours before they were harvested. Prior to cell seeding, 200 µL of serum free medium with 0.001% of Collagen type I from calf skin (Sigma) was placed in the upper part of the 8 µm pore size ThinCerts^{TM} inserts (Greiner bio-one) and 500 µL of serum free medium in the bottom and left for 1 hour in the incubator. After trypsinization, detached cells were washed two times in serum-free medium and resuspended in PBS, 1% BSA. In selected experiments, cells were previously incubated 20 min with anti-sialyl Lewis X (Clone CSLEX1) mouse monoclonal antibody (BD biosciences, 1:10). The cell inserts were emptied and $3.5x10^4$ cells for Capan-1 and $2.5x10^4$ for BxPC-3 in a final volume of 100 µL were seeded in the top chamber and 500 µL of medium containing 10% FBS for BxPC-3 and 20% FBS for Capan-1 was added to the bottom as chemoattractant. Cells were let to migrate in the incubator for 18 hours. After that inserts were washed with PBS and fixed with a 4% paraformaldehyde (PFA) solution in PBS (Santa Cruz Biotechnology) for 15 min, and stained 30 minutes in 0.3% violet crystal solution. After 3 washes with PBS, non-migrated cells were removed from the top surface of the insert using cotton swabs. Then, at least 20 random camps were photographed under the microscope with a CKX41 inverted microscope (Olympus) and the covered area was quantified using ImageJ software.

19. Transwell invasion assay

Cell invasion was evaluated using modified Boyden chambers in 24-well plates. Cells were grown in absence of FBS for 24 hours before they were harvested. Prior to cell seeding, chambers were precoated with 25 µg of Matrigel (Corning) diluted with cold PBS (final volume per well: 50 µL, 1/20 dilution). Then, the mixture was allowed to polymerize 1 hour at 37ºC. After trypsinization, detached cells were washed two times in serum-free medium and resuspended in PBS 1% BSA. The cell inserts were emptied and $5x10^4$ cells for Capan-1 and $4x10^4$ for BxPC-3 in a final volume of 150 µL were seeded in the top chamber. In selected experiments, cells were previously incubated 20 min with anti-sialyl Lewis X (Clone CSLEX1) mouse monoclonal antibody (BD biosciences, 1:10) or with

57/27 Anti-sialyl Lewis A (SLeA), mouse monoclonal antibody (De Bolós 1995, 1:2). After 30 min, 500 µL of medium containing 10% FBS for BxPC-3 or 20%FBS for Capan-1 cells was added to the bottom as chemoattractant. Cells remained in the incubator for 24 hours, after that inserts were washed with PBS and fixed with a 4% paraformaldehyde (PFA) solution in PBS (Santa Cruz Biotechnology) for 15 min, stained 30 minutes in 0,3% violet crystal solution and washed 3 times. Non-invaded cells were removed from the top surface of the insert using cotton swabs. Then at least 20 random camps were photographed at 10x magnification under the microscope with a CKX41 inverted microscope (Olympus) and the covered area was quantified using ImageJ software.

20. Code for cell coverage analysis.

The following code was used to generate a Macro for Fiji software in order to automate image processing. Written by X. Sanjuan. Important note: In order to reduce the code, each jump of paragraph of the code has been represented as (JUMP):

run("Options...", "iterations=1 count=1 black edm=Overwrite do=Nothing"); (JUMP) MyDir = getDirectory("Choose a Directory"); (JUMP) MyList = getFileList(MyDir); (JUMP) for(i=0;i<lengthOf(MyList);i=i+1) (JUMP) { (JUMP) if(endsWith(MyList[i], ".tif")) (JUMP) { (JUMP) open(MyDir+MyList[i]); (JUMP) MyImatge= getTitle(); (JUMP) MyImatge_ID= getImageID(); (JUMP) run("Set Scale...", "distance=0 known=0 pixel=1 unit=pixel"); (JUMP) selectImage(MyImatge_ID); (JUMP) run("Split Channels"); (JUMP) selectImage(MyImatge + " (green)"); (JUMP) MyTrueImatge_ID= getImageID(); (JUMP) selectImage(MyImatge + " (blue)"); (JUMP) run("Close"); (JUMP) selectImage(MyImatge + " (red)"); (JUMP) run("Close"); (JUMP) selectImage(MyTrueImatge_ID); (JUMP) run("Median...", "radius=1"); (JUMP) run("Threshold..."); (JUMP) waitForUser("if neede adjust threshold"); (JUMP) run("Convert to Mask"); (JUMP) run("Options...", "iterations=1 count=1 black edm=Overwrite do=Open"); (JUMP) run("Set Measurements...", "area area_fraction redirect=None decimal=2"); (JUMP) run("Measure"); (JUMP) selectImage(MyTrueImatge_ID); (JUMP) close(); (JUMP) selectWindow("Threshold"); (JUMP) run("Close"); (JUMP) } (JUMP) }

21. PDMS devices fabrication and assembling of microfluidic devices.

Microfluidic polydimethylsiloxane (PDMS) devices were manufactured by mixing vigorously the SYLGARD® 184 silicone elastomer base with the SYLGARD® 184 curing agent in a 10:1 ratio. The mixture was poured onto the selected molded wafer in a Petri dish (100 mm in diameter) and it was degassed in the vacuum from 40 minutes to O/N. After removing all the possible remained air bubbles trapped in patterns with a pipette tip, the dish was placed to cure on hot plate at 85ºC for an hour and a half. After incubation, the cured PDMS was demolded from the negative master by using a scalpel blade and individual PDMS devices were cut and pierced (0.5 mm diameter) to form inlet and outlet ports according to the designed pattern.

For the assembling of the device, PDMS surface was cleaned with tape several times to avoid small particles, which can cause leakage of the bonded device. After cleaning, the devices were sonicated in 100% fresh ethanol for 5 min. Devices were then rinsed and dried with air around the holes and edges. Rectangular cover slips (25x75 mm) with a thick between .13-.17 mm were cleaned and dried. PDMS devices with features side up and the cover slips were placed in a plasma cleaner machine and vacuumed for at least 5 min for pressure dropping. After incubation, a plasma treatment was done for 2 min 15 sec (A pale violet color should be observed in the vacuum chamber during this process). Plasma treatment of PDMS will increase the exposition of silanol groups at the surface of the PDMS layers enabling the formation of covalent bonds within the glass cover slips. After placing features down on activated cover slides, devices were left for 2 min before add the diluted collagen for migration assay or the corresponding antibody for flow-based assays (see below).

22. Flow-based adhesion assays.

PDMS-based devices were fabricated using a photolithography and standard replica molding technique as previously described. Once the PDMS was linked to the cover slide, 20 µL of Goat Anti-Human IgG Antibody, Fc, FITC conjugate (Millipore) at a final concentration of 10 µg/mL was added to one end of the device for 10 min at RT. Twice washes of 3 min each with 100 µL of PBS were performed. After washing, devices were coated for 1hour at RT with 20 µL of recombinant human E-Selectin/CD62E Fc Chimera (R&D Systems) concentrated at 10 µg/mL. After incubation, three washes were performed and devices were blocked with a solution of PBS 1% BSA (50 µL) for another hour at RT. Finally, devices were washed out again and pancreatic cancer cells (BxPC-3 and Capan-1) were resuspended at $3x10^5$ and $2.5x10^5$ cells/mL respectively in PBS, 0.1% BSA. Cells were perfused into the inlet channel and allowed to flow via gravity over the immobilized E-selectin-coated devices at prescribed wall shear stresses using a parallel microfluidic flow chamber. The dimensions of the device channel (**figure 17**) were 2 cm x 1000 µm x 22.5 µm (length x width x height). The extent of adhesion was quantified by enumerating the total number of binding events in a single field of view during a 2-min period recorded with a phase contrast 10x Ph1 objective of a Nikon Inverted microscope.

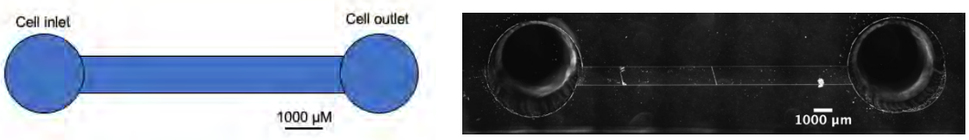

Figure 17 | Flow chambers devices. Left: schematic representation of flow chambers. Right: cross image of flow chamber PDMS-Devices (Scale bars: 1000 µm).

23. PDMS-based microchannel migration assay.

PDMS-based microchannels devices were fabricated using a photolithography and standard replica molding technique as previously described. Each device comprises a series of parallel 200 µm-long and 10 µm-high microchannels of prescribed widths varying from 6, 10, 20 to 50 µm arrayed perpendicularly between a cell and chemoattractant inlet lines with 50 µm-high (**figure 18**).

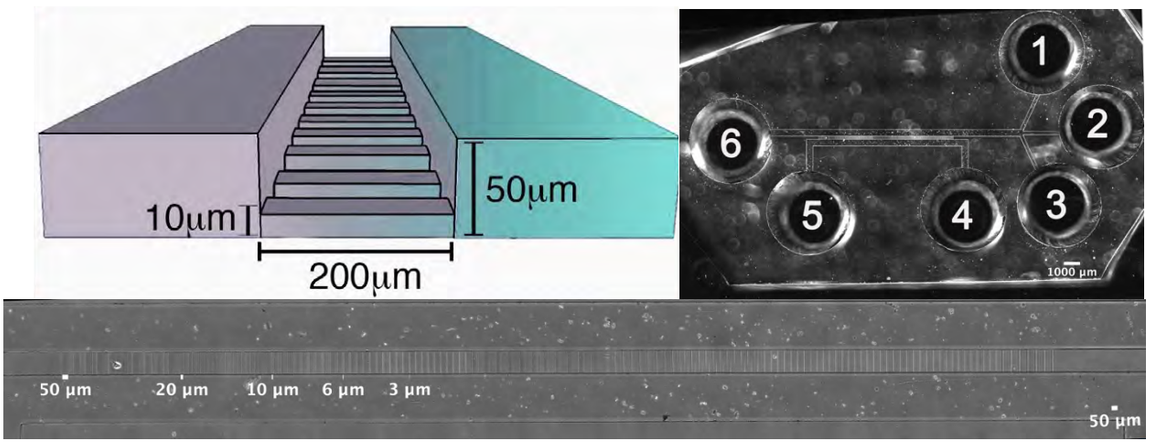

Figure 18 | Microchannel device for cell migration. Up left: schematic representation of microchannel device, extracted from [283]. Up right: cross image of entire PDMS-Device (Scale bar: 1000 µm). Down: cross image of central channels with different widths (Scale bars: 50,20,10,6 and 3 µm).

The microchannels devices were coated with 80 µL of collagen type I diluted in PBS (20 µg/mL) in inlets port number 1,2,3 and 4 and then incubated for 1h at 37ºC to adsorb collagen to facilitate cell adhesion. Microchannel devices were kept at 4ºC O/N. Cells were trypsinized, counted and resuspended at $1x10^6$ cells/mL. Devices were washed with PBS for 1 min before seeding cells and 30 µL of medium was added to port 3. 50 µL of cell suspension ($5x10^4$ cells) was then added to cell inlet number 5. 20 s later, 25 µL from port 5 was transferred to port 4 and devices were incubated for 15-30 min. After incubation, cell media were aspirated and 100 µL of complete media were added to all ports and devices were placed in the microscopy. Cell migration was visualized and recorded via time-lapse live microscopy in an enclosed, humidified microscope stage maintained at 37°C and 5% CO_2 using software-controlled stage automation and an inverted Eclipse Ti microscope (Nikon). Phase contrast time-lapse images were taken at every 10 min for 24 hours with a 10x Ph1 objective. The spatial x and y positions of all non-dividing and viable cells that entered and migrated in the microchannels were tracked

overtime with the Manual Tracking plugin in ImageJ. Motility parameters, namely velocity, speed and persistence, were computed using a custom-written MATLAB code as previously described [288,289].

24. MATLAB code for motility analysis.

Written by Kimberly M. Stroka [290] for motility analysis.

Confined cell migration analysis consideration before the use of the code:

1. Input is a set of Excel files of tracked cells using Manual Tracker in ImageJ

2. Files should be saved alternating data (xy1, xy2, etc.) with reference files (xy1_ref, xy2_ref, etc.)

3. Change Matlab "current folder" to the one with the files to be analyzed and then choose "add path" at prompt after running the program

4. Positive velocity represents migration towards top of device (chemoattractant) and negative velocity towards bottom of device.

5. Enter "scale" and "time_int" to correct values according to the microscope setings.

Important note: In order to reduce the code, each jump of paragraph of the code has been represented as (JUMP):

close all (JUMP) clear all (JUMP) clear all (JUMP) clc (JUMP) P=0; (JUMP) Vmean=[]; (JUMP) Smean=[]; (JUMP) dchange=[]; (JUMP) CI2=[]; (JUMP) xlsFiles = dir('*.xls'); (JUMP) for k = 1:2:length(xlsFiles)-1 (JUMP) P=P+1; (JUMP) clearvars -except k xlsFiles P Vmean Smean dchange CI2 (JUMP) scale = 0.8810170 (JUMP) time_int =10; (JUMP) dc=0; (JUMP) filename = xlsFiles(k).name; (JUMP) ref = xlsFiles(k+1).name; (JUMP) xy = dlmread(filename,'\t',1,1); (JUMP) x = xy(:,3); (JUMP) y = xy(:,4); (JUMP) N = xy(:,1); (JUMP) slice = xy(:,2); (JUMP) Dis=xy(:,5); (JUMP) Vel=xy(:,6); (JUMP) xy_ref = dlmread(ref,'\t',1,3); (JUMP) x_ref = xy_ref(:,1); (JUMP) y_ref = xy_ref(:,2); (JUMP) xc = x_ref-x_ref(1); (JUMP) yc = y_ref-y_ref(1); (JUMP) Vsum = zeros(N(end),1); (JUMP) Ssum = zeros(N(end),1); (JUMP) for i = 1:N(end) (JUMP) d=0 (JUMP) for g = 1:length(x) (JUMP) if Dis(g)==-1 && Vel(g)==-1 (JUMP) slice2=slice-slice(g)+1; (JUMP) end (JUMP) if N(g) == i (JUMP) last=g; (JUMP) xc1(g) = x(g) - xc(slice(g)); (JUMP) yc1(g) = y(g) - yc(slice(g)); (JUMP) if slice2(g)~=1 (JUMP) v(g) = (scale*60/time_int).*(sqrt((xc1(g)-xc1(g-1))^2+(yc1(g)-yc1(g-1))^2)); (JUMP) sign(g) = yc1(g-1)-yc1(g); (JUMP) d = d + (sqrt((xc1(g)-xc1(g-1))^2+(yc1(g)-yc1(g-1))^2)); (JUMP) end (JUMP) if slice2(g) == 1 (JUMP) v(g) = 0; (JUMP) sign(g) = 0; (JUMP) first=g; (JUMP) end (JUMP) if sign(g)~=0 (JUMP) sign1(g) = sign(g)/abs(sign(g)); (JUMP) end (JUMP) if sign(g) == 0 (JUMP) sign1(g) = 0; (JUMP) endV(g) = v(g).*sign1(g); (JUMP) if slice2(g)>2 (JUMP) if V(g)/V(g-1)==-1 (JUMP) dc=dc+1; (JUMP) end (JUMP) end (JUMP) if slice2(g) ~=1 (JUMP) Vsum(i) = Vsum(i)+V(g); (JUMP) Ssum(i) = Ssum(i)+v(g); (JUMP) end (JUMP) slice_max(i) = slice2(g)-1; (JUMP) end (JUMP) end (JUMP) dchange=[dchange,dc]; (JUMP) CI=(sqrt((xc1(first)-xc1(last))^2+(yc1(first)-yc1(last))^2))/d; (JUMP) CI2=[CI2,CI]; (JUMP) end (JUMP) Vmean = [Vmean; Vsum./slice_max.']; (JUMP) Smean = [Smean; Ssum./slice_max.']; (JUMP) end (JUMP) CI2=CI2'; (JUMP) mkdir('Matlab_results'); (JUMP) dlmwrite('Matlab_results/Velocities.xls',Vmean,'\t',0,0) (JUMP) dlmwrite('Matlab_results/Speeds.xls',Smean,'\t',0,0) (JUMP) dlmwrite('Matlab_results/Chemotactic_Index.xls',CI2,'\t',0,0)

25. Statistical analyses

All data are presented as mean ± SEM. or SD. from 3 independent experiments. Statistical significance was determined between pairs of data with a t-test, or between groups of data with one-way ANOVA and a Tukey's Multiple Comparison post-hoc test. Dunnett's multiple comparisons test was used to compare each of the shRNAs to scramble in migration microdevices. Figures were designed with Prism7- GraphPad.

IV. Results

Results – Chapter 1

Microfibril Associated Protein 4 (MFAP4) is a carrier of the tumor associated carbohydrate sialyl Lewis X (SLe^X) in pancreatic adenocarcinoma.

1.1 Analysis of sialyl Lewis X determinant expression in PDA.

Pancreatic tissue lysates coming from twenty-five PDA of different stages and six control tissues, including three non-tumor pancreas from PDA patients and three pancreas of individuals with non-pancreatic related disorders, were electrophoresed in 8% polyacrylamide gel and transferred onto PVDF membranes to analyze by western blot the Sialyl Lewis X (SLe^X) levels in total protein tissue lysates with CSLEX1 clone, which specifically recognizes SLe^X determinants. **Figure 19** depicts an illustrative example including tumor and non-tumor tissues.

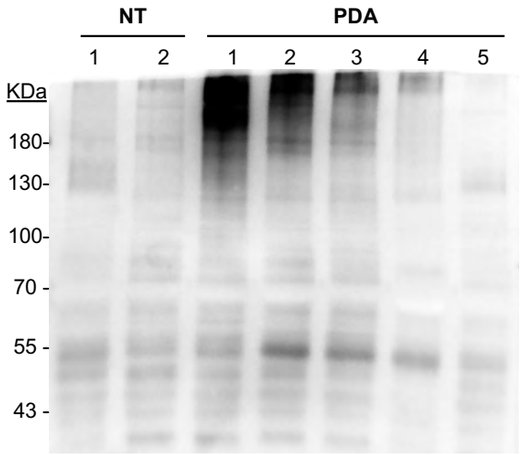

Figure 19 | Evaluation of Sialyl Lewis X expression in different pancreatic samples. Representative example of SLe^X immunodetection of 20 µg of total protein lysates from pancreatic tissue samples. NT 1 and 2 corresponds to non-tumor pancreatic tissue from the PDA patients T3 and T2 respectively. PDA, corresponds to the tumor tissues from pancreatic ductal adenocarcinoma patients.

Most of the PDA samples showed stronger positive SLe^X signal, in contrast with negative samples, in agreement with previous studies [291]. Different immunoreactive bands corresponding to proteins of several molecular weight (MW) were observed in most PDA samples. However, SLe^X immunodetection was clearly more pronounced in high MW glycoproteins (over 130 KDa), probably corresponding to mucins. Mucins are heavily glycosylated proteins containing several O and N-glycosylation sites and that have been reported to carry sialyl Lewis determinants in PDA and other tumors [291–293]. The variable signal of SLe^X shown in **figure 19** where the same total protein amount was loaded, indicates the differences in the expression levels of SLe^X on glycoproteins from different PDA samples.

1.2 Identification of glycoproteins with SLe^X in PDA through two dimensional electrophoresis and mass spectrometry.

Despite a common approach for enriching glycoproteins carrying SLe^X would be by the use of antibodies against SLe^X, CSLEX (Anti-sialyl Lewis X Antibody) which is an IgM subtype that could not immunoprecipitate SLe^X protein carriers in previous attempts. Thus, other alternatives such as the 2DE approach to comprehensively identify SLe^X carriers in PDA were exploited. 2DE allowed to obtain a protein map containing a wider range of MW proteins than the previous SDS-PAGE analysis, having in this way higher resolution, and a better separation of the proteins of interest for its subsequent MS analysis. For that, Immobiline® dry strips pH: 3–10 to separate the proteins according to their isoelectric point followed by a second-dimension separation in gradient 4–15% pre-cast polyacrylamide gels were used. Gradient gels were used to facilitate the entry of high MW proteins into the second-dimension gel. All initial samples were run in parallel, one gel was Coomassie blue stained, and the duplicate gel was transferred onto PVDF membrane for SLe^X immunodetection. Three pancreatic samples were thus analyzed (two PDA samples and one control sample from an individual with non-pancreatic-related disorders). Analyses of the PDA samples yielded very reproducible 2DE profiles. **Figure 20** shows the pattern of PDA 18 as a representative profile of the tumor sample. Several positive spots for SLe^X from the immunodetection (**figure 20B**) of the PDA samples could be identified in the Coomassie gel (**figure 20A**). The Coomassie spots with stronger SLe^X immunoreactivity were then excised, trypsin digested and analyzed by mass spectrometry (MS). The peptide mapping results followed by bioinformatics analysis allowed the identification of the corresponding carrier proteins. After MS analysis of several defined SLe^X positive spots of both PDA samples, those proteins with potential glycosylation sites that showed higher score and peptide coverage were selected. Spots 1, 2 and 3 of 36 KD of MW and isoelectric points (pIs) ranging from 4.9 to 5.2, were found to contain a promising novel candidate; the microfibril associated glycoprotein 4 (MFAP4). At this point to further validate these findings, stripping of the SLe^X membranes was performed an the membranes were probed with MFAP4 antibodies. MFAP4 immunostaining appeared in at least seven visible isoforms with different intensities and pIs ranging from 4.7 to 5.6. The five spots with PIs from 4.8 to 5.4 showed much higher intensity in the

immunodetection than the spots at pIs 4.7 and 5.6, which was very weak. Membrane stripping and MFAP4 immunostaining allowed us to confirm the co-localization of the identified MS MFAP4 spots with their corresponding SLe^X ones at a pI of 4.9 for spot 1, 5.1 for spot 2 and 5.2 for spot number 3 (**figure 20C**). Spots at pI 4,8 and 5.4, for MFAP4 showed a slight staining for SLe^X, but as they were also less intense for MFAP4 they could not be identified in the Coomassie gel. No SLe^X spots at these pI and MW regions were detected in the pancreatic control.

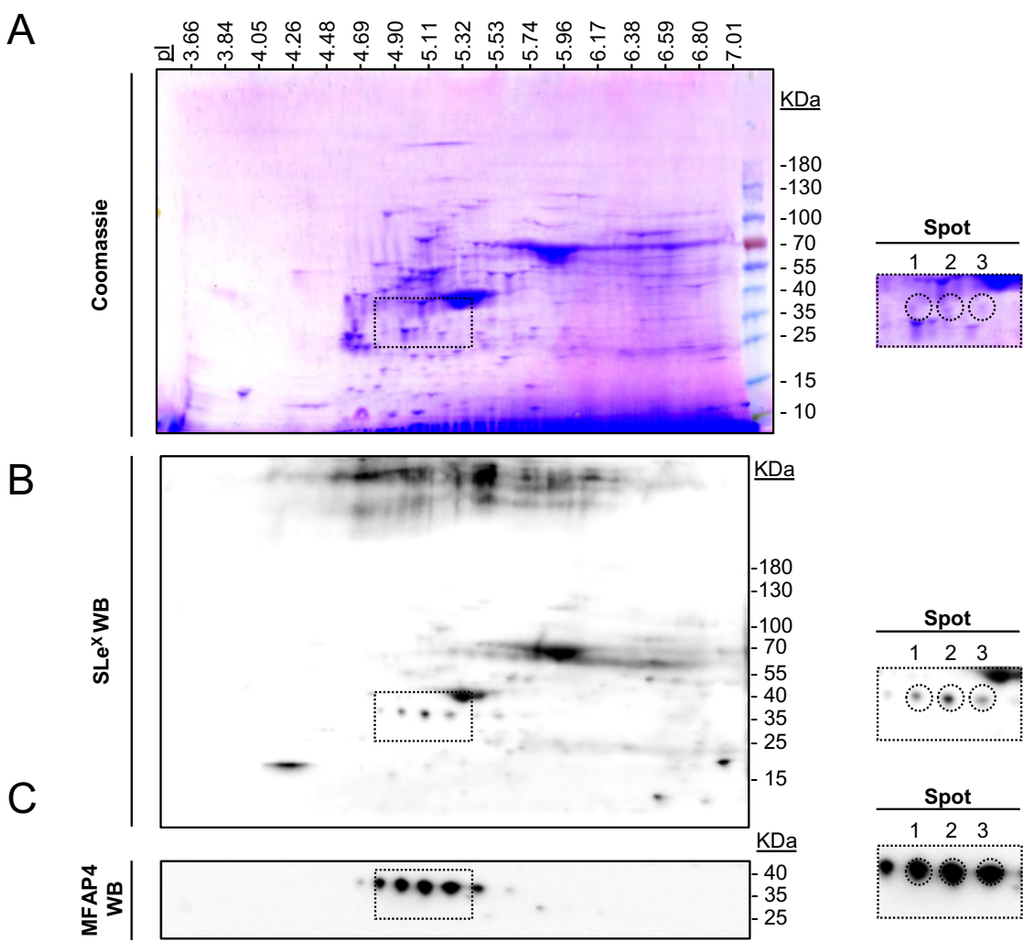

Figure 20 | Identification of glycoproteins with increased levels of SLe^X in PDA using two-dimensional electrophoresis (2DE). A) Left: Proteome pattern obtained from a representative pancreatic ductal adenocarcinoma tissue (PDA 18) stained with Coomassie after 2DE. Right: Amplification of the selected spots (S1, S2 and S3) that were positive for SLe^X (shown in panel B) and that were further identified by MS. B) Left: Immunodetection of SLe^X pattern from the same representative PDA tissue (PDA 18) after 2DE, run in parallel with that shown in panel A. Right: Amplification of the positive spots for SLe^X that were identified on the Coomassie stained gel (S1, S2 and S3) in panel A. C) Left: Immunodetection of MFAP4 after stripping treatment of the membrane of panel B. Right: Amplification of the selected spots (S1, S2 and S3).

Next, we aimed to confirm glycosylation and presence of N-glycans on MFAP4 from pancreatic tissue samples (both PDA and control samples) since there is no literature about MFAP4 glycosylation in pancreas. Thus, 10 µg of pancreatic tissue lysates were treated with the enzyme PNGase F, which digests the N-glycans from glycoproteins, and with sialidase, which digests terminal sialic acids linked to N-glycans, in order to facilitate PNGase F digestion. Samples were run in 10% polyacrylamide gels under reducing conditions and an immunoblot against MFAP4 was performed (**figure 21**).

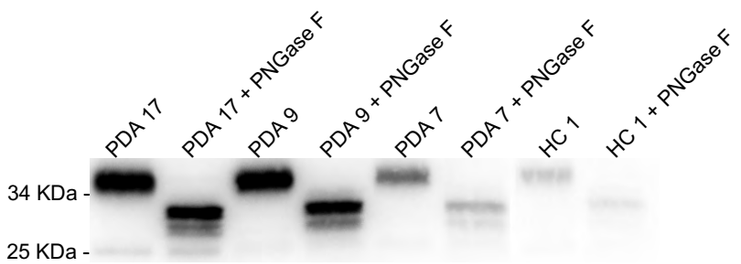

Figure 21 | MFAP4 deglycosylation with PNGase F. MFAP4 immunodetection of 10 µg of total cell lysates from pancreatic tissue samples treated with PNGase F and sialidase and their corresponding non-treated samples.

Deglycosylated samples showed greater MFAP4 electrophoretic mobility, which migrated at a band at 30 KDa, compared to the MFAP4 band at 36 KDa of the non-treated samples. This change in MFAP4 MW in the deglycosylated samples could be attributed to the loss of MFAP4 N-glycan/s, thus confirming the presence of N-glycosylation in MFAP4 from pancreatic samples.

1.3 Expression of microfibril associated glycoprotein 4 (MFAP4) in human pancreatic cancer cell lines and tissues by western blot and immunohistochemistry.

MFAP4 protein expression was investigated in pancreatic cancer cells and tissues. The expression of MFAP4 was first explored by western blot in cell lysates from a pancreatic cancer cell panel that included the seven cell lines: AsPC-1, BxPC-3, Capan-1, Capan-2, HPAF-II, Panc 10.05 and SW 1990. These cell lines represent varying degrees of pancreatic cancer genetic complexity and different grades of neoplastic differentiation. Nevertheless, MFAP4 was not detected in any of the protein cell lysates. Since MFAP4

is present in the extracellular matrix, we investigated whether this protein was present in the conditioned media from the same cell lines, but no presence of MFAP4 was either detected in any of the PDA cell lines in both reducing and unreducing conditions (data not shown). The analysis of MFAP4 expression was then further investigated in pancreatic tissue lysates under reducing conditions by WB (**figure 22**).

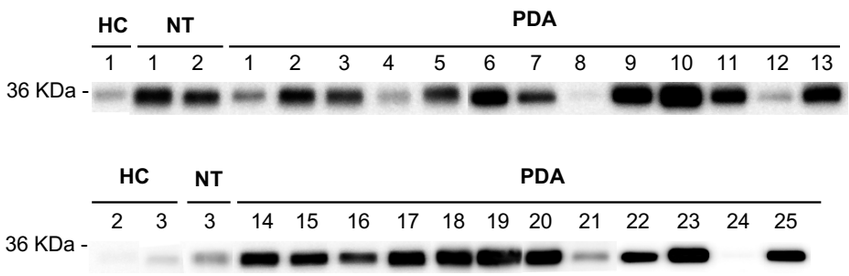

Figure 22 | Western blot analysis of MFAP4 expression in human pancreatic tissues. MFAP4 immunodetection of 10 µg of total cell lysates from pancreatic tissue samples. HC represents control pancreas from non-pancreatic-related disorders, NT represents no tumor biopsies from PDA patients, and PDA samples from pancreatic ductal adenocarcinoma.

In contrast with the cell line results, MFAP4 immunodetection (observed in a band at an approximate MW of 36 KDa), revealed a moderate to high expression of MFAP4 in human pancreatic tissues with different degrees of intensity when loading 10 µg of total protein onto the electrophoresis. MFAP4 protein was detected in most of the PDA lysates, (being positive in 23 out of the 25 PDA samples) and its expression was in general much higher in comparison with control pancreas (HC) 1, 2 and 3 from donors with non-pancreatic disorders. Interestingly, two-thirds of the non-tumor samples (NT), which come from the non-tumor part of the pancreatic tissue from PDA patients, showed also high-expression of MFAP4.

In order to assess MFAP4 location in the pancreatic tissues, immunohistochemistry analysis with paraffin sections of PDA specimens, non-tumor pancreas and chronic pancreatitis tissues was performed in parallel to this work [294]. Staining of tissues of different staging and the corresponding staining with hematoxylin eosin is shown in **figure 23.**

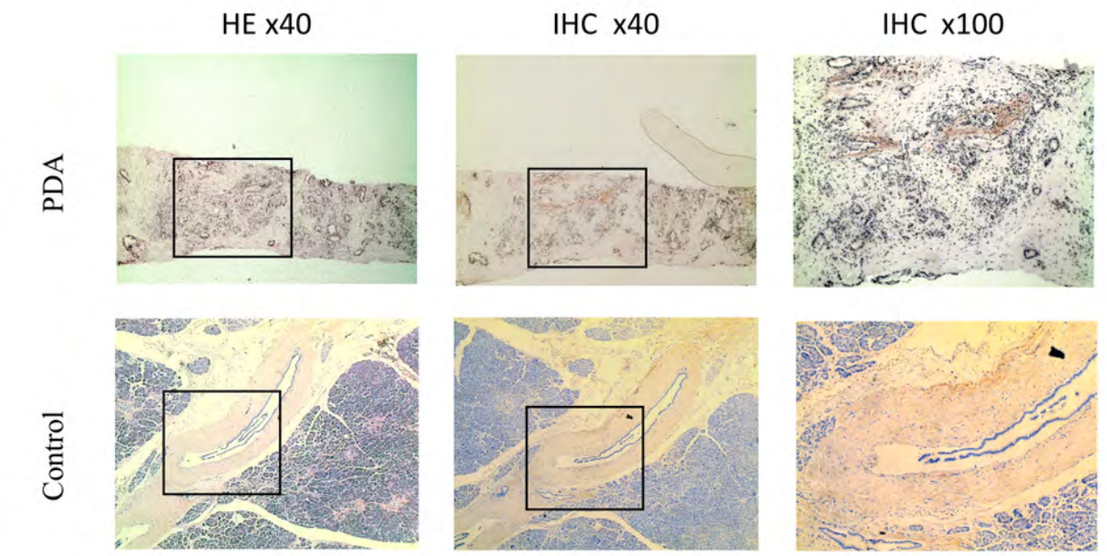

Figure 23 | Immunohistochemistry staining of MFAP4 in human pancreatic tissues. Immunohistochemistry (IHC) staining of MFAP4 at different magnification (x40 and x100) and the corresponding hematoxylin eosin (HE) staining (x40) of a representative pancreatic cancer tissue (top) and one control tissue (bottom). Images extracted and modified from [294].

MFAP4 staining was detected in 11 out of the 31 tissues of pancreatic adenocarcinoma in the extracellular matrix surrounding glands and ductal structures (**figure 23**, top panel) but not in their neoplastic cells. The different degree of MFAP4 expression between the pancreatic tissue lysates and the tissue immunohistochemistry could be explained by the use of a different antibody against MFAP4. However, the lack of expression of the protein in the neoplastic cells is consistent with the results from the adenocarcinoma cell lines' lysates that did not show any MFAP4 expression either. Tissue Immunohistochemistry (IHC) analyses showed that MFAP4 glycoprotein is found in the stroma of the PDA samples in agreement with the data reported in the Human Protein Atlas /Cancer Genome Atlas Database (TCGA), which also showed that most of the PDA tissues analyzed did not show any positivity in the neoplastic cells either. The non-tumor pancreatic and the chronic pancreatitis tissues showed a weak staining also in the extracellular matrix surrounding some ducts (**figure 23**, bottom panel).

1.4 SLe^X on 2DE MFAP4 spots from PDA samples.

To analyze the occurrence of the specific glycoform of MFAP4 with SLe^X in more PDA samples, the purification of the protein from PDA samples with high MFAP4 content by immunoprecipitation (IP) to perform MFAP4 glycan sequencing was first assessed. However, the few commercial antibodies available for MFAP4 IP free of glycoproteins in their storing buffers did not work efficiently for that purpose. Therefore, to demonstrate the presence of SLe^X in the N-glycans of MFAP4 in a larger cohort of PDA samples, 2DE, with SLe^X and MFAP4 immunoblotting, was performed. The tissue samples were: , six more PDA samples (previously selected to express high or medium levels of both SLe^X and MFAP4), two more NT (non-tumor pancreatic tissues samples from PDA patients) and one more control sample (HC, control pancreas from donor with non-pancreatic disorders). Representative images of these analyses are shown in **figure 24**.

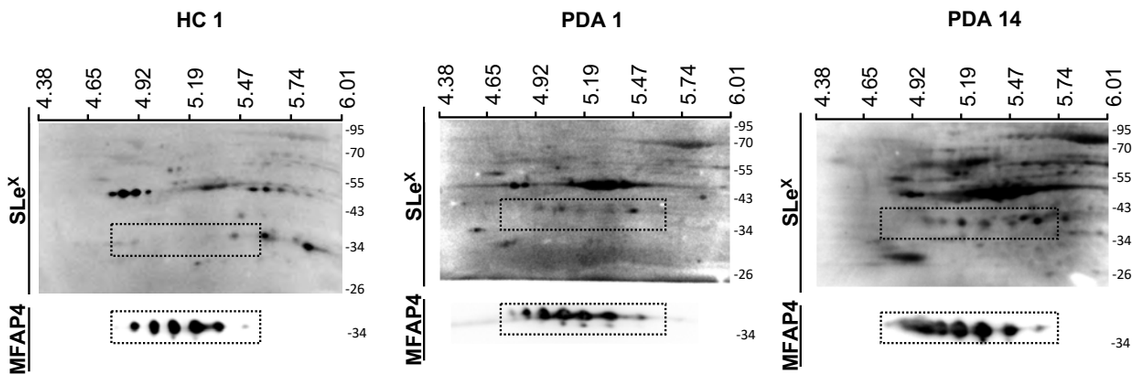

Figure 24 | SLe^X colocalization over MFAP4 spots. Up: Immunodetection of SLe^X pattern from different pancreatic tissues after 2DE. Down: Immunodetection of MFAP4 after stripping treatment from the membrane of upper panel. Boxes in dark represents the exactly location of the membranes for colocalization visualization. pI was calculated based on the distance according to the pH gradient data supplied by the manufacturer.

All PDA samples showed colocalization of SLe^X and MFAP4 spots, WB analysis also revealed that despite the protein MFAP4 was present in all different samples (PDA, NT and HC), SLe^X expression and colocalization with MFAP4 was present only in PDA, and both control pancreas and NT samples did not shown immunoreactivity for SLe^X and MFAP4 spots. Collectively, these findings reveal that the MFAP4 glycoform carrying SLe^X is a feature of PDA and could be a future biomarker candidate in pancreatic malignancy.

Results – Chapter 2

Knock-down of α2,3-sialyltransferases in pancreatic cancer cells impairs their migration, invasion and E-selectin adhesion.

2.1 Expression of sialylated glycan determinants, α2,3-sialyltransferases and α1,3/4-fucosyltransferases in a panel of PDA cells.

In order to investigate the contribution of the α2,3-sialyltransferases ST3GAL3 and ST3GAL4 to the adhesive and invasive capabilities of PDA cells, the levels of these STs as well as the expression levels of sialyl Lewis X (SLe^X), sialyl Lewis A (SLe^A) and different sialic acid determinants (α2,3 and/or α2,6) were characterized in a panel of seven different pancreatic cancer cell lines (AsPC-1, BxPC-3, Capan-1, Capan-2, HPAF-II, Panc 10.05 and SW 1990). These cell lines represent varying degrees of pancreatic cancer genetic complexity and different grades of neoplastic differentiation.

Cell surface glycan expression was first analyzed by flow cytometry with specific monoclonal antibodies (mAb) against SLe^X and SLe^A antigens and lectins: *Sambucus Nigra* Lectin (SNA) which binds preferentially to sialic acid attached to terminal galactose in α2,6-linkage, *Maackia Amurensis* Lectin II (MAA II) that binds sialic acid in an α2,3-linkage. Flow cytometry experiments with anti-SLe^X mAb showed different expression of SLe^x on the cell surface of the diverse cell lines (**figure 25,** top left panel).

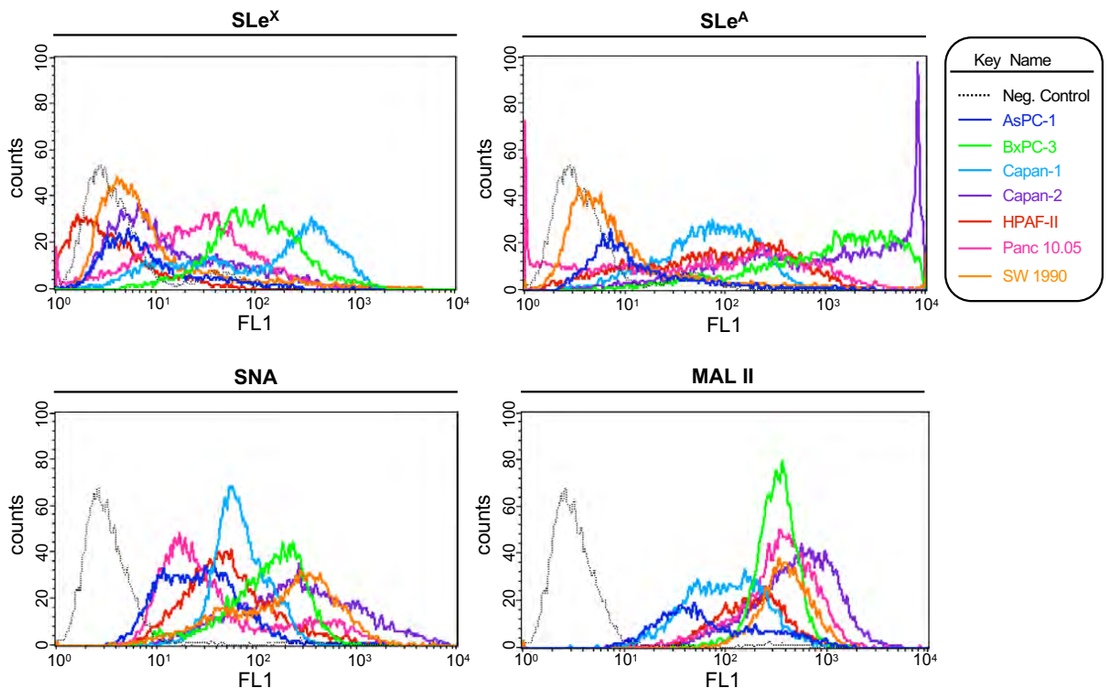

Figure 25 | FC analysis of the cell surface glycan structures in pancreatic cancer cell lines. Representative cytometry histograms of the different glycan structures in cell surface of the seven PDA cell lines: Sialyl Lewis X (top left), sialyl Lewis A (top right), α2,6-sialic acid detected with SNA lectin (bottom left) and α2,3-sialic acid detected with MAL II lectin (bottom right). Color Legend: Negative control is represented with a continuous dot outline: (...), AsPC-1 (dark blue line), BxPC-3 (green line) Capan-1 (light blue line), Capan-2 (purple line), HPAF-II (red line), Panc 10.05 (pink line), SW 1990 (orange line).

BxPC-3 and Capan-1 showed the highest levels compared with the rest of the PDA cell lines, being Capan-1 levels 2-fold higher than BxPC-3. Among the other cell lines, Panc 10.05 showed moderate SLe^X levels, and Capan-2, AsPC-1, HPAF-II and SW 1990 cells displayed lower SLe^X contents. The analysis of SLe^A antigen showed that BxPC-3 and especially Capan-2 cells had the highest levels of SLe^A compared with medium-high levels from Capan-1, HPAF-II and Panc 10.05, while AsPC-1 and SW 1990 cells showed the lowest levels (**figure 25**, top right panel). The same analyses were performed for the expression of α2,6 and α2,3-sialic acid determinants using SNA and MAL II, respectively (**figure 25,** bottom panel). In decreasing order Capan-2, SW 1990, BxPC-3 and Capan-1 showed high-medium levels of α2,6-SA by SNA analysis. Analysis with MAL II lectin revealed that Capan-2 was again the cell line with the highest levels, whereas BxPC-3, Panc 10.05, HPAF-II, SW 1990 and Capan-1 showed high medium levels and AsPC-1 low-medium levels.

The expression of SLe^X and SLe^A determinants in protein cell lysates and secreted glycoconjugates from conditioned media was analyzed by western blot (**figure 26**).

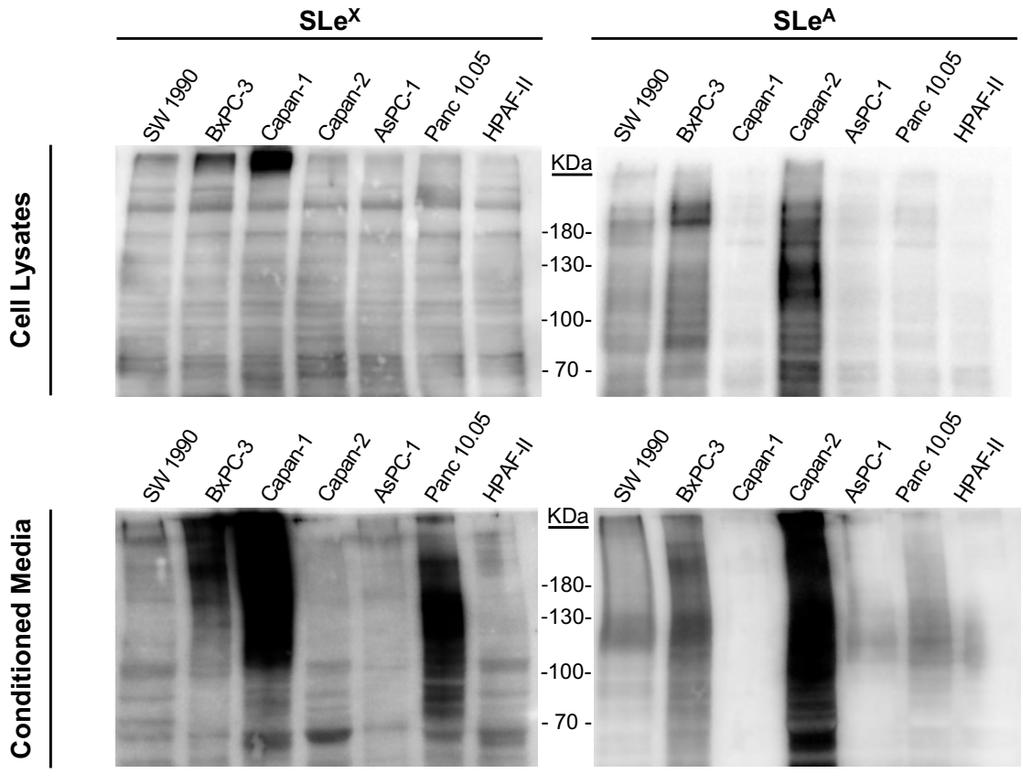

Figure 26 | WB analysis of the cell surface glycan structures in pancreatic cancer cell lines. Immunodetection by western blot of SLe^X (left) and SLe^A (right) content in proteins from total cell lysates (top) and conditioned media (bottom) of the PDA cells. Blots were probed with clones CSLEX1 mAb against sialyl Lewis X and the clone 57/27 mAb against sialyl Lewis A.

The results were similar to the ones obtained for cell membrane glycoconjugates determined by flow cytometry. The most expressing SLe^X cell lines were Capan-1 and BxPC-3, and for SLe^A were Capan-2 and BxPC-3, in both cell lysates and cell conditioned media, but the signal was higher in secreted glycoproteins of the conditioned media. The main differences of sialylated determinants between cell lines were specially detected in the high molecular weight region, which could correspond to highly glycosylated mucins, among others, as reported previously [291].

To identify the most appropriate cell lines to knock-down ST3GAL3 and ST3GAL4, the mRNA expression levels of the α2,3-ST and the fucosyltransferase genes that codify for the enzymes that act in the last steps of SLe antigens' biosynthesis were determined (**figure 27**).

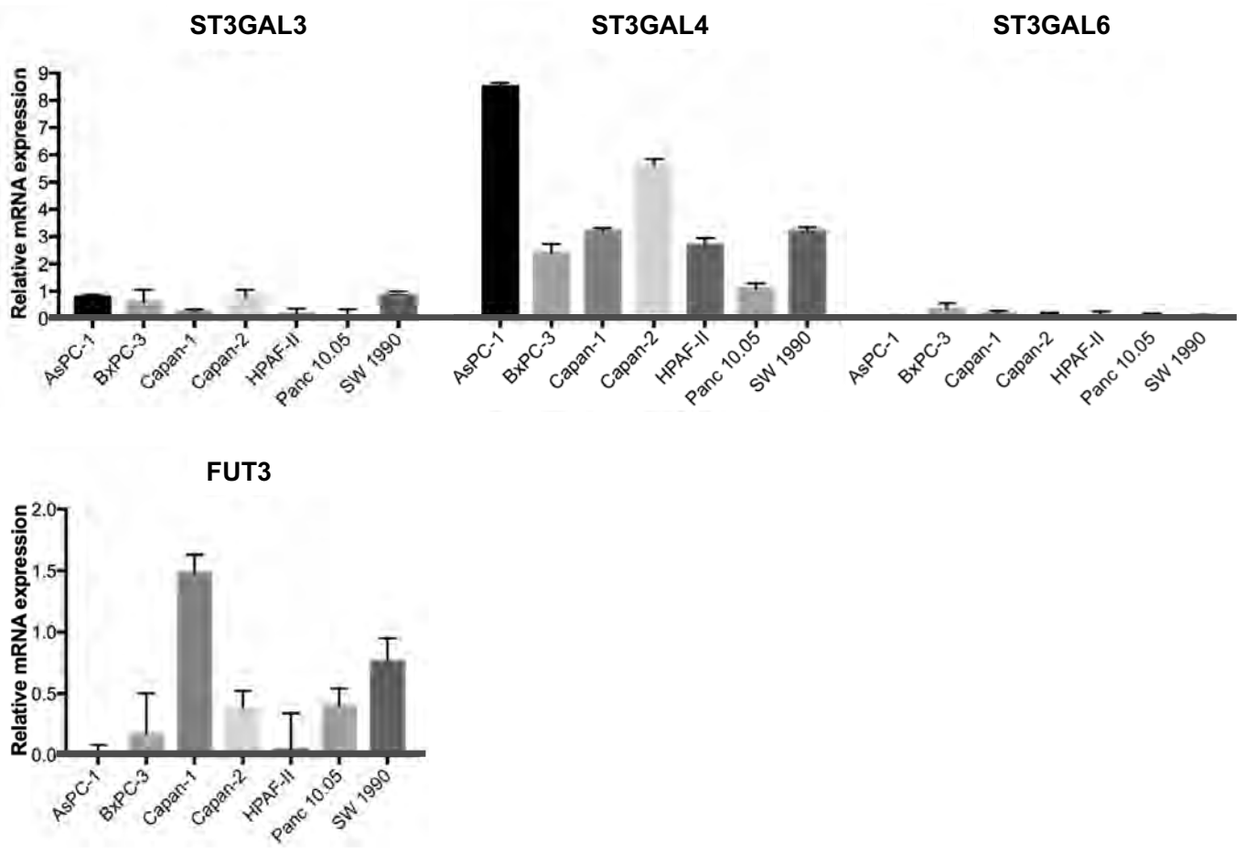

Figure 27 | Relative quantification of α2,3-sialyltransferases and α1,3/4-fucosyltransfereases. Quantification of ST3GAL3, ST3GAL4, ST3GAL6 and FUT3 mRNA levels by RT-qPCR in the pancreatic cancer cell panel. RNA levels were normalized using TBP as a housekeeping gene. Data represents mean±SD.

Regarding α2,3-ST expression, ST3GAL3, ST3GAL4 and ST3GAL6 mRNA levels were analyzed. ST3GAL6 levels were much lower than ST3GAL3 and ST3GAL4 ones for all cell lines. Within these low ST3GAL6 levels, Capan-1 and BxPC-3 were the cell lines with the highest ones. ST3GAL3 expression was also lower than ST3GAL4 for all cell lines, being between 4- to 20-fold less expressed, depending on the cell line. The cells with higher ST3GAL3 expression were AsPC-1, BxPC-3, Capan-2 and SW 1990. Regarding ST3GAL4 mRNA, AsPC-1 was the cell line with the highest level and Panc 10.05 the cell line with the lowest level. The expression of α1,3/4-fucosyltransferases, involved in the synthesis of SLe^X and SLe^A in mammalian cell lines (FUTs 3, 5, 6 and 7) [198] showed that these cell lines exhibited very low expression for FUT5, FUT6 and FUT7 (data not shown). FUT3 was the main fucosyltransferase expressed, which was found in five (Capan-1, SW 1990, Panc 10.05, Capan-2 and BxPC-3) out of the seven cell lines, being Capan-1 the cell line with the highest levels (**figure 27**).

This analysis prompted us to select BxPC-3 and Capan-1 cells, which display high SLe^X expression and high to moderate SLe^A expression, for knock-down ST3GAL4 and ST3GAL3, in order to assess the effect of these STs on their biosynthesis as well as their influence in other processes, which may involve SLe^X/SLe^A biological interactions.

2.2 Stable silencing of ST3GAL4 and ST3GAL3 in BxPC-3 and Capan-1 cells.

To investigate the role of ST3GAL4 and ST3GAL3 in PDA malignant progression, both genes were targeted for silencing through shRNA technology in BxPC-3 and Capan-1 cell lines. Knock-down experiments by inserting the pLKO.1-puro vectors containing the shRNAs against the target genes were first attempted with liposome-based transfection reagents and with specific electroporation kits, but the transfection efficiency for these pancreatic cell lines was very low. Therefore, the knock-down (KD) of ST3GAL4 and ST3GAL3 genes were performed by lentiviral delivery of the pLKO.1-puro vector containing the shRNAs against the target genes. PDA cells lines (BxPC-3 and Capan-1) were transduced with 5 different shRNAs for each target sialyltransferase and the

respective knock-downs were designated as sh-1 to sh-5 for shRNAs against ST3GAL4 and as sh-6 to sh-10 for the ST3GAL3 KD cells. Parental cells were simultaneously transduced with a scramble control containing a non-targeting sequence. No changes in cell morphology or proliferation were observed in the stable transduced cells.

After one-week puromycin selection, ST3GAL4 and ST3GAL3 mRNA expression levels were determined by reverse transcription quantitative PCR (RT-qPCR) (**figure 28**).

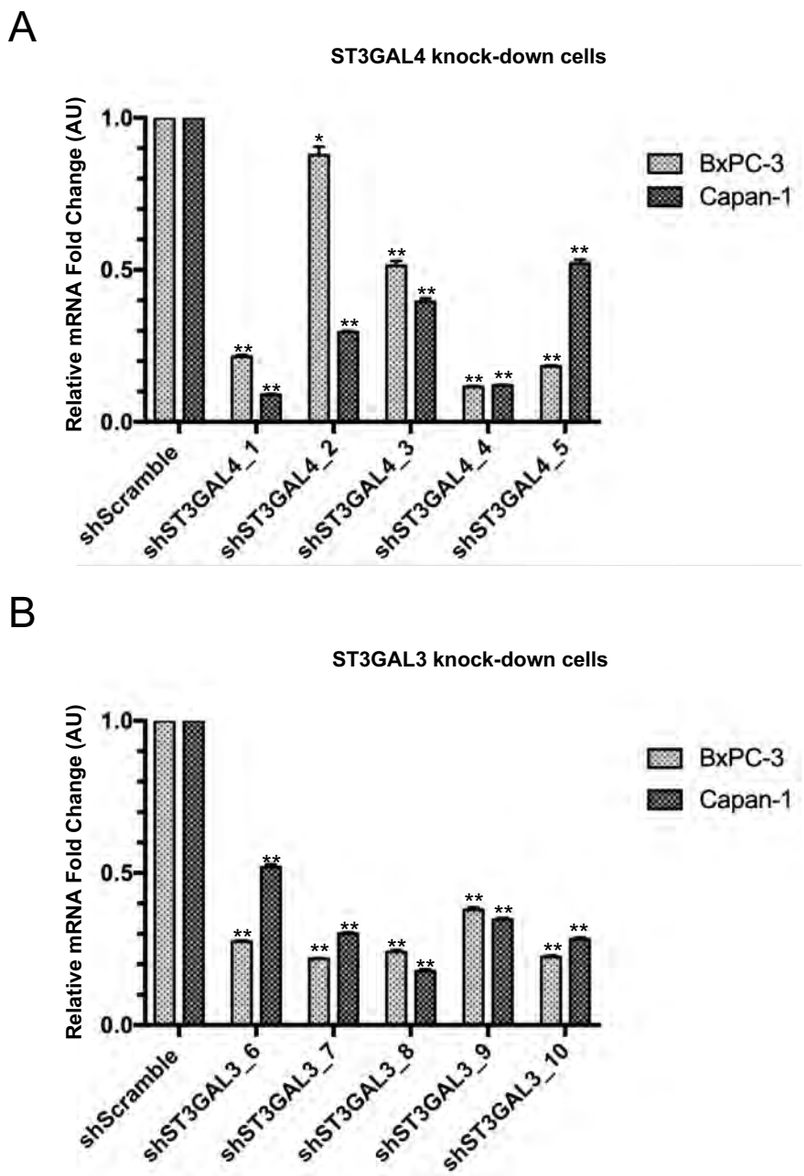

Figure 28 | Relative quantification of ST3GAL3 and ST3GAL4 mRNA expression in pancreatic cells after shRNA transfection. A) RT-qPCR validation of the knock-down of ST3GAL4 (shST3GAL4_1-5 cells) in Capan-1 and BxPC-3. Control cells (shScramble), were generated by stable transfection with non-target scramble vector. B) RT-qPCR validation of the knock-down of ST3GAL3 (shST3GAL3_6-10 cells) in Capan-1 and BxPC-3. RNA levels were normalized using TBP as a housekeeping gene. Data are expressed as means ± SD. of three independent experiments * represents $P < 0.05$; **$P < 0.01$ (Student's t test).

No changes in ST3GAL4/3 expression levels were detected between parental cells and scramble cells, therefore scramble cells were used as a negative control for expression changes in further experiments. For ST3GAL4 KD cells (**figure 28A**), shST3GAL4_1 and shST3GAL4_4 were the ones with the highest knock-down efficiency for Capan-1, showing a decrease of 91 and 87%, respectively. The highest reduction in ST3GAL4 expression in BxPC-3 cells was generated by short hairpins RNAs 1, 4 and 5 with 78, 88 and 81% decrease, respectively. The five different shRNAs designed to silence ST3GAL3 (**figure 28B**) resulted in varying levels of knock-down, all of them greater than 48%. For ST3GAL3 KD cells, shST3GAL3_7 and shST3GAL3_10 showed the best knock-down efficiencies for BxPC-3 (78 and 77% reduction respectively) and shST3GAL3_8 and shST3GAL3_10 for Capan-1 (82 and 71% respectively). To confirm that the knock-down of ST3GAL4 or ST3GAL3 genes did not affect the expression levels of the other ST3GAL genes, we determined the mRNA expression of ST3GAL3, ST3GAL4 and ST3GAL6 genes in all silenced cell lines. As expected, the ST3GAL3 knock-down cells did not show significant changes in ST3GAL4 or ST3GAL6 gene expression. Likewise, the ST3GAL4 knock-down cells did not show significant changes in ST3GAL3 or ST3GAL6 gene expression (data not shown).

2.3 Down-regulation of ST3GAL4 and ST3GAL3 in BxPC-3 and Capan-1 cells reduces SLe^X expression.

To explore how the reduction in ST3GAL4 and ST3GAL3 expression levels leads to changes in cell sialylated glycans in BxPC-3 and Capan-1 cells, glycan expression pattern was analyzed by flow cytometry and western blot in all ten knock-down cells (sh-1 to sh-10), and their respective controls (scramble and parental cells). The knock-down cells that showed major decrease in sialyl Lewis antigens are described below and were selected for further *in vitro* analyses.

In particular, for BxPC-3, shST3GAL4_1 cells were the ones with the most prominent reduction in SLe^X membrane expression –up to 67%– when compared to scramble median values, as shown by flow cytometry **(figure 29**) and western blot (**figure 30**).

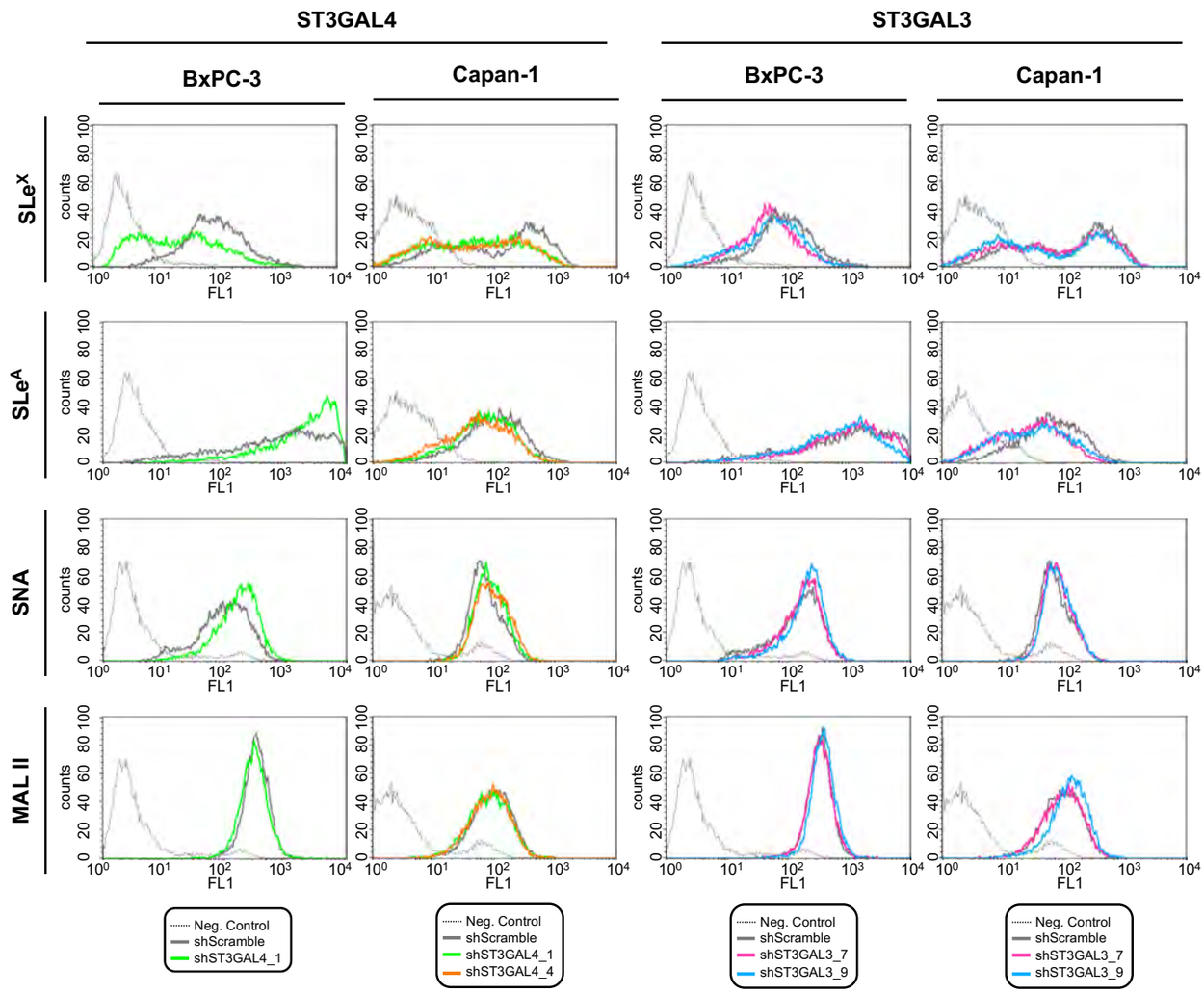

Figure 29 | Glycan analysis of the ST3GAL4 and ST3GAL3 KD BxPC-3 and Capan-1 cells by FC. Sialic acid determinants were analyzed in shRNA stably transduced BxPC-3 and Capan-1 cells. Representative flow cytometry profiles of the cell surface glycans structures detected with SLe^X and SLe^A antibodies and the lectins SNA and MAL II in knock-down ST3GAL4 cells (left) and ST3GAL3 cells (right) over different knock-down cells of BxPC-3and Capan-1. Negative controls (without the primary antibodies or lectins) are represented in a continuous black dot outline: (...), shScramble (black line), shST3GAL4_1 (green line), shST3GAL4_4 (orange line), shST3GAL3_7 (pink line), shST3GAL3_9 (blue line)

Surprisingly, knock-down of this gene led to an increase of SLe^A on cell membrane glycoconjugates detected by flow cytometry (**figure 29**), when we initially expected either to keep the same SLe^A levels or a decrease in SLe^A since ST3GAL4 has been reported to act also on type-1 structures [203]. To confirm these results, CA 19-9 levels, which correspond to the SLe^A antigen, of the total cell lysates were quantified using the mAb 1116-NS-19-9. The levels of CA 19-9 in shST3GAL4_1 BxPC-3 cells confirmed these

previous results and showed a 30% increase in comparison with the ones of scramble BxPC-3 cells.

Lectins' analyses of shST3GAL4_1 BxPC-3 cells showed an increase of 53% in α2,6-sialic acid using SNA (**figure 29**), evidencing a multiple enzymatic competition of α2,3- and α2,6-STs for type-2 chains. This is in agreement with our previous work that describes that increasing levels of SLe^X in the cells are accompanied by a decrease in α2,6-sialic acid content of membrane glycoconjugates [203]. MAL II analysis did not reveal any significant differences in the total amount of α2,3-sialic acid content (**figure 29**). Sialic acid determinants of protein lysates from the selected silenced cells were also tested by western blot using SNA and MAL II lectins. The changes detected in the specific glycan determinants showed the same tendency as the ones obtained by flow cytometry and were found mainly in high molecular weight glycoproteins (data not shown).

For Capan-1, ST3GAL4 KD cells also showed a reduction in SLe^X content and in addition, a decrease of SLe^A levels (**figure 29**). The cells with highest decrease in SLe^X were shST3GAL4_1 and shST3GAL4_4 (64% and 63% reduction respectively), confirmed by western blot of their cell lysates (**figure 30**).

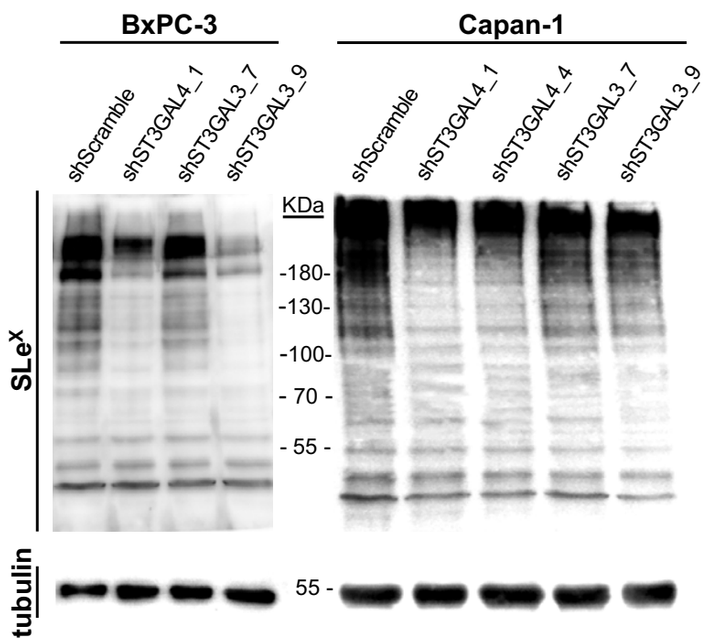

Figure 30 | Glycan analysis of the ST3GAL4 and ST3GAL3 KD BxPC-3 and Capan-1 cells by WB. Immunodetection by western blot showing the reduction of SLe^X antigens in selected cell lysates from total protein on BxPC-3 cells (top left) and Capan-1 (top right) with anti-SLe^x antibody (clone CSLEX). Anti-tubulin western blot of the corresponding membrane is showed on the bottom panel.

They also showed a decrease of 32 and 45% in SLe^A on membrane glycoconjugates, suggesting that ST3GAL4 is also involved in SLe^A biosynthesis in Capan-1 cells as previously described [204]. Increased signal in α2,6-SA content was additionally detected in shST3GAL4_1 and shST3GAL4_4 (35 and 24% in the median values compared with the scramble cells) (**figure 29**). No significant changes in MAL II detected glycans were found either by flow cytometry or western blot.

For BxPC-3, shST3GAL3_7 and shST3GAL3_9 cells displayed the highest reduction in SLe^x with a decrease of 33% and 38% in median values over scramble cells (**figure 29**), as also shown by western blot of their cell lysates (**figure 30**). As expected, ST3GAL3 KD also led to a reduction of SLe^A, which was much more marked in the shST3GAL3_9 cells (31% decrease) than in the shST3GAL3_7 cells (with a very slight decrease of 4%) (**figure 29**). Due to the high SLe^A content of BxPC-3 cells and to overcome the possible saturation in the immunodetection by immunofluorescence, CA 19-9 content was also determined by the quantitative immunoassay and showed a 28% reduction in the shST3GAL3_7 and a 78% reduction in the shST3GAL3_9 cells. Regarding α2,6-SA content, flow cytometry results indicated an increase up to 22% for sh-7 and to 42% for sh-9 (**figure 29**). Both ST3GAL3 KD cells showed also a slight increase in α2,3-SA content in flow cytometry analyses using MAL II lectin (**figure 29**). This result could be explained in part because MAL II lectin is unable to bind to SLe^X / SLe^A structures.

For Capan-1, shST3GAL3_7 and shST3GAL3_9 cells also showed the highest SLe^X reduction, 60% for shST3GAL3_7 and 73% for shST3GAL3_9 (**figure 29**), which was corroborated by western blot of the protein cell lysates and the changes detected were mainly found in high molecular weight glycoproteins (**figure 30**). Reduction of ST3GAL3 also led to a decrease in sialyl Lewis A antigen around 40-50% for both silenced cells (**figure 29**). Regarding the expression of α2,6-SA, there was an increase of 20% for shST3GAL3_7 and 11% in shST3GAL3_9, detected using SNA (**figure 29**). MAL II analyses by flow cytometry did not show differences among clones except for an increase

(39%) shST3GAL3_9 (**figure 29**), which was also confirmed by WB of the protein cell lysates.

Overall, the knock-down of both ST3GAL4 and ST3GAL3 decreased SLe^X levels, in a similar degree for all Capan-1 knock-down cells, whereas in the case of BxPC-3, the reduction of SLe^X expression was more pronounced for the ST3GAL4 KD cells. ST3Gal III enzyme is mostly related with the addition of α2,3-sialic acid upon terminal galactose on type-1 chains (SLe^A precursor) while ST3Gal IV plays the major role in the synthesis of sialylated type-2 chains (SLe^X precursor). However, these results have shown the important role of ST3GAL3 in the SLe^X biosynthesis too. The decrease in SLe^X was more pronounced in Capan-1 ST3GAL3 knock-down cells than in the corresponding BxPC-3 ones. This difference between cell lines could be explained by the Capan-1 lower expression levels of this gene compared to BxPC-3.

The reduction of SLe^A was observed in all ST3GAL3 knock-down cells, being also more pronounced for Capan-1 cells. ST3GAL4 knock-down also resulted in a decrease on SLe^A but only in the Capan-1 cells. BxPC-3 with very high levels of SLe^A did not show a decrease in their corresponding ST3GAL4 knock-down cells, but an unexpected increase. In all cases, the reduction in the α2,3-sialylated Lewis antigens was compensated by an increase of α2,6-sialylated structures, which can be explained by the competition of the α2,6-STs for the same substrates that the α2,3-STs.

Next, the behavior of these knock-down cells, which showed the greatest reduction in SLe^x antigens, was analyzed in cell adhesion and migration processes *in vitro* and in microfluidic devices.

2.4 ST3GAL4 and ST3GAL3 knock-down in BxPC-3 and Capan-1 impaired pancreatic cancer cell migration.

Sialyltransferases have been described to play an important role mediating migration and dissemination events in different cancer cells. In addition, sialylated-Lewis antigens overexpressed upon cell membrane glycoconjugates enhance and modulate a wide variety of pathological events in cancer including the migration degree of tumor cells as previously shown [203,204]. Thus, to determine whether the reduction of those sialylated antigens had a phenotypic effect upon PDA cells, the characterization of their role in cell adhesion and migration events was performed using the ST3GAL4 and ST3GAL3 KD cells with reduced levels of SLe^X on cell surface glycoconjugates.

ST3GAL4 KD cells (shST3GAL4_1 for BxPC-3 and shST3GAL4_1 and shST3GAL4_4 for Capan-1), and ST3GAL3 knock-down cells (shST3GAL3_7 and shST3GAL3_9 for both BxPC-3 and Capan-1) were allowed to migrate using modified Boyden chambers and FBS as chemoattractant. Downregulation of α2,3-STs significantly suppressed cancer cell migration in PDA cells in comparison with scramble cells for both cell lines (**figure 31**).

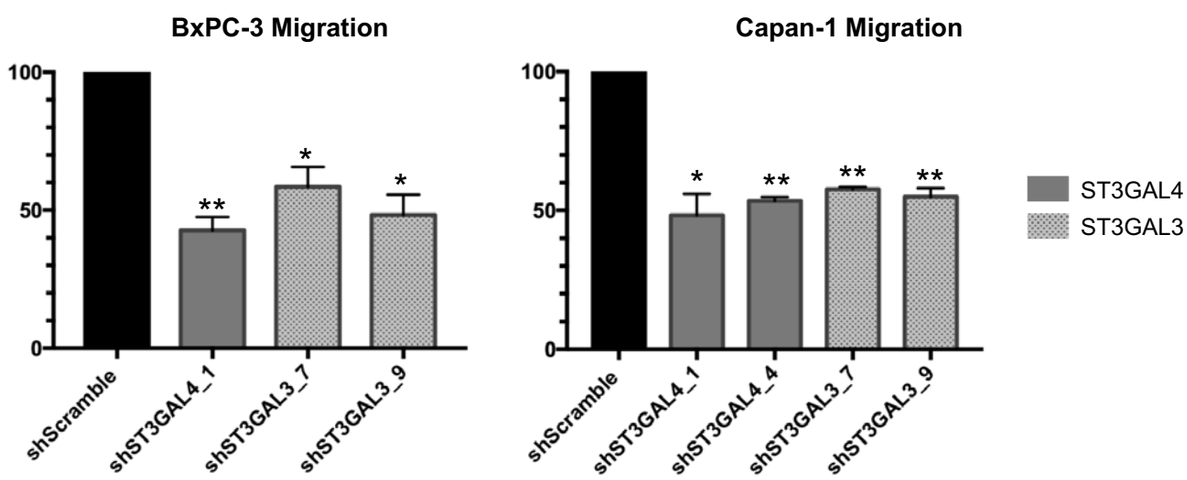

Figure 31 | SLe^X reduction induces impaired cell migration. Relative quantification of cell migration over shScramble cells of BxPC-3 knock-down cells (shST3GAL4_1, shST3GAL3_7 and shST3GAL3_9) (left) and Capan-1 cells (shST3GAL4_1, shST3GAL4_4, shST3GAL3_7 and shST3GAL3_9) (right). Cells were allowed to migrate on 8 µm-pores-type 1-collagen coated Boyden chambers. Migrated cells were fixed and counted. Results are presented as means ± SEM. of three independent experiments * represents significantly different, $p<0.05$, ** $p<0.01$.

In BxPC-3 cells, cell migration was significantly decreased between 41% and 57% of reduction relative to scramble control cells, being shST3GAL4_1 BxPC-3 the cells with higher cell migration reduction (57%). Similar results were obtained with Capan-1 cells which showed also a reduced migration capacity between 42 and 51%. There were no significant differences among the KD cell lines.

To assess whether SLe^X reduction of the ST knock-down cells was a main factor that could explain the decrease in cell migration, scramble cells were incubated with anti-SLe^X mAb CSLEX1 prior to their seeding. Both treated BxPC-3 and Capan-1 scramble cells showed a reduction in migration, up to 59% in BxPC-3, and up to 71% in Capan-1(data not shown). In scramble Capan-1 cells treated with anti-SLe^X antibody, the decrease in migration was notably higher compared to their corresponding silenced clones. The marked decrease degree in cell migration in the α2,3-ST knock-down cells as well as in in the scramble cells treated with anti-SLe^X antibody indicates that SLe^X plays a major part in this process.

The role of α2,3-sialyltransferases knock-down in the promotion of cell migration was also assessed in a different physical microenvironment. In physiological conditions, circulating tumor cells migrate in 3D microenvironments through the degradation of extracellular matrix but also through longitudinal tracks within the ECM (that range from less less than 1 μm to 20 μm in diameter) or bordering with 2D interfaces that generate channel-like tracks created by anatomical structure [282,284]. By using the microfluidic device described in (methods, section 23.PDMS-based microchannel migration assay), the migration of BxPC-3 and Capan-1 KD cells was characterized in both confined (with channels width more narrow than the cell diameter) and unconfined (channels wider than the cell diameter) microchannels of 200 μm of length, coated with collagen type 1 in a polydimethylsiloxane (PDMS) microfluidic chip, mimicking the tunnel-line tracks structures that migrating tumor cells use to reach host tissues.

Unfortunately, Capan-1 cells formed aggregates or died inside the channels and therefore their analysis was not possible. For BxPC-3, shST3GAL4_1 cells, which were the silenced cells with higher reduction in SLe^X, showed significantly suppressed

chemotactically-driven cell migration inside in both confined and unconfined microchannels (**figure 32**).

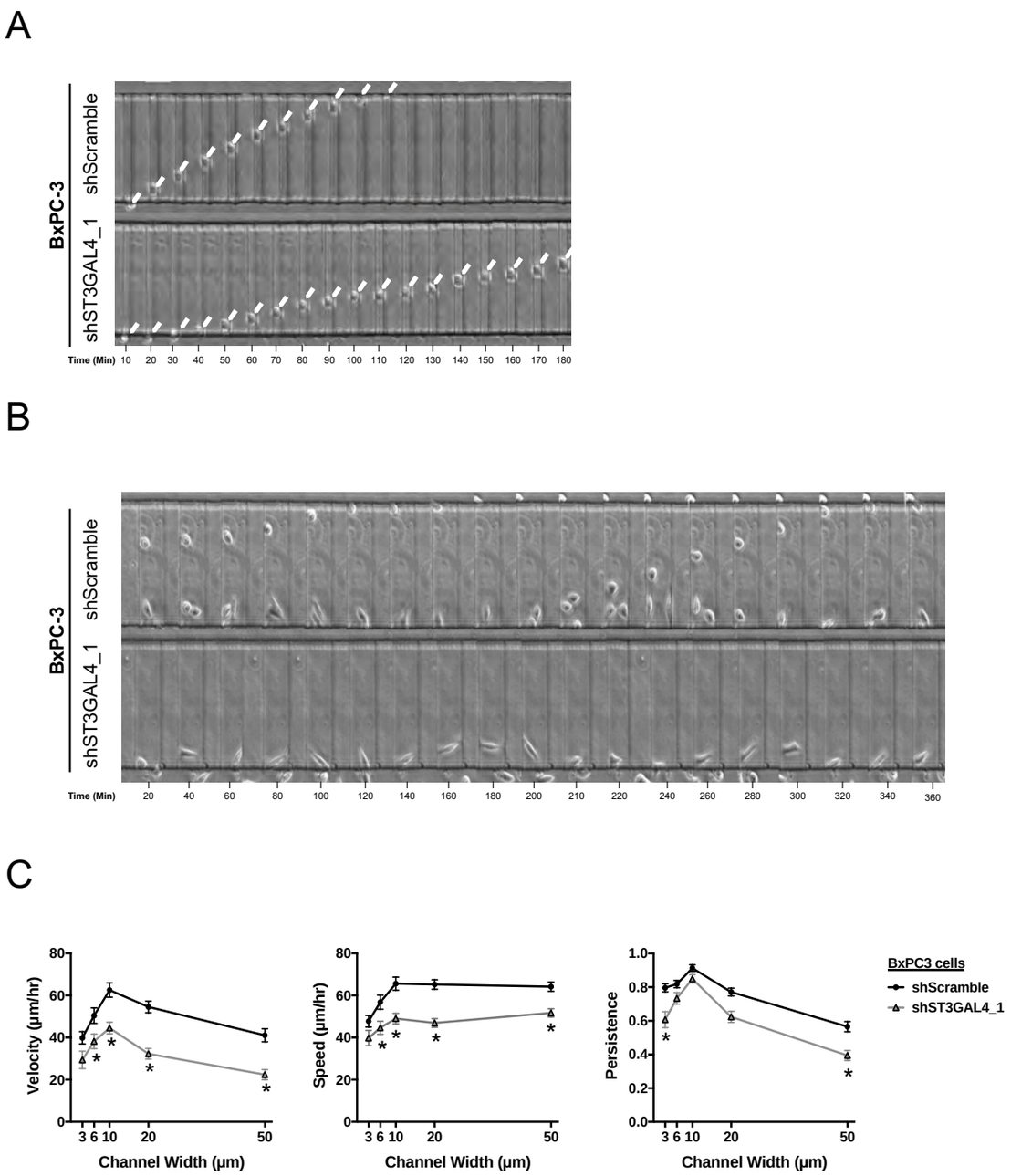

Figure 32 | ST3GAL4 KD in BxPC-3 cells impaired cell confined and unconfined chemotactic migration. A) For depicting the changes in cell velocity illustrative pictures were taken in 10-minute intervals of BxPC-3 shScramble cells (top row) and shST3GAL4_1 BxPC-3 cells (bottom row) migrating inside 10 μm-wide confined microchannels. Arrowheads indicate the leading edge of a migrating cell. B) Illustrative picture showing differences in cell persistence between BxPC-3 shScramble cells (top row) and shST3GAL4_1 BxPC-3 cells (bottom row) migrating inside 50 μm-wide unconfined microchannels in 20-minute time intervals. C) Migration velocity (left panel), speed (middle panel) and persistence (right panel) of scramble control and shST3GAL4_1 BxPC-3 cells in PDMS-based microchannels of 10 μm in height, 200 μm in length, and either 6, 10, 20 or 50 μm in width. Data represent the mean±S.E.M from at least 3 independent experiments. * represents significantly different, $p<0.05$.

BxPC-3 shST3GAL4_1 cells showed a significant lower mobility parameters of speed, velocity in all 6, 10, 20 and 50 µm wide microchannels and reduced persistence in 3, 20 and 50 µM channels in comparison with shScramble BxPC-3 cells. These results confirm that ST3GAL4 knock-down BxPC-3 cells reduce their migration also in a microfluidic system, which closely mimics the physiological conditions.

2.5 ST3GAL4 and ST3GAL3 knock-down reduced cell invasion *in vitro*

To determine whether the decrease in ST3GAL4 and ST3GAL3 expression and their concomitant reduction in SLe^X also impaired the invasion of pancreatic cancer BxPC-3 and Capan-1 cells, transwell invasion assays coated with Matrigel, which mimics a complex extracellular matrix, were performed with the KD cells.

The invasion ability of BxPC-3 knock-down cells was significantly reduced compared with scramble cells (**figure 33**).

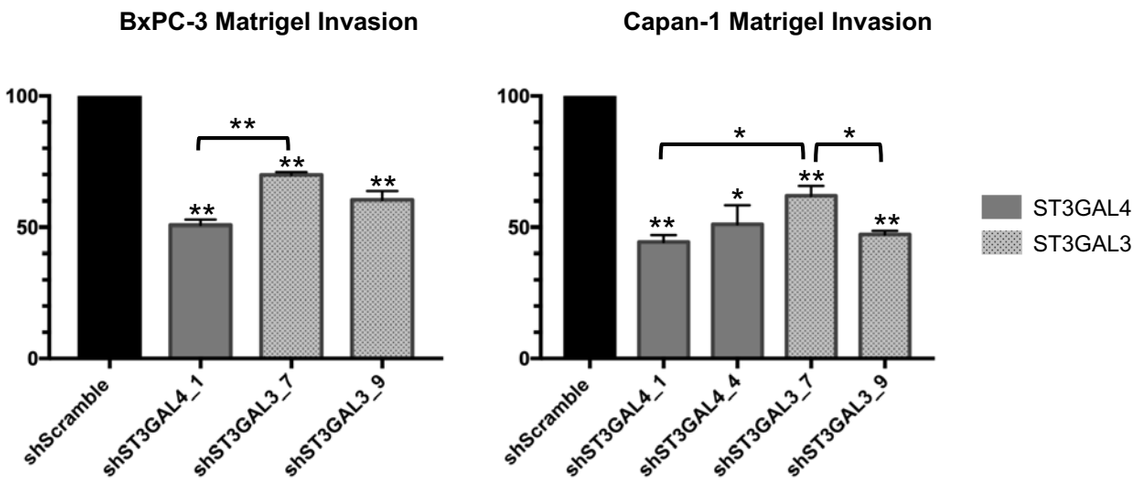

Figure 33 | SLe^X reduction induces impaired cell Matrigel invasion *in vitro*. Tumor cell invasion was evaluated using Boyden chambers in 24-well plates with Matrigel coated inserts. Invading capacity was assessed by quantifying the number of cells that invade in BxPC-3 knock-down (left) and Capan-1 knock-down cells (right) relative to scramble. * represents significantly different, $p<0.05$, ** $p<0.01$.

The shST3GAL4_1 cells showed up to a 49% reduction in cell invasion, significantly higher than the 30% reduction of the ST3GAL3 knock-down shST3GAL3_7 cells. This difference between ST3GAL4 and ST3GAL3 KD cells could be explained by the higher reduction of SLe^X in the former ones (67% vs. 33-38%). Capan-1 KD cells (**figure 33**)

showed also a significant impaired invasive capacity between 55% and 38% with respect to scramble cells. The highest invasive reduction was found for shST3GAL4_1 in the Capan-1 ST3GAL4 KD cells and for shST3GAL3_9 cells in the ST3GAL3 KD cells in analogous percentages, which also showed similar percentages of SLe^X decrease.

To further describe the underlying mechanism of sialylation effect in cell invasion *in vitro*, we performed the invasion assay with blocking antibodies against SLe^X antigens. Scramble Capan-1 and BxPC-3 cells showed an impaired invasion, when treated with anti SLe^X antibody, with decreases of 39% and 55%, respectively. Altogether, these results indicate a positive link between the expression of SLe^X expression and the invasion capability of PDA cells.

2.6 Reduced levels of SLe^X in ST3GAL4 and ST3GAL3 knock-down cells led to a decrease in E-selectin binding.

E-selectin from activated endothelial cells plays a key role in tumor cell-endothelium interactions in the first steps of the tumor extravasation through the binding with sialyl Lewis ligands on tumor cells. The impact of ST3GAL4 and ST3GAL3 KD in both BxPC-3 and Capan-1 cells over E-selectin was explored to examine if sialyl Lewis antigen decrease on surface glycoconjugates of the KD cells was able to induce changes in E-selectin adhesion. To pursue this objective, we first performed an *in vitro* assay to measure the binding of the cells to recombinant human E-selectin (rh-E-selectin) (**figure 34A**).

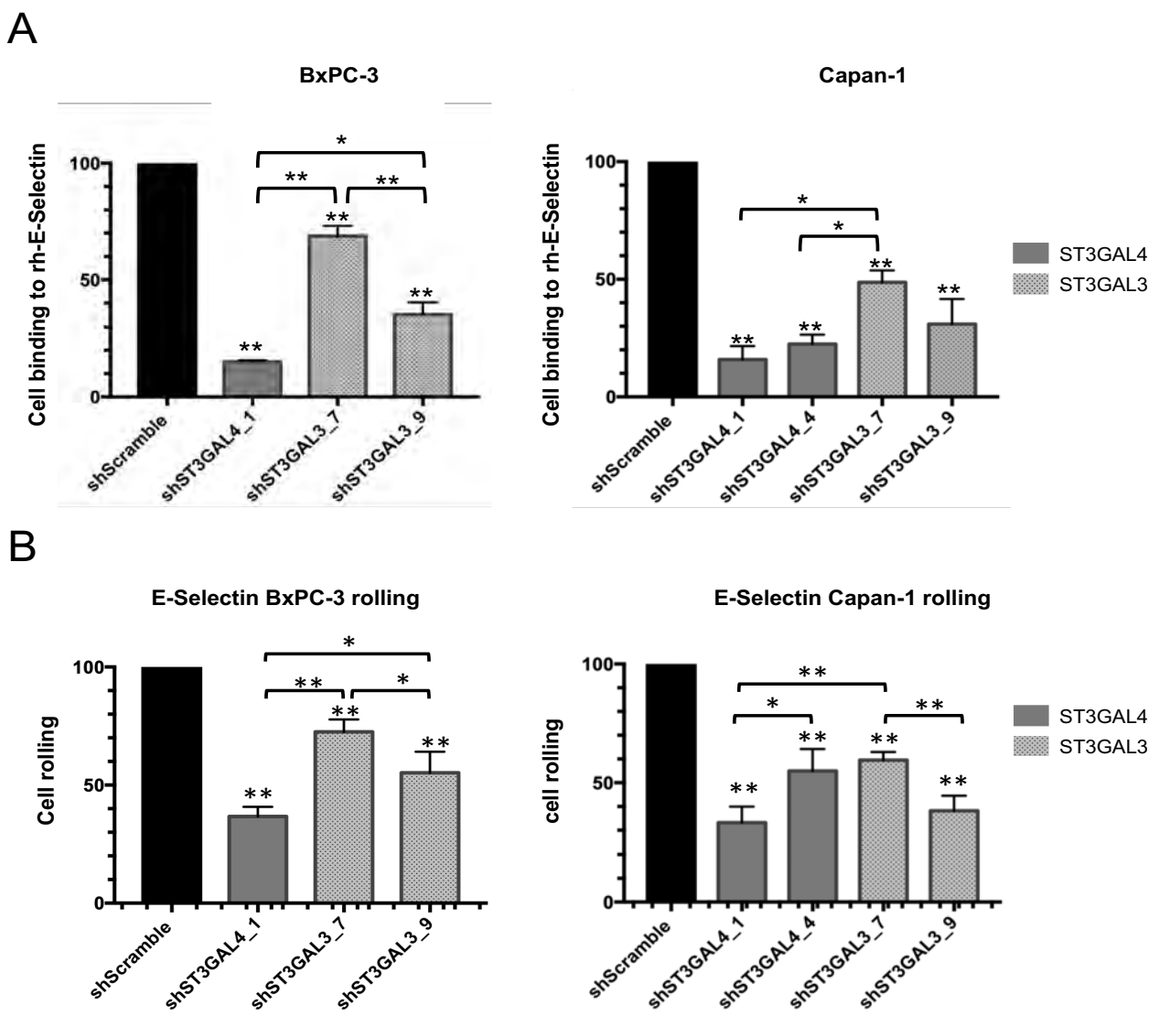

Figure 34 | ST3GAL4 and ST3GAL3 KD inhibited cell adhesion to rh-E-selectin and induced impaired cell arrest and rolling to rh-E-selectin in parallel flow chamber. A) BxPC-3 (left) and Capan-1 cells (right) were incubated over E-selectin coated 96-well plates and allowed to adhere at 37ºC. Adherent cells were quantified after 1h incubation with MTS-based colorimetric assay. Experiments were performed in triplicate. Results are presented as Mean ±S.E.M of adherent cells respect shScramble cells of the independent experiments. * significantly different, P< 0.05, ** p <0.01. B) Reduction in BxPC-3 (left) and Capan-1 (right) knock-down cells arrest and rolling over rhE-selectin in comparison with ST3GAL4 and ST3GAL3 scrambled cells flowed over immobilized E-selectin. Graphs depict means and SD. from at least three independent experiments.

Both cell lines, BxPC-3 and Capan-1, displayed similar adhesion levels to E-selectin and all KD cells significantly decreased their adhesion to rh-E-selectin compared to their respective scramble cells, which could be explained by their reduction of the sialyl Lewis antigens' levels compared to their corresponding scramble cells.

In BxPC-3, The shST3GAL4_1 cells presented an 84% reduction in adhesion compared to scramble cells, significantly higher than the decrease shown for the ST3GAL3 knock-down cells shST3GAL3_7 and shST3GAL3_9 (reduction in 31% and 64%, respectively). The higher decrease of the ST3GAL4 KD cells (shST3GAL4_1) could be explained by their higher reduction in SLe^X levels compared with the ST3GAL3 KD cells. Among the ST3GAL3 KD cells, shST3GAL3_7 displayed a lower reduction in SLe^X and SLe^A than shST3GAL3_9 cells, which could explain their lower decrease in E-selectin adhesion compared to shST3GAL3_9.

In Capan-1, the ST3GAL4 KD cells, shST3GAL4_1 and shST3GAL4_4, also showed higher reduction in E-selectin adhesion (84% and 77%, respectively vs. scramble cells) compared to the 51% and 69% reduction in rh-E-selectin binding of the ST3GAL3 knock-down cells shST3GAL3_7 and shST3GAL3_9 respectively, being significantly different between shST3GAL4_1, shST3GAL4_4 and shST3GAL3_7. The significant differences in E-selectin binding between Capan-1 ST3GAL4 and ST3GAL3 knock-down cells could not be explained by their SLe^X and SLe^A levels since both levels were quite similar between them.

Nevertheless, the importance of SLe antigens in E-selectin binding was demonstrated when scramble BxPC-3 and Capan-1 cells were incubated with anti-SLe^X. Their adhesion to E-selectin was abrogated impairing the binding up to the 82% of the pre-incubated cells with antibodies against SLe^X, which indicates that SLe^X drives the main mechanisms involved in the binding to human E-selectin *in vitro.* However, other factors apart from sialyl Lewis expression may influence to explain the differences in E-selectin adhesion between the ST3GAL4 and ST3GAL3 knock-down cells.

To further investigate the functional importance of ST3GAL4 and ST3GAL3 in the binding of pancreatic tumor cells to E-selectin, this interaction using a microfluidic system was analyzed. For that, a perfusion under a physiologically level of shear stress of the BxPC-3 and Capan-1 scramble and KD cells over immobilized E-selectin was performed and changes in cell arrestment and the interaction of cell singlets were counted (**figure 34B**). Scramble cells for both cell lines showed again more interactions with E-selectin in comparison with KD cells corroborating what had been observed in the previous experiments. In the case of the BxPC-3 cells, ST3GAL4 KD cells, shST3GAL4_1 were again the ones that showed less interactions with E-selectin. For Capan-1 cells, the highest reduction was found for shST3GAL4_1 in the Capan-1 ST3GAL4 KD cells and for shST3GAL3_9 cells in the ST3GAL3 KD cells in analogous percentages.

Altogether, these results highlight the role of these α2,3-STs in key steps of cell metastases. They show that the reduction of sialyl Lewis X can be used as a target in key steps of metastasis, since we observed a strong decrease in the reduction of migration, invasion and binding to E-selectin in all the ST3GAL4 and ST3GAL3 KD PDA cells with reduced sialyl Lewis X levels.

V. Discussion

Pancreatic ductal adenocarcinoma (PDA) the most common pancreatic cancer type, is a very aggressive malignancy associated with poor prognosis because of recurrence, metastasis, and high treatment resistance. The overall 5-year survival rates of only 9% reflects the grim prognosis of PDA patients. This dismal scenario is frequently attributed, at least partially, to late-staging at the time of diagnosis, when metastasis has occurred or the disease is already unresectable. By 2030 in USA, PDA is estimated to surpass from the fourth leading cause of cancer-related death to become the second [16,17] . This estimation is consequence of unfruitful efforts in identifying accurate predictive biomarkers and almost no progress in therapeutic approaches [295]. The need for prompt detection is recognized globally as one of the most promising approaches to significantly improve the long-term survival of PDA patients, and it has been also recommended by health organizations [151,296].

Cancer biomarkers are a useful tool for early detection, diagnosis and prognosis of the disease. They are also heavily relied on management of patients, assessment of pharmacodynamics of drugs, and relapse of the disease [297]. Efforts in the research have been made with diverse new methodologies such as genomics and proteomics towards the identification of novel candidates. However, many of them fail in FDA verification or lack sensitivity and specificity enough, being elevated in other cancers or benign pathologies. Thus, difficulties arise in clinically differentiating the two different conditions and in decreasing the number of false positives.

Interestingly, changes in glycosylation upon cell surface during cancer development have been a hallmark of cancer transformation for decades. Those glycoproteins which are structurally altered in their glycan moieties and aberrantly expressed upon cancer [105] offer a fruitful opportunity in the discovery of novel cancer biomarkers. Importantly, most cancer biomarkers which are routinely used in the clinical setting such PSA, AFP, CEA, CA 15-3, CA 125 and CA 19-9 among others are glycoproteins [298]. Interestingly, CA 19-9 measures the glycan moiety of a mucin and is used as a marker for the monitoring of pancreatic cancer.

Still, the use of glycoproteins as tumor markers is typically focused on the detection of the protein levels. However, the clinical monitoring in the changes of certain glycans on the glycoprotein (protein glycoforms) has shown that is a powerful tool. In fact, this is already used for alpha-fetoprotein (AFP) in hepatocellular carcinoma and CA 15-3 for breast cancer. Nonetheless its use is still scarce nowadays [297,299]. In order to overcome this problem, in recent years, the use of lectins (a group of proteins of nonimmune origin that bind with high specificity to mono and oligosaccharides) for screening of potential biomarkers has gained increased importance in cancer research. The inclusion of lectins against specific glycan determinants associated to cancer or TACAs, has allowed the detection of those glycan changes in glycoconjugates in biological fluids of cancer patients. As a matter of fact, work developed in our laboratory has proven the utility of glycosylation changes in PSA by using lectins and specific PSA glycoforms have shown to improve the specificity of this tumor marker to identify high-risk prostate cancer patients [300,301]. In particular, by chromatography with *Pholiota squarrosa* (PhoSL) and *Sambucus nigra* agglutinin (SNA) lectins (against core fucosylation and α2,6-sialic acid respectively upon PSA), we could identify a significant decrease in the core fucosylation and an increase in the α2,3-sialic acid percentage of PSA in high-risk prostate cancer patients with higher sensitivity and specificity than using PSA biomarker alone [300]. Other methods that could help in measuring potential changes in the glycan moieties of glycoproteins, includes either antibodies against carbohydrate structures or glycan binding proteins.

Anomalous glycosylation therefore, represents a feature that could bring new biomarker candidates to prompt detection of PDA, an urgent need to significantly improve the survival of cancer patients as mentioned before. In a previous review, our group evaluated the potential of several candidates that could work as possible biomarkers for pancreatic cancer such as mesothelin, IGFBP-3, IGFBP-2, REG family member including REG1A/1B/3A/4, TIMP-1 and HER-2 [298]. Also, recent work from our group showed that TACAs (tumor-associated antigens distinctly expressed in large number of tumor tissues, but not in their corresponding non-tumor tissue) represent a rich source for the identification of novel PDA cancer markers. Among these glycosylation changes, variations in sialylation levels and linkage during cancer progression have been

thoroughly reported in literature since a wide spectrum of sialylated glycoproteins are secreted by the tumor [302].

In this work, we have focused our attention on the carbohydrate structure sialyl Lewis X (SLe^X), which is a TACA in PDA. SLe^X is commonly expressed over 80% of PDAs [303,304] while it is not detected in healthy pancreatic specimens [303]. Also, SLe^X could be reflected in the serum secreted tumor proteins. In this regard, our group already described in 2010 an increase in the levels of SLe^X of several serum glycoproteins in advanced PDA [286]. However, these reported glycoproteins carrying SLe^X were acute-phase proteins mainly liver derived and did not shown enough specificity for PDA. On this subject, our group has also described the presence of glycoforms containing SLe^X in glycoproteins such as Mucin 5AC (MUC5AC) and ceruloplasmin (CP) as potential serum PDA biomarkers [291,305].

Overall, TACAs are already involved in practically all stages of tumor progression and ultimately contribute to more aggressive cell phenotypes including PDA [306]. Therefore, this work has highlighted the transversal role of SLe^X in PDA for improving two key aspects of patient's survival in the disease: Early detection and new targets for treatment. The dual approach of this work intends to provide on the one hand, new potential biomarkers carrying SLe^X for PDA early detection before the disease turns to unresectable. On the other hand, this work has focused on understanding the SLe^X contribution on PDA biology through the analysis of the role of STs and SLe^X in tumor migration, invasion and adhesion in order to evaluate in future the utility of these enzymes as PDA therapeutic targets against disease evolution.

Microfibril Associated Protein 4 (MFAP4) is a carrier of the tumor associated carbohydrate sialyl Lewis X (SLe^X) in pancreatic adenocarcinoma.

The first objective of this thesis, which is focused on finding novel biomarkers for PDA based on SLe^X carrier glycoproteins that could come from the pancreatic tumor tissue, has been developed by a glycoproteomic approach. To accomplish this goal, we analyzed target proteins containing SLe^X in their glycans from PDA tissues by using 2DE and

immunodetection techniques. This approach has led to the identification by mass spectrometry of the protein Microfibril Associated Protein 4 (MFAP4) as potential novel PDA biomarker.

MFAP4, is an extracellular glycoprotein of about 36 KDa that form disulfide-linked higher structures of homodimers, trimeric and hexameric structures mainly [307]. The N-terminus of MFAP4 has a conserved Arg-Gly-Asp (RGD) sequence associated with cell adhesiveness and as ligand for cell surface integrins [308,309] and a C-terminal fibrinogen-related domain (FReD). MFAP4 is typically found in extracellular matrix fibers, being MFAP4 highly expressed in blood vessels [310,311], elastic tissues and vascular walls [312]. Concerning the biological role of this protein, it is well stablished that, MFAP4 has a dynamic role in elastic fiber assembly and in the maintenance of ECM proteins. MFAP4 binds fibrillin-1 [313] and fibrillin-2, in presence of calcium, MFAP4 can also bind to desmosine (involved in elastin cross-link) and to tropoelastin, promoting its self-assembly (coacervation) [307]. Several models describing the role of MFAP4 in elastic fiber assembly have been proposed (**figure 35**).

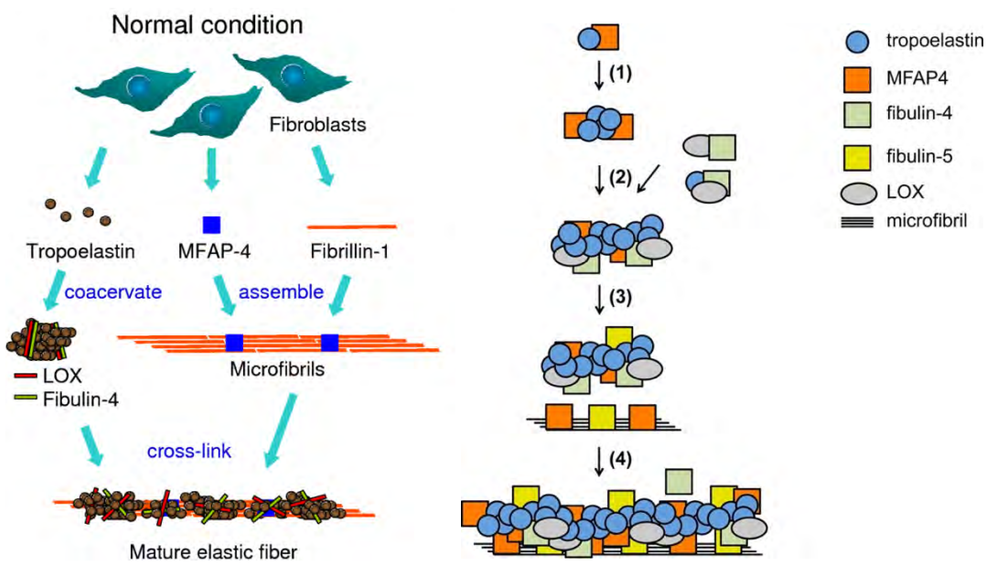

Figure 35 | Diverse models of the role of MFAP4 in elastic fiber assembly. Schematic representations extracted from [313] (left) and [307] (right).

In general, the abundance of microfibril-associated proteins in the extracellular matrix of both developing and mature tissues, suggests that those microfibril-associated proteins generate a niche that influences cellular phenotypes, such as the regulation of tissue development and repair [314]. Furthermore, it has been described that MFAP4 can induce

cell migration and proliferation dependent on integrin-associated signaling in vascular smooth muscle [310]. The role of MFAP4 in malignancy remains not well understood; it has been associated so far with mechanism of fibrogenesis: plasma levels of MFAP4 are associated with liver fibrosis [315], and serum levels are also increased in hepatic cirrhosis patients with hepatitis C [316,317]. MFAP4 has also been associated with pulmonary diseases [318], atherosclerotic [310] and diabetic neuropathy [319] and has been found upregulated in pleomorphic adenoma [320].

Despite changes in MFAP4 expression have already been described in other malignancies and human cancers, this study represents the first investigation of this glycoprotein in pancreatic cancer samples (including different PDA cell lines and their corresponding conditioned media and PDA patients' tissues). Our results revealed that MFAP4 was not detected in any the whole range of the PDA cells analyzed in this work, either in cell lysates or in conditioned media, but was found in the pancreatic extracellular matrix of the PDA patients. Therefore, the presence of MFAP4 in the stroma would come from some of the different cellular types found in PDA stroma, such as fibroblasts [313].

Interestingly, we have observed a trend where MFAP4 protein levels in pancreatic tissue samples seems to be higher in the PDA samples in comparison with samples from non-tumor pancreas. In other carcinomas, is not clear yet if MFAP4 expression is associated with malignancy since there are relatively few and not always coincident data in the literature. Thus, MFAP4 has been found to be upregulated in aggressive prostate cancer [321] but on the contrary, other study described MFAP4 downregulation in prostate cancer compared to benign prostate hyperplasia [322]. Recently it has been described that MFAP4 downregulation by microRNA-147b can promote lung adenocarcinoma invasion and migration [323]. MFAP4 is also upregulated in low-risk breast cancer in comparison with high-risk [324]. Also, an OMICS analysis which analyzed MFAP4 expression as a novel biomarker in human cancer, found a dual role of this protein. MFAP4 is frequently downregulated in human cancers, however high levels of MFAP4 predicted poor prognosis in advanced stages of lung, breast and stomach cancer [325]. MFAP4 mRNA levels have been described as prognostic marker in renal cancer

(unfavorable), head and neck cancer (favorable), ovarian cancer (unfavorable) and urothelial cancer (unfavorable), but not in PDA [326], https://www.proteinatlas.org/ENSG00000166482-MFAP4/pathology.

Since MFAP4 is highly expressed in extracellular matrix fibers and blood vessels [310], elastic tissues and vascular walls [312], we hypothesize that the increase of MFAP4 in PDA could be directly explained for presence of the highly dense fibrotic stromal reaction that occurs in PDA, known as desmoplasia. The positive staining for MFAP4 in the IHC analysis has shown the localization of this glycoprotein in the stroma of PDA tissues. Stroma is mainly composed of abundant extracellular matrix, myofibroblast-like cells (pancreatic stellate cells), fibroblasts, blood vessels, immune cells and a dense environment of cytokines, growth factors and proteins that favor tumor progression and invasion [13,28,29]. In this fibrotic and vascular environment MFAP4 overexpression seems reasonable. Although more studies are needed to determine whether the protein level of MFAP4 alone or in combination with other biomarkers could have diagnostic ability in early stage of PDA, our results made us to focus not just in the protein levels, but also in its glycosylation.

Previous N-glycan analysis of MFAP4 had shown that this glycoprotein contained two N-glycosylation sites occupied in human liver tissue F**N**GSVSFFR (N87) and VDLEDFE**N**NTAYAK (N137) [327], and one of them was also found in a broad analysis of human plasma N-glycoproteins [328]. Very recently, a study focused on a glycoproteomic analysis shed light onto some of the glycopeptides present in MFAP4 in the aortic ECM [311]. While the glycosite N87 was occupied by high-manose class glycans, in N137 other hybrid and complex structures containing fucose and sialic acid residues were found. Those changes in the glycan composition of MFAP4 such as increasing of negative charge due to sialic acid presence, may confer a higher electrostatic affinity to proteins with positive charge [314]. In this work, we have described that MFAP4 carries the SLe^X structure in their N-glycans in PDA tissues.

Although the specific role or influence of this MFAP4-SLe^X glycoform in the biological function of stromal pancreatic cancer cells remains to be elucidated, our group among others, has described that SLe^X antigen is expressed during malignant transformation and induces an increase in the invasive capability in PDA [203,204] and in gastric carcinoma. In this last, SLe^X upon glycoproteins, is able to induce c-Met activation and downstream signaling pathways [254]. Hence, we could hypothesize that MFAP4 could play a not yet understood role in carcinogenesis and fibrosis, not only at the protein level, but also regarding the changes in its glycan content, especially the MFAP4-SLe^X glycoform.

Another member of the microfibril associated protein family, MFAP2, has been found in ovarian cancer and its expression has been shown to correlate with poor prognosis. MFAP2 can bind and activate αVβ3 integrin and downstream effectors, contributing to ovarian cancer cell survival, adhesion and also endothelial cell motility and survival in ovarian serous cancer cells [329]. In agreement with those observations, it has been reported that MFAP4 may also induce integrin αVβ3–mediated human VSMC migration and proliferation [312], and it has been described that TGF-β signaling can induce MFAP4 expression [311]. In addition, it has been reported that MFAP4 plays essential roles in the maintenance of ECM proteins such as collagen I contributing to maintenance of tissue integrity [313]. Among these ECM proteins, especially collagen but also others such as laminin and fibronectin, are associated with chemo-resistance in PDA *in vitro* providing physical barriers to drugs [38,330]. ECM proteins play an important role in mediated malignant phenotype, since proteins such as collagen I in PDA can enhance its proliferation and migration via integrin-ECM pathways [331,332]. Despite the effect of MFAP4 expression seems to be different over different carcinomas, MFAP4 potential role in cancer cell motility and survival should be studied deeper to a better depict the MFAP4 role in PDA.

In summary, in this part of the work MFAP4 glycoprotein has been identified as a carrier of SLe^X antigen in pancreatic cancer tissues and not in pancreatic control tissues, which suggests that this particular MFAP4 glycoform could be investigated as a potential

diagnostic or prognostic biomarker for pancreatic cancer. The presence of this glycoprotein was not detected in PDA cells but in the stroma of the PDA tissues. Thus, we could hypothesize that MFAP4-SLe^X glycoform may have a role interacting with the PDA dense fibrotic stroma and ECM proteins. Taking into account that desmoplasia is one of the PDA hallmarks favoring the invasive and metastatic capabilities of cancer cells, changes in MFAP4 glycosylation, specially the presence of sialylated structures as SLe^X may result in important functional differences not only in microfibril development but also due to changes in the interaction of MFAP4 with other ECM proteins in stroma remodeling.

Knock-down of α2,3-sialyltransferases in pancreatic cancer cells impairs their migration, invasion and E-selectin adhesion.

Another mayor cause of PDA poor prognosis is the high chemo resistance of the disease, where most of treatment options fail in their effectiveness. For this reason, the other topic this thesis has focused on, is the study of potential gene targets to reduce cancer cell migration and metastasis. Gene knock-down technology represents a relatively simple methodology that allows to study gene functions in living organisms. Through the inactivation of gene expression and its correspondent reduction in protein expression, we are able to determine the phenotypic change produced by silencing gene expression. Therefore, we could depict the implication of the target gene in cancer progression in order to develop new drugs to inhibit the gene if it favors carcinogenesis.

To accomplish this goal, we relied again in glycobiology. Approximately half of all mammalian proteins are glycosylated and more than 200 glycosyltransferases act in the regulation of glycosylation. Such a complex machinery is also altered in cancer. Thus, aberrant glycosylation is closely involved in cancer progression, triggering processes, such as immune modulation, tumor cell dissociation, migration and invasion among others. Sialylation is a common example of those altered glycosylation during malignant transformation since altered sialylation has been associated with tumor cell survival

pathways, immune regulation for cancer progression, EMT induction and promotion of cancer cell migration and invasion [302].

Changes in glycosyltransferases and genes involved in the sialylation pathway are highly dysregulated in cancer processes. However, nowadays still exists a dearth of knowledge regarding the significances of these changes in the sialyltransferase genes. For this reason, in this work we have addressed the impact of knocking-down the α2,3-sialyltransferases ST3GAL3 and ST3GAL4 that lead to SLe^X and SLe^A biosynthesis in the migration, invasion and E-selectin adhesion capability of pancreatic cancer cells.

Diversity in sialyl Lewis antigens' and their corresponding glycogenes' expression in PDA cells.

First, the expression levels of the α2,3-sialyltransferases and α1,3/4-fucosytransferases involved in the biosynthesis of SLe^X and SLe^A in mammals as well as the levels of these sialyl Lewis antigens in cell surface, lysates and conditioned media were evaluated in seven pancreatic cancer cell lines of different genetic complexity that cover the wide tumor heterogeneity that can be found in PDA.

In all PDA cells, ST3GAL4 was much more expressed than ST3GAL3 (from 4 to 20-fold increase depending on the cells line). These results were in accordance with the higher expression level of ST3GAL4 compared to ST3GAL3 described in pancreatic adenocarcinoma tissues, where ST3GAL4 levels were about four-fold higher than the mean of pancreatic control tissue, while ST3GAL3 levels were only two-fold higher compared to pancreatic control tissue [204]. Similar results on higher ST3GAL4 expression compared to ST3GAL3 expression have also been reported in gastric carcinoma [333]. ST3GAL6 was expressed at very minor levels and could only be detected in Capan-1 and BxPC-3, at much lower levels than for ST3GAL3, in agreement with our previous data [256].

The expression levels of the α1,3/4-fucosyltransferases (FUT3, 5, 6, 7 and 9) that catalyze the transference of fucose residues to the N-acetylglucosamine (GlcNAc) on the α2,3-sialylated type-1 and type-2 precursors [197] were also analyzed. We found that among the α1,3/4-fucosyltransferases, the only α1,3/4-fucosyltransferase that presented noticeable levels was FUT3, which showed higher mRNA expression in five out of the

seven pancreatic cancer cell lines, being Capan-1 the one with highest level, in agreement with recent published data, which found FUT3 between the top-upregulated genes in the aggressive pancreatic cancer cell line Capan-1 [334].

The levels of SLe^X and SLe^A epitopes on the glycoconjugates of the seven PDA cells were variable among them as expected by their different α2,3-sialyltransferases' and α1,3/4-fucosytransferases' expression. SLe^X levels detected in the cell glycoconjugates by flow cytometry were in accordance with the levels detected in the glycoproteins from cell lysates and cell conditioned media, while for SLe^A there were some discordances in some of the cell lines, which showed moderate levels by flow cytometry and almost undetectable levels from the cell lysates and conditioned media (Capan-1, HPAF-II and Panc 10.05) or *viceversa* (SW 1990). These discordances could be in part attributed to the different type-1 acceptors that lead to SLe^A antigen, which could differ between cell lines. These antigens could be found on glycolipids when mainly detected by flow cytometry or on glycoproteins when mainly detected from the cell lysates and conditioned media.

Regarding the different SLe^X levels between cell lines, they could not be explained by a simple combination of a specific α1,3/4-FucTs or an α2,3-ST but through the combination of the several expressed FucTs and α2,3-STs, considering that ST3GAL4 was not a limiting gene in these cells. AsPC-1 and HPAF-II showed almost undetectable levels of SLe^X and SLe^A antigens probably due to very low levels of α1,3/4-FucT, FUT3, and on the contrary Capan-1 that showed the highest SLe^X levels was the one with the highest levels of FUT3.

SNA and MAA analysis also showed different expression levels of α2,6 and α2,3-sialic acid determinants' expression among these seven PDA cell lines. The wide diversity in glycan expression of these different PDA cell lines is a reflection of their different phenotype and metastatic potential in agreement with the results obtained from the analyses of N-glycans determinants of several PDA cells [335].

From the seven pancreatic cancer cell lines, Capan-1 and BxPC-3, were the ones chosen to knock-down the α2,3-STs (ST3GAL4 and ST3GAL3) because they presented the

highest levels of SLe^X in their cell glycoconjugates, total protein lysates and conditioned media determined by flow cytometry and western blot analysis respectively, and also showed high to moderate levels of SLe^A.

ST3GAL4 and ST3GAL3 knock-down effects on SLe^X/ SLe^A cell levels

Both ST3GAL4 and ST3GAL3 gene silencing resulted in a significant reduction of SLe^X in both cell models on their cell glycoconjugates and glycoproteins. For Capan-1 cells the decrease was similar (60-67%) for all knock-down cells while for BxPC-3 cells, the decrease in SLe^X, was significantly higher for ST3GAL4 knock-down cells (70%) than for ST3GAL3 knock-down ones (32-40%), reinforcing the role of ST3GAL4 in SLe^X biosynthesis as previously described [201,202]. However, ST3GAL3, which codifies for the main enzyme involved in the synthesis of α2,3-sialylated type-1 structures that lead to SLe^A biosynthesis, has also a master role in the SLe^X biosynthesis in both pancreatic cancer cell models. These results are also in agreement with other studies on pancreatic, gastric and breast cancer cells where the overexpression of ST3GAL3 led also to an increase of SLe^X antigen [203,250,253].

Regarding the changes in SLe^A amounts, Capan-1 cells showed a decrease in SLe^A expression by flow cytometry in a range of 30-50% in both ST3GAL4 and ST3GAL3 knock-down cells, while for BxPC-3 the decrease in SLe^A was only detected in one of the ST3GAL3 knock-down cells (shST3GAL3_9) in a 30% decrease. The silenced ST3GAL3 knock-down cells that presented this reduction (shST3GAL3_9) showed much higher changes in their functional properties than the ST3GAL3 knock-down cells that did not present a reduction in SLe^A (shST3GAL3_7), as discussed below. ST3GAL3 codifies for the enzyme that preferentially acts on the type-1 structures over type-2 structures while ST3GAL4 is more active on type-2 and type-3 structures than on type-1 structures [336], which explains the decrease in SLe^A in the ST3GAL3 silenced cells.

Reduction of the α2,3 sialylated-Lewis antigens in the knock-down cells also led to an increase in α2,6-sialic, which can be explained through enzymatic competition of α2,3

and α2,6-STs for type-1 and 2 chains, determined by SNA, in agreement with our previous works [203].

ST3GAL4 and ST3GAL3 silencing effects on migration and invasion capabilities of the tumor cells

The KD of both ST3GAL4 and ST3GAL3 generated a significantly reduction in the migratory (42-57%) and invasiveness ability (33-67%) in both BxPC-3 and Capan-1. Within each cell line, there were not significant differences between the ST3GAL4 and ST3GAL3, except for the matrigel invasive experiments, where the ST3GAL4 knock-down cells shST3GAL4_1 for both BxPC-3 and Capan-1 and the ST3GAL3 knock-down cells shST3GAL3_9 for Capan-1 showed the highest reduction. The reduction of these motility capacities was shown to be mediated by the decrease in the sialyl Lewis antigens as demonstrated with blocking experiments using antibodies against SLe^X that led also to a reduction in cell migration and invasion. These results are in agreement with previous works that show that the increase of SLe^X via ST3GAL4 or ST3GAL3 overexpression in other carcinomas such as pancreas, gastric or breast leads to an increased invasive phenotype [203,204,250,253]. ST3GAL4 KD cells have also been reported resulting in decreased ability of cancer cells to adhere to selectins [201] and to invade and migrate *in vitro* in gastric cancer [337]. Given the importance of the desmoplasia in PDA, these results highlight the contribution of SLe^X, at least in part, to the regulatory mechanism for the cells to become more motile among the dense stroma characteristic of this tumor favoring its metastatic capability.

Recently, KD experiments in Capan-1 cells of one of the fucosyltransferases (FUT3) involved in the linking of terminal fucose monosaccharides in α1,3 and α1,4-linkage in the latest steps of SLe^X and SLe^A respectively, showed a high reduction in colony formation and migration through wound closure in those silenced FUT3 Capan-1 cells [334].

Regarding the mechanisms underlying the described phenotypic changes, it has been described that one of the possible molecular mechanisms that could explain the increased invasive phenotype in overexpressed ST3GAL4 in gastric cancer cells with a concomitant

increase in SLe^X could be mediated through the activation of tyrosine kinase receptors such as c-Met and their associated downstream signaling effectors [254]. This activation has been postulated to be initiated by secreted and membrane glycoproteins carrying SLe^X. In this regard, we have also shown that an increase in SLe^X in pancreatic cancer cells overexpressing ST3GAL3 alters the glycosylation pattern and modulates the function of important cell membrane glycoproteins, such as α2β1 integrin and E-cadherin, involved in tumor cell adhesion and invasion mechanisms [257]. Altogether these works evidence the importance of the sialic acid determinants, in particular of SLe^X in the tumor cell progression steps. Further research is therefore needed to elucidate the SLe^X carriers and their specific interactions with glycoproteins involved in mediating cell-ECM or cell-cell interactions and migration.

ST3GAL4 and ST3GAL3 silencing effects on E-selectin binding of tumor cells

Metastasis is one of the main targets to fight against PDA. Metastasis consists of a multistep process which starts from the tumor cell migration in the primary tumor until the development of secondary tumors in a distant organ. In between, cancerous cells have had to extravasate the endothelium in the blood vessels, being sialyl Lewis antigens crucial ligands involved in the initial steps of rolling and arresting of the tumor cells on the activated endothelial [214]. Those inhibition of selectin-ligands, has been widely reported as a potential tool to fight against metastasis and tumor growth over the last decades.

In this work, we have demonstrated significant impaired binding to human recombinant E-selectin of the ST3GAL4 and ST3GAL3 KD BxPC-3 and Capan-1 cells, in cell-protein binding experiments that were further validated with microfluidic chambers. In general, higher reduction in E-selectin binding was found in the ST3GAL4 KD cells compared to ST3GAL3 silenced cells in both cell models for *in vitro* and microfluidic assays. Among the ST3GAL3 KD cells, the shST3GAL3_9 cells were the ones that for both cell models showed higher reduction in E-selectin adhesion, which could be explained by their higher decrease in their sialyl Lewis expression levels.

These results suggest the strong value of sialyl Lewis antigens, and in particular of SLe^X, in the adhesion to E-selectin, involved in the initial steps of pancreatic cancer cell arrestment on endothelial cells. In agreement with this, the overexpression of FUT1, which competes for the same substrate that α2,3-STs, in BxPC-3 pancreatic cancer cells resulted in a decrease in SLe^X levels, which was associated with a reduction in E-selectin-expressing CHO cells binding and an impaired metastatic potential into xenograft transplantation [276,277]. This mechanism is also shared with other neoplasms like in human lung carcinoma cells, in which the up-regulation of FUT3 by TNF-α resulted in an increase of SLe^X expression, which mediates enhanced invasion and E-selectin binding [338]. Studies with metastatic prostate cancer cells also showed an increase in adhesion to E-selectin and migration and invasion after cell treatment with TNF-α that led to an increase of SLe^X [339], and further cell treatment with an antibody against SLe^X compromised the prostate cell migration and invasion with similar results to those obtained in our cell models.

The importance of targeting the sialyltransferases involved in the late steps of SLe^X/ SLe^A biosynthesis has also been shown in other carcinomas such as in lung cancer. In this regard, Yoshihama et al., [340] also reported that the KD of ST3GAL4 in lung metastatic H1299 cells inhibit SLe^X expression reducing cell adhesion to HUVEC cells, which suggests its potential as a target for cell metastasis. In ovarian cancer, ST3GAL3 KD sensitized ovarian cancer cells to cisplatin and paclitaxel induced apoptosis [341,342]. Intriguingly, the induction of EMT in colon cancer led to the upregulation of FUT3, ST3GAL3 and ST3GAL4, which are implicated in the final steps of the biosynthesis of $SLe^{X/A}$, suggesting a significant link between those Lewis antigens and EMT in colon carcinoma [343]. We have shown that the KD of ST3GAL4 and ST3GAL3 in cells implies a partial reduction but not a complete abrogation of the sialyl Lewis antigens ($SLe^{X/A}$), similarly to other reports [201]. However, the effects of such reduction were enough to downgrade *in vitro* some of the malignant properties of PDA cells. Blockade of sialic acid transfer using a cell permeable sialyltransferase inhibitor has shown to reduce significantly the synthesis of sialoglycans both α2,3 and α2,6, and it has diminished the adhesive and migratory capability of melanoma cells [242] and suppressed tumor growth

by enhancing T-cell mediated tumor immunity [344]. Another sialyltransferase inhibitor, Soyasaponin I (SsaI), that targets α2,3-STs, in particular ST3Gal I, inhibited tumor cell migration and dissemination in the *in vivo* mouse model with transplanted ovarian cancer cells [345]. Furthermore, this inhibitor targeted ST3Gal IV in breast cancer cells and also modified their invasive behavior [245].

Overall, we have shown that STs, and in particular ST3GAL4 and ST3GAL3 that lead to the $SLe^{X/A}$ biosynthesis can be considered as new therapeutic targets against pancreatic cancer. This opens a new window to the investigation of compounds that inhibit the corresponding STs to block SLe^{A} and neo-expressed SLe^{x} in pancreatic tumor cells to avoid or reduce their metastasis to other organs.

VI. Conclusions

1. Glycoproteins from pancreatic ductal adenocarcinoma tissues have shown altered glycosylation. Specifically, an increase of glycoproteins carrying the carbohydrate antigen Sialyl Lewis X were detected in PDA compared with control tissues.

2. The separation of glycoproteins containing SLe^X from PDA tissue lysates through 2DE and immunodetection, allowed us to identify the glycoprotein microfibril associated protein 4 (MFAP4) as a SLe^X carrier in PDA tissues by mass spectrometry. The posterior analysis of co-localization revealed the presence of SLe^X over MFAP4 only in PDA tissues and not in control pancreatic tissues, suggesting that the glycoform SLe^X-MFAP4 could be used as a potential diagnostic or prognostic biomarker for pancreatic cancer.

3. MFAP4 expression was in general much higher in human pancreatic adenocarcinoma tissues than in control pancreas or tissues from donors with non-pancreatic disorders. Further MFAP4 expression analysis of cell lysates by western blot displayed that this glycoprotein is not produced by PDA cells. IHC analyses revealed its presence in the pancreatic extracellular matrix of tissue samples meaning that its synthesis is probably driven by stromal fibroblasts.

4. Inhibition of both ST3GAL3 and ST3GAL4 genes using specific shRNAs in PDA cell lines BxPC-3 and Capan-1, resulted in a decrease in sialyl Lewis antigens both in cell glycoconjugates and in glycoproteins from cell lysates and conditioned media, analyzed by flow cytometry and western blot respectively.

5. Reduction of the α2,3-sialyltransferases expression ST3GAL3 and ST3GAL4 in knock-down cells shBxPC-3 and shCapan-1 showed a significant decrease in their adhesion and rolling to human recombinant E-selectin, consistent with the lower expression of sialyl Lewis antigens within the different clones of each cell line.

6. Cellular migration and invasion *in vitro* (analyzed with transwells and microfluidic devices) of the of ST3GAL3 and ST3GAL4 knock-down PDA cells (shBxPC-3and shCapan-1), showed a significant reduction compared to their corresponding control cells, demonstrating the role of the α2,3-sialyltransferases ST3GAL3 and ST3GAL4 in the regulation of the adhesive and migratory potential of pancreatic adenocarcinoma cells.

7. Inhibition of α2,3-sialyltransferases expression has partially reversed the highly invasive phenotype of PDA, which makes them potential tumor therapeutic targets.

VII. References

1. Moreno Planas JM, Sánchez Ortega AS, García Bueno JM, Ramírez Castillejo C. Avances en cáncer de páncreas, del laboratorio a la clínica. 2010. 15–339 p.

2. Bardeesy N, DePinho RA. Pancreatic cancer biology and genetics. Nat Rev Cancer. 2002; 2: 897–909. doi: 10.1038/nrc949.

3. Guest PC. Biogenesis of the Insulin Secretory Granule in Health and Disease. 2019. p. 17–32. doi: 10.1007/978-3-030-12668-1_2.

4. Benitez CM, Goodyer WR, Kim SK. Deconstructing Pancreas Developmental Biology. Cold Spring Harb Perspect Biol. 2012; 4: a012401–a012401. doi: 10.1101/cshperspect.a012401.

5. Longnecker D. Anatomy and Histology of the Pancreas. Pancreapedia Exocrine Pancreas Knowl Base. 2014; : 1–26. doi: 10.3998/panc.2014.3.

6. Sastre J, Sabater L, Aparisi L. Fisiología de la secreción pancreática. Gastroenterol Hepatol. 2005; 28: 3–9. doi: 10.1157/13071380.

7. Haugk B. Pancreatic intraepithelial neoplasia - can we detect early pancreatic cancer? Histopathology. 2010; 57: 503–14. doi: 10.1111/j.1365-2559.2010.03610.x.

8. Yao JC, Hassan M, Phan A, Dagohoy C, Leary C, Mares JE, Abdalla EK, Fleming JB, Vauthey J-N, Rashid A, Evans DB. One Hundred Years After “Carcinoid”: Epidemiology of and Prognostic Factors for Neuroendocrine Tumors in 35,825 Cases in the United States. J Clin Oncol. 2008; 26: 3063–72. doi: 10.1200/JCO.2007.15.4377.

9. Halfdanarson TR, Rubin J, Farnell MB, Grant CS, Petersen GM. Pancreatic endocrine neoplasms: epidemiology and prognosis of pancreatic endocrine tumors. Endocr Relat Cancer. 2008; 15: 409–27. doi: 10.1677/ERC-07-0221.

10. Kleeff J, Korc M, Apte M, La Vecchia C, Johnson CD, Biankin A V., Neale RE, Tempero M, Tuveson DA, Hruban RH, Neoptolemos JP. Pancreatic cancer. Nat Rev Dis Prim. Macmillan Publishers Limited; 2016; 2: 16022. doi: 10.1038/nrdp.2016.22.

11. Matthaei H, Semaan A, Hruban RH. The genetic classification of pancreatic neoplasia. J Gastroenterol. 2015; 50: 520–32. doi: 10.1007/s00535-015-1037-4.

12. Siegel RL, Miller KD, Jemal A. Cancer statistics, 2019. CA Cancer J Clin. 2019; 69: 7–34. doi: 10.3322/caac.21551.

13. Adamska A, Domenichini A, Falasca M. Pancreatic Ductal Adenocarcinoma: Current and Evolving Therapies. Int J Mol Sci. 2017; 18: 1338. doi: 10.3390/ijms18071338.

14. Hruban RH, Canto MI, Goggins M, Schulick R, Klein AP. Update on Familial Pancreatic Cancer. Adv Surg. 2010; 44: 293–311. doi: 10.1016/j.yasu.2010.05.011.

15. Moutinho-Ribeiro P, Macedo G, Melo SA. Pancreatic Cancer Diagnosis and Management: Has the Time Come to Prick the Bubble? Front Endocrinol (Lausanne). 2019; 9: 1–11. doi: 10.3389/fendo.2018.00779.

16. Siegel R, Ma J, Zou Z, Jemal A. Cancer statistics, 2014. CA Cancer J Clin. 2014; 64: 9–29. doi: 10.3322/caac.21208.

17. Rahib L, Smith BD, Aizenberg R, Rosenzweig AB, Fleshman JM, Matrisian LM. Projecting Cancer Incidence and Deaths to 2030: The Unexpected Burden of Thyroid, Liver, and Pancreas Cancers in the United States. Cancer Res. 2014; 74: 2913–21. doi: 10.1158/0008-5472.CAN-14-0155.

18. Wu S ta, Fowler AJ, Garmon CB, Fessler AB, Ogle JD, Grover KR, Allen BC, Williams CD, Zhou R, Yazdanifar M, Ogle CA, Mukherjee P. Treatment of pancreatic ductal adenocarcinoma with tumor antigen specific-targeted delivery of paclitaxel loaded PLGA nanoparticles. BMC Cancer. BMC Cancer; 2018; 18: 1–13. doi: 10.1186/s12885-018-4393-7.

19. Fokas E, O'Neill E, Gordon-Weeks A, Mukherjee S, McKenna WG, Muschel RJ. Pancreatic ductal adenocarcinoma: From genetics to biology to radiobiology to oncoimmunology and all the way back to the clinic. Biochim Biophys Acta - Rev Cancer. 2015; 1855: 61–82. doi: 10.1016/j.bbcan.2014.12.001.

20. Erkan M, Kurtoglu M, Kleeff J. The role of hypoxia in pancreatic cancer: a potential therapeutic target? Expert Rev Gastroenterol Hepatol. 2016; 10: 301–16. doi: 10.1586/17474124.2016.1117386.

21. Siegel R, Ward E, Brawley O, Jemal A. Cancer statistics, 2011. CA Cancer J Clin. 2011; 61: 212–36. doi: 10.3322/caac.20121.

22. Wolfgang CL, Herman JM, Laheru DA, Klein AP, Erdek MA, Fishman EK, Hruban RH. Recent progress in pancreatic cancer. CA Cancer J Clin. 2013; 63: 318–48. doi: 10.3322/caac.21190.

23. Kamisawa T, Wood LD, Itoi T, Takaori K. Pancreatic cancer. Lancet. Elsevier Ltd; 2016; 388: 73–85. doi: 10.1016/S0140-6736(16)00141-0.

24. Lynch HT, Lynch JF, Lanspa SJ. Familial Pancreatic Cancer. Cancers (Basel). 2010; 2: 1861–83. doi: 10.3390/cancers2041861.

25. Jaffee EM, Hruban RH, Canto M, Kern SE. Focus on pancreas cancer. Cancer Cell. 2002; 2: 25–8. doi: 10.1016/S1535-6108(02)00093-4.

26. Tjomsland V, Niklasson L, Sandström P, Borch K, Druid H, Bratthäll C, Messmer D, Larsson M, Spångeus A. The desmoplastic stroma plays an essential role in the accumulation and modulation of infiltrated immune cells in pancreatic adenocarcinoma. Clin Dev Immunol. 2011; 2011. doi: 10.1155/2011/212810.

27. Xie D, Xie K. Pancreatic cancer stromal biology and therapy. Genes Dis. Elsevier Taiwan LLC and the; 2015; 2: 133–43. doi: 10.1016/j.gendis.2015.01.002.

28. Xu Z. Pancreatic cancer and its stroma: A conspiracy theory. World J Gastroenterol. 2014; 20: 11216. doi: 10.3748/wjg.v20.i32.11216.

29. Apte M V., Park S, Phillips PA, Santucci N, Goldstein D, Kumar RK, Ramm GA, Buchler M, Friess H, McCarroll JA, Keogh G, Merrett N, Pirola R, et al. Desmoplastic reaction in pancreatic cancer: Role of pancreatic stellate cells. Pancreas. 2004; 29: 179–87. doi: 10.1097/00006676-200410000-00002.

30. Neesse A, Bauer CA, Öhlund D, Lauth M, Buchholz M, Michl P, Tuveson DA, Gress TM. Stromal biology and therapy in pancreatic cancer: ready for clinical translation? Gut. 2019; 68: 159–71. doi: 10.1136/gutjnl-2018-316451.

31. Olive KP. Stroma, Stroma Everywhere (Far More Than You Think). Clin Cancer Res. 2015; 21: 3366–8. doi: 10.1158/1078-0432.CCR-15-0416.

32. Nielsen MFB, Mortensen MB, Detlefsen S. Key players in pancreatic cancer-stroma

interaction: Cancer-associated fibroblasts, endothelial and inflammatory cells. World J Gastroenterol. 2016; 22: 2678. doi: 10.3748/wjg.v22.i9.2678.

33. Johnsen AK, Templeton DJ, Sy M, Harding C V. Deficiency of transporter for antigen presentation (TAP) in tumor cells allows evasion of immune surveillance and increases tumorigenesis. J Immunol. 1999; 163: 4224–31. Available from http://www.ncbi.nlm.nih.gov/pubmed/10510359

34. Clark CE, Hingorani SR, Mick R, Combs C, Tuveson DA, Vonderheide RH. Dynamics of the Immune Reaction to Pancreatic Cancer from Inception to Invasion. Cancer Res. 2007; 67: 9518–27. doi: 10.1158/0008-5472.CAN-07-0175.

35. Rucki AA, Zheng L. Pancreatic cancer stroma: Understanding biology leads to new therapeutic strategies. World J Gastroenterol. 2014; 20: 2237–46. doi: 10.3748/wjg.v20.i9.2237.

36. Apte M V., Yang L, Phillips PA, Xu Z, Kaplan W, Cowley M, Pirola RC, Wilson JS. Extracellular matrix composition significantly influences pancreatic stellate cell gene expression pattern: Role of transgelin in PSC function. Am J Physiol - Gastrointest Liver Physiol. 2013; 305. doi: 10.1152/ajpgi.00016.2013.

37. Dangi-Garimella S, Sahai V, Ebine K, Kumar K, Munshi HG. Three-Dimensional Collagen I Promotes Gemcitabine Resistance In Vitro in Pancreatic Cancer Cells through HMGA2-Dependent Histone Acetyltransferase Expression. Cukierman E, editor. PLoS One. 2013; 8: e64566. doi: 10.1371/journal.pone.0064566.

38. Miyamoto H, Murakami T, Tsuchida K, Sugino H, Miyake H, Tashiro S. Tumor-Stroma Interaction of Human Pancreatic Cancer: Acquired Resistance to Anticancer Drugs and Proliferation Regulation Is Dependent on Extracellular Matrix Proteins. Pancreas. 2004; 28: 38–44. doi: 10.1097/00006676-200401000-00006.

39. Michl P, Gress TM. Improving drug delivery to pancreatic cancer: breaching the stromal fortress by targeting hyaluronic acid. Gut. 2012; 61: 1377–9. doi: 10.1136/gutjnl-2012-302604.

40. Provenzano PP, Cuevas C, Chang AE, Goel VK, Von Hoff DD, Hingorani SR. Enzymatic Targeting of the Stroma Ablates Physical Barriers to Treatment of Pancreatic Ductal Adenocarcinoma. Cancer Cell. 2012; 21: 418–29. doi:

10.1016/j.ccr.2012.01.007.

41. Hezel AF. Genetics and biology of pancreatic ductal adenocarcinoma. Genes Dev. 2006; 20: 1218–49. doi: 10.1101/gad.1415606.

42. Vincent A, Herman J, Schulick R, Hruban RH, Goggins M. Pancreatic cancer. Lancet. 2011; 378: 607–20. doi: 10.1016/S0140-6736(10)62307-0.

43. Matthaei H, Schulick RD, Hruban RH, Maitra A. Cystic precursors to invasive pancreatic cancer. Nat Rev Gastroenterol Hepatol. 2011; 8: 141–50. doi: 10.1038/nrgastro.2011.2.

44. Makohon-Moore A, Iacobuzio-Donahue CA. Pancreatic cancer biology and genetics from an evolutionary perspective. Nat Rev Cancer. 2016; 16: 553–65. doi: 10.1038/nrc.2016.66.

45. Hruban RH, van Mansfeld AD, Offerhaus GJA, van Weering DH, Allison DC, Goodman SN, Kensler TW, Bose KK, Cameron JL, Bos JL. K-ras oncogene activation in adenocarcinoma of the human pancreas. A study of 82 carcinomas using a combination of mutant-enriched polymerase chain reaction analysis and allele-specific oligonucleotide hybridization. Am J Pathol. 1993; 143: 545–54. Available from http://www.ncbi.nlm.nih.gov/pubmed/8342602

46. Liang WS, Craig DW, Carpten J, Borad MJ, Demeure MJ, Weiss GJ, Izatt T, Sinari S, Christoforides A, Aldrich J, Kurdoglu A, Barrett M, Phillips L, et al. Genome-Wide Characterization of Pancreatic Adenocarcinoma Patients Using Next Generation Sequencing. Sarkar FH, editor. PLoS One. 2012; 7: e43192. doi: 10.1371/journal.pone.0043192.

47. Vogelstein B, Kinzler KW. Cancer genes and the pathways they control. Nat Med. 2004; 10: 789–99. doi: 10.1038/nm1087.

48. Loc WS. Novel strategies for managing pancreatic cancer. World J Gastroenterol. 2014; 20: 14717. doi: 10.3748/wjg.v20.i40.14717.

49. Lanfredini S, Thapa A, O'Neill E. RAS in pancreatic cancer. Biochem Soc Trans. 2019; 47: 961–72. doi: 10.1042/BST20170521.

50. Rozenblum E, Schutte M, Goggins M, Hahn SA, Panzer S, Zahurak M, Goodman

SN, Sohn TA, Hruban RH, Yeo CJ, Kern SE. Tumor-suppressive pathways in pancreatic carcinoma. Cancer Res. 1997; 57: 1731–4. Available from http://www.ncbi.nlm.nih.gov/pubmed/9135016

51. Li D, Xie K, Wolff R, Abbruzzese JL. Pancreatic cancer. Lancet. 2004; 363: 1049–57. doi: 10.1016/S0140-6736(04)15841-8.

52. Sherr CJ. Principles of Tumor Suppression. Cell. 2004; 116: 235–46. doi: 10.1016/S0092-8674(03)01075-4.

53. Okano K. Strategies for early detection of resectable pancreatic cancer. World J Gastroenterol. 2014; 20: 11230. doi: 10.3748/wjg.v20.i32.11230.

54. Iacobuzio-Donahue CA, Fu B, Yachida S, Luo M, Abe H, Henderson CM, Vilardell F, Wang Z, Keller JW, Banerjee P, Herman JM, Cameron JL, Yeo CJ, et al. DPC4 Gene Status of the Primary Carcinoma Correlates With Patterns of Failure in Patients With Pancreatic Cancer. J Clin Oncol. 2009; 27: 1806–13. doi: 10.1200/JCO.2008.17.7188.

55. Yonezawa S, Higashi M, Yamada N, Goto M. Precursor Lesions of Pancreatic Cancer. Gut Liver. 2008; 2: 137–54. doi: 10.5009/gnl.2008.2.3.137.

56. Ghaneh P, Costello E, Neoptolemos JP. Biology and management of pancreatic cancer. Postgrad Med J. 2008; 84: 478–97. doi: 10.1136/gut.2006.103333.

57. Wei P, Tang H, Li D. Insights into Pancreatic Cancer Etiology from Pathway Analysis of Genome-Wide Association Study Data. Zhao Z, editor. PLoS One. 2012; 7: e46887. doi: 10.1371/journal.pone.0046887.

58. Costello E, Greenhalf W, Neoptolemos JP. New biomarkers and targets in pancreatic cancer and their application to treatment. Nat Rev Gastroenterol Hepatol. Nature Publishing Group; 2012; 9: 435–44. doi: 10.1038/nrgastro.2012.119.

59. Kruger S. Translational research in pancreatic ductal adenocarcinoma: Current evidence and future concepts. World J Gastroenterol. 2014; 20: 10769. doi: 10.3748/wjg.v20.i31.10769.

60. Sato N, Fukushima N, Chang R, Matsubayashi H, Goggins M. Differential and

Epigenetic Gene Expression Profiling Identifies Frequent Disruption of the RELN Pathway in Pancreatic Cancers. Gastroenterology. 2006; 130: 548–65. doi: 10.1053/j.gastro.2005.11.008.

61. Matsubayashi H, Sato N, Fukushima N, Yeo CJ, Walter KM, Brune K, Sahin F, Hruban RH, Goggins M. Methylation of cyclin D2 is observed frequently in pancreatic cancer but is also an age-related phenomenon in gastrointestinal tissues. Clin Cancer Res. 2003; 9: 1446–52. Available from http://www.ncbi.nlm.nih.gov/pubmed/12684418

62. Fukushima N, Sato N, Sahin F, Su GH, Hruban RH, Goggins M. Aberrant methylation of suppressor of cytokine signalling-1 (SOCS-1) gene in pancreatic ductal neoplasms. Br J Cancer. 2003; 89: 338–43. doi: 10.1038/sj.bjc.6601039.

63. Collisson EA, Bailey P, Chang DK, Biankin A V. Molecular subtypes of pancreatic cancer. Nat Rev Gastroenterol Hepatol. Springer US; 2019; 16: 207–20. doi: 10.1038/s41575-019-0109-y.

64. Bailey P, Chang DK, Nones K, Johns AL, Patch A-M, Gingras M-C, Miller DK, Christ AN, Bruxner TJC, Quinn MC, Nourse C, Murtaugh LC, Harliwong I, et al. Genomic analyses identify molecular subtypes of pancreatic cancer. Nature. Nature Publishing Group; 2016; 531: 47–52. doi: 10.1038/nature16965.

65. Collisson EA, Sadanandam A, Olson P, Gibb WJ, Truitt M, Gu S, Cooc J, Weinkle J, Kim GE, Jakkula L, Feiler HS, Ko AH, Olshen AB, et al. Subtypes of pancreatic ductal adenocarcinoma and their differing responses to therapy. Nat Med. 2011; 17: 500–3. doi: 10.1038/nm.2344.

66. Puleo F, Nicolle R, Blum Y, Cros J, Marisa L, Demetter P, Quertinmont E, Svrcek M, Elarouci N, Iovanna J, Franchimont D, Verset L, Galdon MG, et al. Stratification of Pancreatic Ductal Adenocarcinomas Based on Tumor and Microenvironment Features. Gastroenterology. Elsevier, Inc; 2018; 155: 1999-2013.e3. doi: 10.1053/j.gastro.2018.08.033.

67. Moffitt RA, Marayati R, Flate EL, Volmar KE, Loeza SGH, Hoadley KA, Rashid NU, Williams LA, Eaton SC, Chung AH, Smyla JK, Anderson JM, Kim HJ, et al. Virtual microdissection identifies distinct tumor- and stroma-specific subtypes of

pancreatic ductal adenocarcinoma. Nat Genet. 2015; 47: 1168–78. doi: 10.1038/ng.3398.

68. Raphael BJ, Hruban RH, Aguirre AJ, Moffitt RA, Yeh JJ, Stewart C, Robertson AG, Cherniack AD, Gupta M, Getz G, Gabriel SB, Meyerson M, Cibulskis C, et al. Integrated Genomic Characterization of Pancreatic Ductal Adenocarcinoma. Cancer Cell. 2017; 32: 185-203.e13. doi: 10.1016/j.ccell.2017.07.007.

69. Follia L, Ferrero G, Mandili G, Beccuti M, Giordano D, Spadi R, Satolli MA, Evangelista A, Katayama H, Hong W, Momin AA, Capello M, Hanash SM, et al. Integrative Analysis of Novel Metabolic Subtypes in Pancreatic Cancer Fosters New Prognostic Biomarkers. Front Oncol. 2019; 9: 1–12. doi: 10.3389/fonc.2019.00115.

70. Kanno A, Masamune A, Hanada K, Maguchi H, Shimizu Y, Ueki T, Hasebe O, Ohtsuka T, Nakamura M, Takenaka M, Kitano M, Kikuyama M, Gabata T, et al. Multicenter study of early pancreatic cancer in Japan. Pancreatology. Elsevier India, a division of Reed Elsevier India Pvt. Ltd; 2018; 18: 61–7. doi: 10.1016/j.pan.2017.11.007.

71. Zhang Q, Zeng L, Chen Y, Lian G, Qian C, Chen S, Li J, Huang K. Pancreatic Cancer Epidemiology, Detection, and Management. Gastroenterol Res Pract. Hindawi Publishing Corporation; 2016; 2016: 1–10. doi: 10.1155/2016/8962321.

72. Poruk KE, Firpo MA, Adler DG, Mulvihill SJ. Screening for Pancreatic Cancer. Ann Surg. 2013; 257: 17–26. doi: 10.1097/SLA.0b013e31825ffbfb.

73. Winter JM, Cameron JL, Lillemoe KD, Campbell KA, Chang D, Riall TS, Coleman J, Sauter PK, Canto M, Hruban RH, Schulick RD, Choti MA, Yeo CJ. Periampullary and Pancreatic Incidentaloma. Ann Surg. 2006; 243: 673–83. doi: 10.1097/01.sla.0000216763.27673.97.

74. Barhli A, Cros J, Bartholin L, Neuzillet C. Prognostic stratification of resected pancreatic ductal adenocarcinoma: Past, present, and future. Dig Liver Dis. Editrice Gastroenterologica Italiana; 2018; 50: 979–90. doi: 10.1016/j.dld.2018.08.009.

75. Chang JC, Kundranda M. Novel Diagnostic and Predictive Biomarkers in Pancreatic Adenocarcinoma. Int J Mol Sci. 2017; 18: 667. doi:

10.3390/ijms18030667.

76. Chu LC, Goggins MG, Fishman EK. Diagnosis and Detection of Pancreatic Cancer. Cancer J. 2017; 23: 333–42. doi: 10.1097/PPO.0000000000000290.

77. Lee ES. Imaging diagnosis of pancreatic cancer: A state-of-the-art review. World J Gastroenterol. 2014; 20: 7864. doi: 10.3748/wjg.v20.i24.7864.

78. Miura F, Takada T, Amano H, Yoshida M, Furui S, Takeshita K. Diagnosis of pancreatic cancer. HPB. 2006; 8: 337–42. doi: 10.1080/13651820500540949.

79. Li H-Y, Cui Z-M, Chen J, Guo X-Z, Li Y-Y. Pancreatic cancer: diagnosis and treatments. Tumor Biol. 2015; 36: 1375–84. doi: 10.1007/s13277-015-3223-7.

80. Agarwal B, Abu-Hamda E, Molke KL, Correa AM, Ho L. Endoscopic ultrasound-guided fine needle aspiration and multidetector spiral CT in the diagnosis of pancreatic cacer. Am J Gastroenterol. 2004; . doi: 10.1111/j.1572-0241.2004.04177.x.

81. Güngör B, Çağlayan K, Polat C, Şeren D, Erzurumlu K, Malazgirt Z. The Predictivity of Serum Biochemical Markers in Acute Biliary Pancreatitis. ISRN Gastroenterol. 2011; 2011: 1–5. doi: 10.5402/2011/279607.

82. E. Poruk K, Z. Gay D, Brown K, D. Mulvihill J, M. Boucher K, L. Scaife C, A. Firpo M, J. Mulvihill S. The Clinical Utility of CA 19-9 in Pancreatic Adenocarcinoma: Diagnostic and Prognostic Updates. Curr Mol Med. 2013; 13: 340–51. doi: 10.2174/1566524011313030003.

83. McGuigan A, Kelly P, Turkington RC, Jones C, Coleman HG, McCain RS. Pancreatic cancer: A review of clinical diagnosis, epidemiology, treatment and outcomes. World J Gastroenterol. 2018; 24: 4846–61. doi: 10.3748/wjg.v24.i43.4846.

84. Callery MP, Chang KJ, Fishman EK, Talamonti MS, William Traverso L, Linehan DC. Pretreatment Assessment of Resectable and Borderline Resectable Pancreatic Cancer: Expert Consensus Statement. Ann Surg Oncol. 2009; 16: 1727–33. doi: 10.1245/s10434-009-0408-6.

85. Ryan DP, Hong TS, Bardeesy N. Pancreatic Adenocarcinoma. N Engl J Med. 2014;

371: 1039–49. doi: 10.1056/NEJMra1404198.

86. Isaji S, Mizuno S, Windsor JA, Bassi C, Fernández-del Castillo C, Hackert T, Hayasaki A, Katz MHG, Kim S-W, Kishiwada M, Kitagawa H, Michalski CW, Wolfgang CL. International consensus on definition and criteria of borderline resectable pancreatic ductal adenocarcinoma 2017. Pancreatology. 2018; 18: 2–11. doi: 10.1016/j.pan.2017.11.011.

87. Jordan EJ, Lowery MA, Basturk O, Allen PJ, Yu KH, Tabar V, Beal K, Reidy DL, Yamada Y, Janjigian Y, Abou-Alfa GK, O'Reilly EM. Brain Metastases in Pancreatic Ductal Adenocarcinoma: Assessment of Molecular Genotype–Phenotype Features—An Entity With an Increasing Incidence? Clin Colorectal Cancer. Elsevier Inc.; 2018; 17: e315–21. doi: 10.1016/j.clcc.2018.01.009.

88. Hartwig W, Werner J, Jäger D, Debus J, Büchler MW. Improvement of surgical results for pancreatic cancer. Lancet Oncol. 2013; 14: e476–85. doi: 10.1016/S1470-2045(13)70172-4.

89. Strobel O, Hank T, Hinz U, Bergmann F, Schneider L, Springfeld C, Jäger D, Schirmacher P, Hackert T, Büchler MW. Pancreatic Cancer Surgery. Ann Surg. 2017; 265: 565–73. doi: 10.1097/SLA.0000000000001731.

90. Gillen S, Schuster T, Büschenfelde CM Zum, Friess H, Kleeff J. Preoperative/neoadjuvant therapy in pancreatic cancer: A systematic review and meta-analysis of response and resection percentages. PLoS Med. 2010; 7: 1–15. doi: 10.1371/journal.pmed.1000267.

91. Andriulli A, Festa V, Botteri E, Valvano MR, Koch M, Bassi C, Maisonneuve P, Sebastiano P Di. Neoadjuvant/Preoperative Gemcitabine for Patients with Localized Pancreatic Cancer: A Meta-analysis of Prospective Studies. Ann Surg Oncol. 2012; 19: 1644–62. doi: 10.1245/s10434-011-2110-8.

92. Garrido-Laguna I, Hidalgo M. Pancreatic cancer: from state-of-the-art treatments to promising novel therapies. Nat Rev Clin Oncol. Nature Publishing Group; 2015; 12: 319–34. doi: 10.1038/nrclinonc.2015.53.

93. BALSANO R, TOMMASI C, GARAJOVA I. State of the Art for Metastatic Pancreatic Cancer Treatment: Where Are We Now? Anticancer Res. 2019; 39: 3405–12. doi:

10.21873/anticanres.13484.

94. Faris JE, Blaszkowsky LS, McDermott S, Guimaraes AR, Szymonifka J, Huynh MA, Ferrone CR, Wargo JA, Allen JN, Dias LE, Kwak EL, Lillemoe KD, Thayer SP, et al. FOLFIRINOX in Locally Advanced Pancreatic Cancer: The Massachusetts General Hospital Cancer Center Experience. Oncologist. 2013; 18: 543–8. doi: 10.1634/theoncologist.2012-0435.

95. Cunningham D, Chau I, Stocken DD, Valle JW, Smith D, Steward W, Harper PG, Dunn J, Tudur-Smith C, West J, Falk S, Crellin A, Adab F, et al. Phase III Randomized Comparison of Gemcitabine Versus Gemcitabine Plus Capecitabine in Patients With Advanced Pancreatic Cancer. J Clin Oncol. 2009; 27: 5513–8. doi: 10.1200/JCO.2009.24.2446.

96. Moore MJ, Goldstein D, Hamm J, Figer A, Hecht JR, Gallinger S, Au HJ, Murawa P, Walde D, Wolff RA, Campos D, Lim R, Ding K, et al. Erlotinib Plus Gemcitabine Compared With Gemcitabine Alone in Patients With Advanced Pancreatic Cancer: A Phase III Trial of the National Cancer Institute of Canada Clinical Trials Group. J Clin Oncol. 2007; 25: 1960–6. doi: 10.1200/JCO.2006.07.9525.

97. Herrmann R, Bodoky G, Ruhstaller T, Glimelius B, Bajetta E, Schüller J, Saletti P, Bauer J, Figer A, Pestalozzi B, Köhne C-H, Mingrone W, Stemmer SM, et al. Gemcitabine Plus Capecitabine Compared With Gemcitabine Alone in Advanced Pancreatic Cancer: A Randomized, Multicenter, Phase III Trial of the Swiss Group for Clinical Cancer Research and the Central European Cooperative Oncology Group. J Clin Oncol. 2007; 25: 2212–7. doi: 10.1200/JCO.2006.09.0886.

98. Gourgou-Bourgade S, Bascoul-Mollevi C, Desseigne F, Ychou M, Bouché O, Guimbaud R, Bécouarn Y, Adenis A, Raoul J-L, Boige V, Bérille J, Conroy T. Impact of FOLFIRINOX Compared With Gemcitabine on Quality of Life in Patients With Metastatic Pancreatic Cancer: Results From the PRODIGE 4/ACCORD 11 Randomized Trial. J Clin Oncol. 2013; 31: 23–9. doi: 10.1200/JCO.2012.44.4869.

99. Conroy T, Desseigne F, Ychou M, Bouché O, Guimbaud R, Bécouarn Y, Adenis A, Raoul J-L, Gourgou-Bourgade S, de la Fouchardière C, Bennouna J, Bachet J-B, Khemissa-Akouz F, et al. FOLFIRINOX versus Gemcitabine for Metastatic

Pancreatic Cancer. N Engl J Med. 2011; 364: 1817–25. doi: 10.1056/NEJMoa1011923.

100. Sirohi B, Dawood S, Rastogi S, Pandey A, Bal M, Shetty N, Shrikhande S. Treatment of patients with metastatic pancreatic cancer: Experience from a tertiary Indian cancer center. Indian J Cancer. 2015; 52: 449. doi: 10.4103/0019-509X.176732.

101. Suker M, Beumer BR, Sadot E, Marthey L, Faris JE, Mellon EA, El-Rayes BF, Wang-Gillam A, Lacy J, Hosein PJ, Moorcraft SY, Conroy T, Hohla F, et al. FOLFIRINOX for locally advanced pancreatic cancer: a systematic review and patient-level meta-analysis. Lancet Oncol. 2016; 17: 801–10. doi: 10.1016/S1470-2045(16)00172-8.

102. Laquente B, Calsina-Berna A, Carmona-Bayonas A, Jiménez-Fonseca P, Peiró I, Carrato A. Supportive care in pancreatic ductal adenocarcinoma. Clin Transl Oncol. 2017; 19: 1293–302. doi: 10.1007/s12094-017-1682-6.

103. Cong L, Liu Q, Zhang R, Cui M, Zhang X, Gao X, Guo J, Dai M, Zhang T, Liao Q, Zhao Y. Tumor size classification of the 8th edition of TNM staging system is superior to that of the 7th edition in predicting the survival outcome of pancreatic cancer patients after radical resection and adjuvant chemotherapy. Sci Rep. Springer US; 2018; 8: 10383. doi: 10.1038/s41598-018-28193-4.

104. Sharma S. Tumor markers in clinical practice: General principles and guidelines. Indian J Med Paediatr Oncol. 2009; 30: 1. doi: 10.4103/0971-5851.56328.

105. Henry NL, Hayes DF. Cancer biomarkers. Mol Oncol. 2012; 6: 140–6. doi: 10.1016/j.molonc.2012.01.010.

106. Füzéry AK, Levin J, Chan MM, Chan DW. Translation of proteomic biomarkers into FDA approved cancer diagnostics: issues and challenges. Clin Proteomics. Clinical Proteomics; 2013; 10: 13. doi: 10.1186/1559-0275-10-13.

107. Duffy MJ. Tumor Markers in Clinical Practice: A Review Focusing on Common Solid Cancers. Med Princ Pract. 2013; 22: 4–11. doi: 10.1159/000338393.

108. Hartwell L, Mankoff D, Paulovich A, Ramsey S, Swisher E. Cancer biomarkers: a systems approach. Nat Biotechnol. 2006; 24: 905–8. doi: 10.1038/nbt0806-905.

109. Lalkhen AG, McCluskey A. Clinical tests: sensitivity and specificity. Contin Educ Anaesth Crit Care Pain. 2008; 8: 221–3. doi: 10.1093/bjaceaccp/mkn041.

110. Holdenrieder S, Pagliaro L, Morgenstern D, Dayyani F. Clinically Meaningful Use of Blood Tumor Markers in Oncology. Biomed Res Int. 2016; 2016: 1–10. doi: 10.1155/2016/9795269.

111. Coppolino G, Bolignano D, Rivoli L, Mazza G, Presta P, Fuiano G. Tumour Markers and Kidney Function: A Systematic Review. Biomed Res Int. Hindawi Publishing Corporation; 2014; 2014: 1–9. doi: 10.1155/2014/647541.

112. Peracaula R, Barrabés S, Sarrats A, Rudd PM, de Llorens R. Altered Glycosylation in Tumours Focused to Cancer Diagnosis. Dis Markers. 2008; 25: 207–18. doi: 10.1155/2008/797629.

113. Svarovsky SA, Joshi L. Cancer glycan biomarkers and their detection – past, present and future. Anal Methods. 2014; 6: 3918–36. doi: 10.1039/C3AY42243G.

114. Adamczyk B, Tharmalingam T, Rudd PM. Glycans as cancer biomarkers. Biochim Biophys Acta - Gen Subj. 2012; 1820: 1347–53. doi: 10.1016/j.bbagen.2011.12.001.

115. Kailemia MJ, Park D, Lebrilla CB. Glycans and glycoproteins as specific biomarkers for cancer. Anal Bioanal Chem. Analytical and Bioanalytical Chemistry; 2017; 409: 395–410. doi: 10.1007/s00216-016-9880-6.

116. Wu J, Xie X, Liu Y, He J, Benitez R, Buckanovich RJ, Lubman DM. Identification and Confirmation of Differentially Expressed Fucosylated Glycoproteins in the Serum of Ovarian Cancer Patients Using a Lectin Array and LC–MS/MS. J Proteome Res. 2012; 11: 4541–52. doi: 10.1021/pr300330z.

117. Alvarez-Manilla G, Warren NL, Atwood J, Orlando R, Dalton S, Pierce M. Glycoproteomic Analysis of Embryonic Stem Cells: Identification of Potential Glycobiomarkers Using Lectin Affinity Chromatography of Glycopeptides †. J Proteome Res. 2010; 9: 2062–75. doi: 10.1021/pr8007489.

118. Mechref Y1, Hu Y, Garcia A, Zhou S, Desantos-Garcia JL HA. Defining Putative Glycan Cancer Biomarkers by Mass Spectrometry. Bioanalysis. 2013; 4: 2457–69. doi: 10.4155/bio.12.246.Defining.

119. Compagno D, Gentilini LD, Jaworski FM, Perez IG, Contrufo G, Laderach DJ. Glycans and galectins in prostate cancer biology, angiogenesis and metastasis. Glycobiology. 2014; 24: 899–906. doi: 10.1093/glycob/cwu055.

120. Mereiter S, Balmaña M, Gomes J, Magalhães A, Reis CA. Glycomic Approaches for the Discovery of Targets in Gastrointestinal Cancer. Front Oncol. 2016; 6. doi: 10.3389/fonc.2016.00055.

121. Hamanaka Y, Hamanaka S, Suzuki M. Sialyl Lewisa Ganglioside in Pancreatic Cancer Tissue Correlates with the Serum CA 19-9 Level. Pancreas. 1996; 13: 160–5. doi: 10.1097/00006676-199608000-00007.

122. Ballehaninna UK, Chamberlain RS. The clinical utility of serum CA 19-9 in the diagnosis, prognosis and management of pancreatic adenocarcinoma: An evidence based appraisal. J Gastrointest Oncol. 2012; 3: 105–19. doi: 10.3978/j.issn.2078-6891.2011.021.

123. Azizian A, Rühlmann F, Krause T, Bernhardt M, Jo P, König A, Kleiß M, Leha A, Ghadimi M, Gaedcke J. CA19-9 for detecting recurrence of pancreatic cancer. Sci Rep. 2020; 10: 1332. doi: 10.1038/s41598-020-57930-x.

124. Goh SK, Gold G, Christophi C, Muralidharan V. Serum carbohydrate antigen 19-9 in pancreatic adenocarcinoma: a mini review for surgeons. ANZ J Surg. 2017; 87: 987–92. doi: 10.1111/ans.14131.

125. Goonetilleke KS, Siriwardena AK. Systematic review of carbohydrate antigen (CA 19-9) as a biochemical marker in the diagnosis of pancreatic cancer. Eur J Surg Oncol. 2007; 33: 266–70. doi: 10.1016/j.ejso.2006.10.004.

126. Su S-B. Carbohydrate antigen 19-9 for differential diagnosis of pancreatic carcinoma and chronic pancreatitis. World J Gastroenterol. 2015; 21: 4323. doi: 10.3748/wjg.v21.i14.4323.

127. Ducreux M, Cuhna AS, Caramella C, Hollebecque A, Burtin P, Goéré D, Seufferlein T, Haustermans K, Van Laethem JL, Conroy T, Arnold D. Cancer of the pancreas: ESMO Clinical Practice Guidelines for diagnosis, treatment and follow-up. Ann Oncol. 2015; 26: v56–68. doi: 10.1093/annonc/mdv295.

128. Swords D, Firpo M, Scaife C, Mulvihill S. Biomarkers in pancreatic

adenocarcinoma: current perspectives. Onco Targets Ther. 2016; Volume 9: 7459–67. doi: 10.2147/OTT.S100510.

129. Humphris JL, Chang DK, Johns AL, Scarlett CJ, Pajic M, Jones MD, Colvin EK, Nagrial A, Chin VT, Chantrill LA, Samra JS, Gill AJ, Kench JG, et al. The prognostic and predictive value of serum CA19.9 in pancreatic cancer. Ann Oncol. 2012; 23: 1713–22. doi: 10.1093/annonc/mdr561.

130. Kannagi R. Carbohydrate antigen sialyl Lewis a--its pathophysiological significance and induction mechanism in cancer progression. Chang Gung Med J. 2007; 30: 189–209. Available from http://www.ncbi.nlm.nih.gov/pubmed/17760270

131. Corbo V, Tortora G, Scarpa A. Molecular Pathology of Pancreatic Cancer: From Bench-to-Bedside Translation. Curr Drug Targets. 2012; 13: 744–52. doi: 10.2174/138945012800564103.

132. Sawada R, Sun S-M, Wu X, Hong F, Ragupathi G, Livingston PO, Scholz WW. Human Monoclonal Antibodies to Sialyl-Lewisa (CA19.9) with Potent CDC, ADCC, and Antitumor Activity. Clin Cancer Res. 2011; 17: 1024–32. doi: 10.1158/1078-0432.CCR-10-2640.

133. Chan A, Diamandis EP, Blasutig IM. Strategies for discovering novel pancreatic cancer biomarkers. J Proteomics. Elsevier B.V.; 2013; 81: 126–34. doi: 10.1016/j.jprot.2012.09.025.

134. Rosen A Von, Linder S, Harmenberg U, Pegert S. Serum Levels of CA 19-9 and CA 50 in Relation to Lewis Blood Cell Status in Patients with Malignant and Benign Pancreatic Disease. Pancreas. 1993; 8: 160–5. doi: 10.1097/00006676-199303000-00004.

135. Hamada S, Shimosegawa T. Biomarkers of Pancreatic Cancer. Pancreatology. IAP and EPC. Published by Elsevier India, a division of Reed Elsevier India Pvt. Ltd.; 2011; 11: 14–9. doi: 10.1159/000323479.

136. Ørntoft TF, Vestergaard EM, Holmes E, Jakobsen JS, Grunnet N, Mortensen M, Johnson P, Bross P, Gregersen N, Skorstengaard K, Jensen UB, Bolund L, Wolf H. Influence of Lewis α1-3/4-L-Fucosyltransferase (FUT3) Gene Mutations on Enzyme Activity, Erythrocyte Phenotyping, and Circulating Tumor Marker Sialyl-

Lewis a Levels. J Biol Chem. 1996; 271: 32260–8. doi: 10.1074/jbc.271.50.32260.

137. Ferri MJ, Saez M, Figueras J, Fort E, Sabat M, López-Ben S, de Llorens R, Aleixandre RN, Peracaula R. Improved Pancreatic Adenocarcinoma Diagnosis in Jaundiced and Non-Jaundiced Pancreatic Adenocarcinoma Patients through the Combination of Routine Clinical Markers Associated to Pancreatic Adenocarcinoma Pathophysiology. Kestler HA, editor. PLoS One. 2016; 11: e0147214. doi: 10.1371/journal.pone.0147214.

138. Park J, Choi Y, Namkung J, Yi SG, Kim H, Yu J, Kim Y, Kwon M-S, Kwon W, Oh D-Y, Kim S-W, Jeong S-Y, Han W, et al. Diagnostic performance enhancement of pancreatic cancer using proteomic multimarker panel. Oncotarget. 2017; 8: 93117–30. doi: 10.18632/oncotarget.21861.

139. Brand RE, Nolen BM, Zeh HJ, Allen PJ, Eloubeidi MA, Goldberg M, Elton E, Arnoletti JP, Christein JD, Vickers SM, Langmead CJ, Landsittel DP, Whitcomb DC, et al. Serum Biomarker Panels for the Detection of Pancreatic Cancer. Clin Cancer Res. 2011; 17: 805–16. doi: 10.1158/1078-0432.CCR-10-0248.

140. Chang ST, Zahn JM, Horecka J, Kunz PL, Ford JM, Fisher GA, Le QT, Chang DT, Ji H, Koong AC. Identification of a biomarker panel using a multiplex proximity ligation assay improves accuracy of pancreatic cancer diagnosis. J Transl Med. 2009; 7: 105. doi: 10.1186/1479-5876-7-105.

141. Gu Y-L, Lan C, Pei H, Yang S-N, Liu Y-F, Xiao L-L. Applicative Value of Serum CA19-9, CEA, CA125 and CA242 in Diagnosis and Prognosis for Patients with Pancreatic Cancer Treated by Concurrent Chemoradiotherapy. Asian Pacific J Cancer Prev. 2015; 16: 6569–73. doi: 10.7314/APJCP.2015.16.15.6569.

142. Nolen BM, Brand RE, Prosser D, Velikokhatnaya L, Allen PJ, Zeh HJ, Grizzle WE, Lomakin A, Lokshin AE. Prediagnostic Serum Biomarkers as Early Detection Tools for Pancreatic Cancer in a Large Prospective Cohort Study. Real FX, editor. PLoS One. 2014; 9: e94928. doi: 10.1371/journal.pone.0094928.

143. Jenkinson C, Earl J, Ghaneh P, Halloran C, Carrato A, Greenhalf W, Neoptolemos J, Costello E. Biomarkers for early diagnosis of pancreatic cancer. Expert Rev Gastroenterol Hepatol. 2015; 9: 305–15. doi: 10.1586/17474124.2015.965145.

144. Kinugasa H, Nouso K, Miyahara K, Morimoto Y, Dohi C, Tsutsumi K, Kato H, Matsubara T, Okada H, Yamamoto K. Detection of K-ras gene mutation by liquid biopsy in patients with pancreatic cancer. Cancer. 2015; 121: 2271–80. doi: 10.1002/cncr.29364.

145. Pedersen KS, Bamlet WR, Oberg AL, de Andrade M, Matsumoto ME, Tang H, Thibodeau SN, Petersen GM, Wang L. Leukocyte DNA Methylation Signature Differentiates Pancreatic Cancer Patients from Healthy Controls. Algül H, editor. PLoS One. 2011; 6: e18223. doi: 10.1371/journal.pone.0018223.

146. Dauksa A, Gulbinas A, Barauskas G, Pundzius J, Oldenburg J, El-Maarri O. Whole Blood DNA Aberrant Methylation in Pancreatic Adenocarcinoma Shows Association with the Course of the Disease: A Pilot Study. Srivastava RK, editor. PLoS One. 2012; 7: e37509. doi: 10.1371/journal.pone.0037509.

147. Mitchell PS, Parkin RK, Kroh EM, Fritz BR, Wyman SK, Pogosova-Agadjanyan EL, Peterson A, Noteboom J, O'Briant KC, Allen A, Lin DW, Urban N, Drescher CW, et al. Circulating microRNAs as stable blood-based markers for cancer detection. Proc Natl Acad Sci. 2008; 105: 10513–8. doi: 10.1073/pnas.0804549105.

148. Komatsu S, Ichikawa D, Miyamae M, Kawaguchi T, Morimura R, Hirajima S, Okajima W, Ohashi T, Imamura T, Konishi H, Shiozaki A, Ikoma H, Okamoto K, et al. Malignant potential in pancreatic neoplasm; new insights provided by circulating miR-223 in plasma. Expert Opin Biol Ther. 2015; 15: 773–85. doi: 10.1517/14712598.2015.1029914.

149. Herreros-Villanueva M, Gironella M, Castells A, Bujanda L. Molecular markers in pancreatic cancer diagnosis. Clin Chim Acta. Elsevier B.V.; 2013; 418: 22–9. doi: 10.1016/j.cca.2012.12.025.

150. Kunovsky L, Tesarikova P, Kala Z, Kroupa R, Kysela P, Dolina J, Trna J. The Use of Biomarkers in Early Diagnostics of Pancreatic Cancer. Can J Gastroenterol Hepatol. Hindawi; 2018; 2018: 1–10. doi: 10.1155/2018/5389820.

151. Pereira SP, Oldfield L, Ney A, Hart PA, Keane MG, Pandol SJ, Li D, Greenhalf W, Jeon CY, Koay EJ, Almario C V, Halloran C, Lennon AM, et al. Early detection of pancreatic cancer. Lancet Gastroenterol Hepatol. Elsevier Ltd; 2020; 21: 334. doi:

10.1016/S2468-1253(19)30416-9.

152. Yachida S, Jones S, Bozic I, Antal T, Leary R, Fu B, Kamiyama M, Hruban RH, Eshleman JR, Nowak MA, Velculescu VE, Kinzler KW, Vogelstein B, et al. Distant metastasis occurs late during the genetic evolution of pancreatic cancer. Nature. 2010; 467: 1114–7. doi: 10.1038/nature09515.

153. Goggins M. Markers of Pancreatic Cancer: Working Toward Early Detection. Clin Cancer Res. 2011; 17: 635–7. doi: 10.1158/1078-0432.CCR-10-3074.

154. Al-Sukhni W, Borgida A, Rothenmund H, Holter S, Semotiuk K, Grant R, Wilson S, Moore M, Narod S, Jhaveri K, Haider MA, Gallinger S. Screening for Pancreatic Cancer in a High-Risk Cohort: An Eight-Year Experience. J Gastrointest Surg. 2012; . doi: 10.1007/s11605-011-1781-6.

155. Pinho SS, Reis CA. Glycosylation in cancer: mechanisms and clinical implications. Nat Rev Cancer. 2015; 15: 540–55. doi: 10.1038/nrc3982.

156. Mann M, Jensen ON. Proteomic analysis of post-translational modifications. Nat Biotechnol. 2003; 21: 255–61. doi: 10.1038/nbt0303-255.

157. Josic D, Martinovic T, Pavelic K. Glycosylation and metastases. Electrophoresis. 2019; 40: 140–50. doi: 10.1002/elps.201800238.

158. Apweiler R. On the frequency of protein glycosylation, as deduced from analysis of the SWISS-PROT database. Biochim Biophys Acta - Gen Subj. 1999; 1473: 4–8. doi: 10.1016/S0304-4165(99)00165-8.

159. Abou-Abbass H, Abou-El-Hassan H, Bahmad H, Zibara K, Zebian A, Youssef R, Ismail J, Zhu R, Zhou S, Dong X, Nasser M, Bahmad M, Darwish H, et al. Glycosylation and other PTMs alterations in neurodegenerative diseases: Current status and future role in neurotrauma. Electrophoresis. 2016; 37: 1549–61. doi: 10.1002/elps.201500585.

160. Rakus JF, Mahal LK. New Technologies for Glycomic Analysis: Toward a Systematic Understanding of the Glycome. Annu Rev Anal Chem. 2011; 4: 367–92. doi: 10.1146/annurev-anchem-061010-113951.

161. Varki A, Cummings RD, Esko JD, Stanley P, Hart GW, Aebi M, Darvill AG, Kinoshita

T, Packer NH, Prestegard JH, Schnaar RL, Seeberger PH. Essentials of glycobiology, third edition. Cold Spring Harbor Laboratory Press. 2017.

162. Varki A, Freeze HH, Manzi AE. Overview of Glycoconjugate Analysis. Curr Protoc Protein Sci. 2009; 57: 1–7. doi: 10.1002/0471140864.ps1201s57.

163. Ma J, Hart GW. O-GlcNAc profiling: from proteins to proteomes. Clin Proteomics. 2014; 11: 8. doi: 10.1186/1559-0275-11-8.

164. Moremen KW, Tiemeyer M, Nairn A V. Vertebrate protein glycosylation: diversity, synthesis and function. Nat Rev Mol Cell Biol. Nature Publishing Group; 2012; 13: 448–62. doi: 10.1038/nrm3383.

165. Bennett EP, Mandel U, Clausen H, Gerken TA, Fritz TA, Tabak LA. Control of mucin-type O-glycosylation: A classification of the polypeptide GalNAc-transferase gene family. Glycobiology. 2012; 22: 736–56. doi: 10.1093/glycob/cwr182.

166. Tran DT, Ten Hagen KG. Mucin-type O -Glycosylation during Development. J Biol Chem. 2013; 288: 6921–9. doi: 10.1074/jbc.R112.418558.

167. Pang X, Li H, Guan F, Li X. Multiple Roles of Glycans in Hematological Malignancies. Front Oncol. 2018; 8: 1–12. doi: 10.3389/fonc.2018.00364.

168. Hanisch F-G. O-Glycosylation of the Mucin Type. Biol Chem. 2001; 382: 143–9. doi: 10.1515/BC.2001.022.

169. Bergstrom KSB, Xia L. Mucin-type O-glycans and their roles in intestinal homeostasis. Glycobiology. 2013; 23: 1026–37. doi: 10.1093/glycob/cwt045.

170. Bhatia R, Gautam SK, Cannon A, Thompson C, Hall BR, Aithal A, Banerjee K, Jain M, Solheim JC, Kumar S, Batra SK. Cancer-associated mucins: role in immune modulation and metastasis. Cancer Metastasis Rev. Cancer and Metastasis Reviews; 2019; 38: 223–36. doi: 10.1007/s10555-018-09775-0.

171. Kaur S, Kumar S, Momi N, Sasson AR, Batra SK. Mucins in pancreatic cancer and its microenvironment. Nat Rev Gastroenterol Hepatol. Nature Publishing Group; 2013; 10: 607–20. doi: 10.1038/nrgastro.2013.120.

172. Vliegenthart JFG. The impact of defining glycan structures. Perspect Sci. Elsevier GmbH.; 2017; 11: 3–10. doi: 10.1016/j.pisc.2016.02.003.

173. BHAGAVAN NV. Carbohydrate Metabolism III: Glycoproteins, Glycolipids, GPI Anchors, Proteoglycans, and Peptidoglycans. Medical Biochemistry. Elsevier; 2002. p. 307–30. doi: 10.1016/B978-012095440-7/50018-4.

174. Fischöder T, Laaf D, Dey C, Elling L. Enzymatic Synthesis of N-Acetyllactosamine (LacNAc) Type 1 Oligomers and Characterization as Multivalent Galectin Ligands. Molecules. 2017; 22: 1320. doi: 10.3390/molecules22081320.

175. Thurin M, Kieber-Emmons T. SA-Le a and Tumor Metastasis: The Old Prediction and Recent Findings. Hybrid Hybridomics. 2002; 21: 111–6. doi: 10.1089/153685902317401708.

176. Ugorski M, Laskowska A. Sialyl Lewis(a): a tumor-associated carbohydrate antigen involved in adhesion and metastatic potential of cancer cells. Acta Biochim Pol. 2002; 49: 303–11. Available from http://www.ncbi.nlm.nih.gov/pubmed/12362971

177. Kannagi R. Molecular mechanism for cancer-associated induction of sialyl Lewis X and sialyl Lewis A expression—The Warburg effect revisited. Glycoconj J. 2003; 20: 353–64. doi: 10.1023/B:GLYC.0000033631.35357.41.

178. Magnani JL. The discovery, biology, and drug development of sialyl Lea and sialyl Lex. Arch Biochem Biophys. 2004; 426: 122–31. doi: 10.1016/j.abb.2004.04.008.

179. Schultz MJ, Swindall AF, Bellis SL. Regulation of the metastatic cell phenotype by sialylated glycans. Cancer Metastasis Rev. 2012; 31: 501–18. doi: 10.1007/s10555-012-9359-7.

180. Harduin-Lepers A, Mollicone R, Delannoy P, Oriol R. The animal sialyltransferases and sialyltransferase-related genes: a phylogenetic approach. Glycobiology. 2005; 15: 805–17. doi: 10.1093/glycob/cwi063.

181. Jeanneau C, Chazalet V, Augé C, Soumpasis DM, Harduin-Lepers A, Delannoy P, Imberty A, Breton C. Structure-Function Analysis of the Human Sialyltransferase ST3Gal I. J Biol Chem. 2004; 279: 13461–8. doi: 10.1074/jbc.M311764200.

182. Lehmann F, Kelm S, Dietz F, von Itzstein M, Tiralongo J. The evolution of galactose α2,3-sialyltransferase: Cionaintestinalis ST3GAL I/II and Takifugu rubripes ST3GAL II sialylate Galβ1,3GalNAc structures on glycoproteins but not glycolipids. Glycoconj J. 2008; 25: 323–34. doi: 10.1007/s10719-007-9078-4.

183. Harduin-Lepers A, Vallejo-Ruiz V, Krzewinski-Recchi M-A, Samyn-Petit B, Julien S, Delannoy P. The human sialyltransferase family. Biochimie. 2001; 83: 727–37. doi: 10.1016/S0300-9084(01)01301-3.

184. Bhide GP, Colley KJ. Sialylation of N-glycans: mechanism, cellular compartmentalization and function. Histochem Cell Biol. Springer Berlin Heidelberg; 2017; 147: 149–74. doi: 10.1007/s00418-016-1520-x.

185. Varki A. Sialic acids in human health and disease. Trends Mol Med. 2008; 14: 351–60. doi: 10.1016/j.molmed.2008.06.002.

186. Higel F, Sandl T, Kao C-Y, Pechinger N, Sörgel F, Friess W, Wolschin F, Seidl A. N-glycans of complex glycosylated biopharmaceuticals and their impact on protein clearance. Eur J Pharm Biopharm. Elsevier; 2019; 139: 123–31. doi: 10.1016/j.ejpb.2019.03.018.

187. Ferreira IG, Pucci M, Venturi G, Malagolini N, Chiricolo M, Dall'Olio F. Glycosylation as a Main Regulator of Growth and Death Factor Receptors Signaling. Int J Mol Sci. 2018; 19: 580. doi: 10.3390/ijms19020580.

188. Schauer R. Achievements and challenges of sialic acid research. Glycoconj J. 2000; 17: 485–99. doi: 10.1023/a:1011062223612.

189. Angata T, Varki A. Chemical Diversity in the Sialic Acids and Related α-Keto Acids: An Evolutionary Perspective. Chem Rev. 2002; 102: 439–69. doi: 10.1021/cr000407m.

190. Bate C, Nolan W, Williams A. Sialic Acid on the Glycosylphosphatidylinositol Anchor Regulates PrP-mediated Cell Signaling and Prion Formation. J Biol Chem. 2016; 291: 160–70. doi: 10.1074/jbc.M115.672394.

191. Ilver D, Johansson P, Miller-Podraza H, Nyholm PG, Teneberg S, Karlsson KA. Bacterium-host protein-carbohydrate interactions. Methods Enzymol. 2003; 363: 134–57. doi: 10.1016/S0076-6879(03)01049-8.

192. Li Y, Chen X. Sialic acid metabolism and sialyltransferases: natural functions and applications. Appl Microbiol Biotechnol. 2012; 94: 887–905. doi: 10.1007/s00253-012-4040-1.

193. Lehmann F, Tiralongo E, Tiralongo J. Sialic acid-specific lectins: occurrence, specificity and function. Cell Mol Life Sci C. 2006; 63: 1331–54. doi: 10.1007/s00018-005-5589-y.

194. PENDU J, MARIONNEAU S, CAILLEAU-THOMAS A, ROCHER J, MOULLAC-VAIDYE B, CLÉMENT M. ABH and Lewis histo-blood group antigens in cancer. APMIS. 2001; 109: 9–26. doi: 10.1111/j.1600-0463.2001.tb00011.x.

195. Lowe JB. Glycosylation in the control of selectin counter-receptor structure and function. Immunol Rev. 2002; 186: 19–36. doi: 10.1034/j.1600-065X.2002.18603.x.

196. Holgersson J, Löfling J. Glycosyltransferases involved in type 1 chain and Lewis antigen biosynthesis exhibit glycan and core chain specificity. Glycobiology. 2006; 16: 584–93. doi: 10.1093/glycob/cwj090.

197. Trinchera M, Aronica A, Dall'Olio F. Selectin Ligands Sialyl-Lewis a and Sialyl-Lewis x in Gastrointestinal Cancers. Biology (Basel). 2017; 6: 16. doi: 10.3390/biology6010016.

198. Mondal N, Dykstra B, Lee J, Ashline DJ, Reinhold VN, Rossi DJ, Sackstein R. Distinct human (1,3)-fucosyltransferases drive Lewis-X/sialyl Lewis-X assembly in human cells. J Biol Chem. 2018; 293: 7300–14. doi: 10.1074/jbc.RA117.000775.

199. Dall'Olio F, Malagolini N, Trinchera M, Chiricolo M. Sialosignaling: Sialyltransferases as engines of self-fueling loops in cancer progression. Biochim Biophys Acta - Gen Subj. 2014; 1840: 2752–64. doi: 10.1016/j.bbagen.2014.06.006.

200. Glavey S V., Manier S, Natoni A, Sacco A, Moschetta M, Reagan MR, Murillo LS, Sahin I, Wu P, Mishima Y, Zhang Y, Zhang W, Zhang Y, et al. The sialyltransferase ST3GAL6 influences homing and survival in multiple myeloma. Blood. 2014; 124: 1765–76. doi: 10.1182/blood-2014-03-560862.

201. Mondal N, Buffone A, Stolfa G, Antonopoulos A, Lau JTY, Haslam SM, Dell A, Neelamegham S. ST3Gal-4 is the primary sialyltransferase regulating the synthesis of E-, P-, and L-selectin ligands on human myeloid leukocytes. Blood. 2015; 125: 687–96. doi: 10.1182/blood-2014-07-588590.

202. Kudo T, Ikehara Y, Togayachi A, Morozumi K, Watanabe M, Nakamura M,

Nishihara S, Narimatsu H. Up-regulation of a set of glycosyltransferase genes in human colorectal cancer. Lab Invest. 1998; 78: 797–811. Available from http://www.ncbi.nlm.nih.gov/pubmed/9690558

203. Pérez-Garay M, Arteta B, Pagès L, de Llorens R, de Bolòs C, Vidal-Vanaclocha F, Peracaula R. α2,3-Sialyltransferase ST3Gal III Modulates Pancreatic Cancer Cell Motility and Adhesion In Vitro and Enhances Its Metastatic Potential In Vivo. Lee T, editor. PLoS One. 2010; 5: e12524. doi: 10.1371/journal.pone.0012524.

204. Pérez-Garay M, Arteta B, Llop E, Cobler L, Pagès L, Ortiz R, Ferri MJ, de Bolós C, Figueras J, de Llorens R, Vidal-Vanaclocha F, Peracaula R. α2,3-Sialyltransferase ST3Gal IV promotes migration and metastasis in pancreatic adenocarcinoma cells and tends to be highly expressed in pancreatic adenocarcinoma tissues. Int J Biochem Cell Biol. Elsevier Ltd; 2013; 45: 1748–57. doi: 10.1016/j.biocel.2013.05.015.

205. Kukowska-Latallo JF, Larsen RD, Nair RP, Lowe JB. A cloned human cDNA determines expression of a mouse stage-specific embryonic antigen and the Lewis blood group alpha(1,3/1,4)fucosyltransferase. Genes Dev. 1990; 4: 1288–303. doi: 10.1101/gad.4.8.1288.

206. Weston BW, Nair RP, Larsen RD, Lowe JB. Isolation of a novel human alpha (1,3)fucosyltransferase gene and molecular comparison to the human Lewis blood group alpha (1,3/1,4)fucosyltransferase gene. Syntenic, homologous, nonallelic genes encoding enzymes with distinct acceptor substrate specific. J Biol Chem. 1992; 267: 4152–60. Available from http://www.ncbi.nlm.nih.gov/pubmed/1740457

207. Weston BW, Smith PL, Kelly RJ, Lowe JB. Molecular cloning of a fourth member of a human alpha (1,3)fucosyltransferase gene family. Multiple homologous sequences that determine expression of the Lewis x, sialyl Lewis x, and difucosyl sialyl Lewis x epitopes. J Biol Chem. 1992; 267: 24575–84. Available from http://www.ncbi.nlm.nih.gov/pubmed/1339443

208. Natsuka S, Gersten KM, Zenita K, Kannagi R, Lowe JB. Molecular cloning of a cDNA encoding a novel human leukocyte alpha-1,3-fucosyltransferase capable of synthesizing the sialyl Lewis x determinant. J Biol Chem. 1994; 269: 16789–94.

Available from http://www.ncbi.nlm.nih.gov/pubmed/8207002

209. Trinchera M, Malagolini N, Chiricolo M, Santini D, Minni F, Caretti A, Dall'Olio F. The biosynthesis of the selectin-ligand sialyl Lewis x in colorectal cancer tissues is regulated by fucosyltransferase VI and can be inhibited by an RNA interference-based approach. Int J Biochem Cell Biol. Elsevier Ltd; 2011; 43: 130–9. doi: 10.1016/j.biocel.2010.10.004.

210. Barthel SR, Wiese GK, Cho J, Opperman MJ, Hays DL, Siddiqui J, Pienta KJ, Furie B, Dimitroff CJ. Alpha 1,3 fucosyltransferases are master regulators of prostate cancer cell trafficking. Proc Natl Acad Sci. 2009; 106: 19491–6. doi: 10.1073/pnas.0906074106.

211. Munkley J, Elliott DJ. Hallmarks of glycosylation in cancer. Oncotarget. 2016; 7: 35478–89. doi: 10.18632/oncotarget.8155.

212. Stowell SR, Ju T, Cummings RD. Protein Glycosylation in Cancer. Annu Rev Pathol Mech Dis. 2015; 10: 473–510. doi: 10.1146/annurev-pathol-012414-040438.

213. Fuster MM, Esko JD. The sweet and sour of cancer: glycans as novel therapeutic targets. Nat Rev Cancer. 2005; 5: 526–42. doi: 10.1038/nrc1649.

214. Dube DH, Bertozzi CR. Glycans in cancer and inflammation — potential for therapeutics and diagnostics. Nat Rev Drug Discov. 2005; 4: 477–88. doi: 10.1038/nrd1751.

215. Nouso K, Amano M, Ito YM, Miyahara K, Morimoto Y, Kato H, Tsutsumi K, Tomoda T, Yamamoto N, Nakamura S, Kobayashi S, Kuwaki K, Hagihara H, et al. Clinical utility of high-throughput glycome analysis in patients with pancreatic cancer. J Gastroenterol. 2013; 48: 1171–9. doi: 10.1007/s00535-012-0732-7.

216. Pan S, Chen R, Tamura Y, Crispin D a, Lai L a, May DH, McIntosh MW, Goodlett DR, Brentnall T a. Quantitative Glycoproteomics Analysis Reveals Changes in N-Glycosylation Level Associated with Pancreatic Ductal Adenocarcinoma. J Proteome Res. 2014; 13: 1293–306. doi: 10.1021/pr4010184.

217. Monzavi-Karbassi B, Pashov A, Kieber-Emmons T. Tumor-Associated Glycans and Immune Surveillance. Vaccines. 2013; 1: 174–203. doi: 10.3390/vaccines1020174.

218. Hossain F, Andreana PR. Developments in Carbohydrate-Based Cancer Therapeutics. Pharmaceuticals. 2019; 12: 84. doi: 10.3390/ph12020084.

219. Itzkowitz S, Kjeldsen T, Friera A, Hakomori S-I, Yang U-S, Kim YS. Expression of Tn, sialosyl Tn, and T antigens in human pancreas. Gastroenterology. Elsevier Inc.; 1991; 100: 1691–700. doi: 10.1016/0016-5085(91)90671-7.

220. Radhakrishnan P, Dabelsteen S, Madsen FB, Francavilla C, Kopp KL, Steentoft C, Vakhrushev SY, Olsen J V., Hansen L, Bennett EP, Woetmann A, Yin G, Chen L, et al. Immature truncated O-glycophenotype of cancer directly induces oncogenic features. Proc Natl Acad Sci. 2014; 111: E4066–75. doi: 10.1073/pnas.1406619111.

221. Feng D, Shaikh AS, Wang F. Recent Advance in Tumor-associated Carbohydrate Antigens (TACAs)-based Antitumor Vaccines. ACS Chem Biol. 2016; 11: 850–63. doi: 10.1021/acschembio.6b00084.

222. RodrÍguez E, Schetters STT, van Kooyk Y. The tumour glyco-code as a novel immune checkpoint for immunotherapy. Nat Rev Immunol. 2018; 18: 204–11. doi: 10.1038/nri.2018.3.

223. Hutchins LF, Makhoul I, Emanuel PD, Pennisi A, Siegel ER, Jousheghany F, Guo X, Pashov AD, Monzavi-Karbassi B, Kieber-Emmons T. Targeting tumor-associated carbohydrate antigens: a phase I study of a carbohydrate mimetic-peptide vaccine in stage IV breast cancer subjects. Oncotarget. American Association for Cancer Research; 2017; 8: 99161–78. doi: 10.18632/oncotarget.21959.

224. Vojta A, Samaržija I, Bočkor L, Zoldoš V. Glyco-genes change expression in cancer through aberrant methylation. Biochim Biophys Acta - Gen Subj. 2016; 1860: 1776–85. doi: 10.1016/j.bbagen.2016.01.002.

225. Dall'Olio F, Trinchera M. Epigenetic Bases of Aberrant Glycosylation in Cancer. Int J Mol Sci. 2017; 18: 998. doi: 10.3390/ijms18050998.

226. Potapenko IO, Lüders T, Russnes HG, Helland Å, Sørlie T, Kristensen VN, Nord S, Lingjaerde OC, Børresen-Dale A-L, Haakensen VD. Glycan-related gene expression signatures in breast cancer subtypes; relation to survival. Mol Oncol.

2015; 9: 861–76. doi: 10.1016/j.molonc.2014.12.013.

227. Bard F, Chia J. Cracking the Glycome Encoder: Signaling, Trafficking, and Glycosylation. Trends Cell Biol. Elsevier Ltd; 2016; 26: 379–88. doi: 10.1016/j.tcb.2015.12.004.

228. Hanahan D, Weinberg RA. Hallmarks of Cancer: The Next Generation. Cell. Elsevier Inc.; 2011; 144: 646–74. doi: 10.1016/j.cell.2011.02.013.

229. Lemieux GA, Bertozzi CR. Modulating cell surface immunoreactivity by metabolic induction of unnatural carbohydrate antigens. Chem Biol. 2001; 8: 265–75. doi: 10.1016/S1074-5521(01)00008-4.

230. Dall'Olio F. Mechanisms of cancer-associated glycosylation changes. Front Biosci. 2012; 17: 670. doi: 10.2741/3951.

231. Varki NM, Varki A. Diversity in cell surface sialic acid presentations: implications for biology and disease. Lab Investig. 2007; 87: 851–7. doi: 10.1038/labinvest.3700656.

232. Lin S, Kemmner W, Grigull S, Schlag PM. Cell Surface α2,6-Sialylation Affects Adhesion of Breast Carcinoma Cells. Exp Cell Res. 2002; 276: 101–10. doi: 10.1006/excr.2002.5521.

233. Bogenrieder T, Herlyn M. Axis of evil: molecular mechanisms of cancer metastasis. Oncogene. 2003; 22: 6524–36. doi: 10.1038/sj.onc.1206757.

234. Seidenfaden R, Krauter A, Schertzinger F, Gerardy-Schahn R, Hildebrandt H. Polysialic Acid Directs Tumor Cell Growth by Controlling Heterophilic Neural Cell Adhesion Molecule Interactions. Mol Cell Biol. 2003; 23: 5908–18. doi: 10.1128/MCB.23.16.5908-5918.2003.

235. Hakomori S. Glycosylation defining cancer malignancy: New wine in an old bottle. Proc Natl Acad Sci. 2002; 99: 10231–3. doi: 10.1073/pnas.172380699.

236. Burchell J, Poulsom R, Hanby A, Whitehouse C, Cooper L, Clausen H, Miles D, Taylor-Papadimitriou J. An 2,3 sialyltransferase (ST3Gal I) is elevated in primary breast carcinomas. Glycobiology. 1999; 9: 1307–11. doi: 10.1093/glycob/9.12.1307.

237. Dimitroff CJ, Pera P, Dall'Olio F, Matta KL, Chandrasekaran EV, Lau JTY, Bernacki RJ. Cell SurfaceN-Acetylneuraminic Acid α2,3-Galactoside-Dependent Intercellular Adhesion of Human Colon Cancer Cells. Biochem Biophys Res Commun. 1999; 256: 631–6. doi: 10.1006/bbrc.1999.0388.

238. Yogeeswaran G, Salk P. Metastatic potential is positively correlated with cell surface sialylation of cultured murine tumor cell lines. Science (80-). 1981; 212: 1514–6. doi: 10.1126/science.7233237.

239. Dall'Olio F, Chiricolo M. Sialyltransferases in cancer. Glycoconj J. 2001; 18: 841–50. doi: 10.1023/a:1022288022969.

240. Kim YJ, Varki A. Perspectives on the significance of altered glycosylation of glycoproteins in cancer. Glycoconj J. 1997; 14: 569–76. doi: 10.1023/a:1018580324971.

241. Szabo R, Skropeta D. Advancement of Sialyltransferase Inhibitors: Therapeutic Challenges and Opportunities. Med Res Rev. 2017; 37: 219–70. doi: 10.1002/med.21407.

242. Bull C, Boltje TJ, Wassink M, de Graaf AMA, van Delft FL, den Brok MH, Adema GJ. Targeting Aberrant Sialylation in Cancer Cells Using a Fluorinated Sialic Acid Analog Impairs Adhesion, Migration, and In Vivo Tumor Growth. Mol Cancer Ther. 2013; 12: 1935–46. doi: 10.1158/1535-7163.MCT-13-0279.

243. Chen J-Y, Tang Y-A, Huang S-M, Juan H-F, Wu L-W, Sun Y-C, Wang S-C, Wu K-W, Balraj G, Chang T-T, Li W-S, Cheng H-C, Wang Y-C. A Novel Sialyltransferase Inhibitor Suppresses FAK/Paxillin Signaling and Cancer Angiogenesis and Metastasis Pathways. Cancer Res. 2011; 71: 473–83. doi: 10.1158/0008-5472.CAN-10-1303.

244. Chiang C-H, Wang C-H, Chang H-C, More S V., Li W-S, Hung W-C. A novel sialyltransferase inhibitor AL10 suppresses invasion and metastasis of lung cancer cells by inhibiting integrin-mediated signaling. J Cell Physiol. 2010; 223: n/a-n/a. doi: 10.1002/jcp.22068.

245. Hsu C-C, Lin T-W, Chang W-W, Wu C-Y, Lo W-H, Wang P-H, Tsai Y-C. Soyasaponin-I-modified invasive behavior of cancer by changing cell surface sialic

acids. Gynecol Oncol. 2005; 96: 415–22. doi: 10.1016/j.ygyno.2004.10.010.

246. Chang W-W, Yu C-Y, Lin T-W, Wang P-H, Tsai Y-C. Soyasaponin I decreases the expression of α2,3-linked sialic acid on the cell surface and suppresses the metastatic potential of B16F10 melanoma cells. Biochem Biophys Res Commun. 2006; 341: 614–9. doi: 10.1016/j.bbrc.2005.12.216.

247. Garnham R, Scott E, Livermore K, Munkley J. ST6GAL1: A key player in cancer (Review). Oncol Lett. 2019; 18: 983–9. doi: 10.3892/ol.2019.10458.

248. Zhou H, Li Y, Liu B, Shan Y, Li Y, Zhao L, Su Z, Jia L. Downregulation of miR-224 and let-7i contribute to cell survival and chemoresistance in chronic myeloid leukemia cells by regulating ST3GAL IV expression. Gene. 2017; 626: 106–18. doi: 10.1016/j.gene.2017.05.030.

249. Colomb F, Krzewinski-Recchi M-A, El Machhour F, Mensier E, Jaillard S, Steenackers A, Harduin-Lepers A, Lafitte J-J, Delannoy P, Groux-Degroote S. TNF regulates sialyl-Lewisx and 6-sulfo-sialyl-Lewisx expression in human lung through up-regulation of ST3GAL4 transcript isoform BX. Biochimie. 2012; 94: 2045–53. doi: 10.1016/j.biochi.2012.05.030.

250. Cui H-X, Wang H, Wang Y, Song J, Tian H, Xia C, Shen Y. ST3Gal III modulates breast cancer cell adhesion and invasion by altering the expression of invasion-related molecules. Oncol Rep. 2016; 36: 3317–24. doi: 10.3892/or.2016.5180.

251. Petretti T, Schulze B, Schlag P., Kemmner W. Altered mRNA expression of glycosyltransferases in human gastric carcinomas. Biochim Biophys Acta - Gen Subj. 1999; 1428: 209–18. doi: 10.1016/S0304-4165(99)00080-X.

252. Gretschel S, Haensch W, Schlag PM, Kemmner W. Clinical Relevance of Sialyltransferases ST6GAL-I and ST3GAL-III in Gastric Cancer. Oncology. 2003; 65: 139–45. doi: 10.1159/000072339.

253. Carvalho AS, Harduin-Lepers A, Magalhães A, Machado E, Mendes N, Costa LT, Matthiesen R, Almeida R, Costa J, Reis CA. Differential expression of α-2,3-sialyltransferases and α-1,3/4-fucosyltransferases regulates the levels of sialyl Lewis a and sialyl Lewis x in gastrointestinal carcinoma cells. Int J Biochem Cell Biol. 2010; 42: 80–9. doi: 10.1016/j.biocel.2009.09.010.

254. Gomes C, Osório H, Pinto MT, Campos D, Oliveira MJ, Reis CA. Expression of ST3GAL4 Leads to SLex Expression and Induces c-Met Activation and an Invasive Phenotype in Gastric Carcinoma Cells. Williams BO, editor. PLoS One. 2013; 8: e66737. doi: 10.1371/journal.pone.0066737.

255. Mereiter S, Magalhães A, Adamczyk B, Jin C, Almeida A, Drici L, Ibáñez-Vea M, Gomes C, Ferreira JA, Afonso LP, Santos LL, Larsen MR, Kolarich D, et al. Glycomic analysis of gastric carcinoma cells discloses glycans as modulators of RON receptor tyrosine kinase activation in cancer. Biochim Biophys Acta - Gen Subj. Elsevier B.V.; 2016; 1860: 1795–808. doi: 10.1016/j.bbagen.2015.12.016.

256. Peracaula R, Tabarés G, López-Ferrer A, Brossmer R, de Bolós C, de Llorens R. Role of sialyltransferases involved in the biosynthesis of Lewis antigens in human pancreatic tumour cells. Glycoconj J. 2005; 22: 135–44. doi: 10.1007/s10719-005-0734-2.

257. Bassagañas S, Carvalho S, Dias AM, Pérez-Garay M, Ortiz MR, Figueras J, Reis CA, Pinho SS, Peracaula R. Pancreatic Cancer Cell Glycosylation Regulates Cell Adhesion and Invasion through the Modulation of α2β1 Integrin and E-Cadherin Function. St-Pierre Y, editor. PLoS One. 2014; 9: e98595. doi: 10.1371/journal.pone.0098595.

258. Bassagañas S, Pérez-Garay M, Peracaula R. Cell Surface Sialic Acid Modulates Extracellular Matrix Adhesion and Migration in Pancreatic Adenocarcinoma Cells. Pancreas. 2014; 43: 109–17. doi: 10.1097/MPA.0b013e31829d9090.

259. Foxall C, Watson S, Dowbenko D, Fennie C, Lasky L, Kiso M, Hasegawa A, Asa D, Brandley B. The three members of the selectin receptor family recognize a common carbohydrate epitope, the sialyl Lewis(x) oligosaccharide. J Cell Biol. 1992; 117: 895–902. doi: 10.1083/jcb.117.4.895.

260. Borsig L. Selectins in cancer immunity. Glycobiology. 2018; 28: 648–55. doi: 10.1093/glycob/cwx105.

261. Keelan ETM, Licence ST, Peters AM, Binns RM, Haskard DO. Characterization of E-selectin expression in vivo with use of a radiolabeled monoclonal antibody. Am J Physiol Circ Physiol. 1994; 266: H279–90. doi: 10.1152/ajpheart.1994.266.1.H279.

262. Sipkins DA, Wei X, Wu JW, Runnels JM, Côté D, Means TK, Luster AD, Scadden DT, Lin CP. In vivo imaging of specialized bone marrow endothelial microdomains for tumour engraftment. Nature. 2005; 435: 969–73. doi: 10.1038/nature03703.

263. Shea DJ, Li YW, Stebe KJ, Konstantopoulos K. E-selectin-mediated rolling facilitates pancreatic cancer cell adhesion to hyaluronic acid. FASEB J. 2017; 31: 5078–86. doi: 10.1096/fj.201700331R.

264. Nakamori S, Kameyama M, Imaoka S, Furukawa H, Ishikawa O, Sasaki Y, Kabuto T, Iwanaga T, Matsushita Y, Irimura T. Increased expression of sialyl Lewisx antigen correlates with poor survival in patients with colorectal carcinoma: clinicopathological and immunohistochemical study. Cancer Res. 1993; 53: 3632–7. Available from http://www.ncbi.nlm.nih.gov/pubmed/8101764

265. Läubli H, Borsig L. Selectins promote tumor metastasis. Semin Cancer Biol. 2010; 20: 169–77. doi: 10.1016/j.semcancer.2010.04.005.

266. Witz IP. The selectin–selectin ligand axis in tumor progression. Cancer Metastasis Rev. 2008; 27: 19–30. doi: 10.1007/s10555-007-9101-z.

267. Bendas G, Borsig L. Cancer Cell Adhesion and Metastasis: Selectins, Integrins, and the Inhibitory Potential of Heparins. Int J Cell Biol. 2012; 2012: 1–10. doi: 10.1155/2012/676731.

268. Fuster MM, Brown JR, Wang L, Esko JD. A disaccharide precursor of sialyl Lewis X inhibits metastatic potential of tumor cells. Cancer Res. 2003; 63: 2775–81. Available from http://www.ncbi.nlm.nih.gov/pubmed/12782582

269. Amado M, Carneiro F, Seixas M, Clausen H, Sobrinho–Simões M. Dimeric sialyl-Lex expression in gastric carcinoma correlates with venous invasion and poor outcome. Gastroenterology. 1998; 114: 462–70. doi: 10.1016/S0016-5085(98)70529-3.

270. Nakayama T, Watanabe M, Katsumata T, Teramoto T, Kitajima M. Expression of Sialyl Lewisa as a new prognostic factor for patients with advanced colorectal carcinoma. Cancer. 1995; 75: 2051–6. doi: 10.1002/1097-0142(19950415)75:8<2051::AID-CNCR2820750804>3.0.CO;2-4.

271. Ogawa J, Sano A, Inoue H, Koide S. Expression of Lewis-related antigen and

prognosis in stage I non—small cell lung cancer. Ann Thorac Surg. 1995; 59: 412–5. doi: 10.1016/0003-4975(94)00866-6.

272. Nakagoe T, Fukushima K, Nanashima A, Sawai T, Tsuji T, Jibiki M, Yamaguchi H, Yasutake T, Ayabe H, Matuo T, Tagawa Y. Comparison of the expression of ABH/Lewis-related antigens in polypoid and non-polypoid growth types of colorectal carcinoma. J Gastroenterol Hepatol. 2001; 16: 176–83. doi: 10.1046/j.1440-1746.2001.02425.x.

273. Jørgensen T, Berner A, Kaalhus O, Tveter KJ, Danielsen HE, Bryne M. Up-regulation of the oligosaccharide sialyl LewisX: a new prognostic parameter in metastatic prostate cancer. Cancer Res. 1995; 55: 1817–9. Available from http://www.ncbi.nlm.nih.gov/pubmed/7728744

274. Kim YJ, Borsig L, Varki NM, Varki A. P-selectin deficiency attenuates tumor growth and metastasis. Proc Natl Acad Sci. 1998; 95: 9325–30. doi: 10.1073/pnas.95.16.9325.

275. Li D, Sun H, Bai G, Wang W, Liu M, Bao Z, Li J, Liu H. α-1,3-Fucosyltransferase-VII siRNA inhibits the expression of SLex and hepatocarcinoma cell proliferation. Int J Mol Med. 2018; 42: 2700–8. doi: 10.3892/ijmm.2018.3850.

276. Aubert M, Panicot L, Crotte C, Gibier P, Lombardo D, Sadoulet MO, Mas E. Restoration of alpha(1,2) fucosyltransferase activity decreases adhesive and metastatic properties of human pancreatic cancer cells. Cancer Res. 2000; 60: 1449–56. Available from http://www.ncbi.nlm.nih.gov/pubmed/10728712

277. Aubert M, Panicot-Dubois L, Crotte C, Sbarra V, Lombardo D, Sadoulet M-O, Mas E. Peritoneal colonization by human pancreatic cancer cells is inhibited by antisenseFUT3 sequence. Int J Cancer. 2000; 88: 558–65. doi: 10.1002/1097-0215(20001115)88:4<558::AID-IJC7>3.0.CO;2-B.

278. Sackmann EK, Fulton AL, Beebe DJ. The present and future role of microfluidics in biomedical research. Nature. 2014; 507: 181–9. doi: 10.1038/nature13118.

279. Rackus DG, Riedel-Kruse IH, Pamme N. “Learning on a chip:” Microfluidics for formal and informal science education. Biomicrofluidics. AIP Publishing LLC; 2019; 13: 041501. doi: 10.1063/1.5096030.

280. Venugopal Menon N, Lim S Bin, Lim CT. Microfluidics for personalized drug screening of cancer. Curr Opin Pharmacol. Elsevier Ltd; 2019; 48: 155–61. doi: 10.1016/j.coph.2019.09.008.

281. Solanki S, Pandey CM, Gupta RK, Malhotra BD. Emerging Trends in Microfluidics Based Devices. Biotechnol J. 2020; : 1900279. doi: 10.1002/biot.201900279.

282. Friedl P, Alexander S. Cancer Invasion and the Microenvironment: Plasticity and Reciprocity. Cell. Elsevier Inc.; 2011; 147: 992–1009. doi: 10.1016/j.cell.2011.11.016.

283. Hung W-C, Chen S-H, Paul CD, Stroka KM, Lo Y-C, Yang JT, Konstantopoulos K. Distinct signaling mechanisms regulate migration in unconfined versus confined spaces. J Cell Biol. 2013; 202: 807–24. doi: 10.1083/jcb.201302132.

284. Paul CD, Mistriotis P, Konstantopoulos K. Cancer cell motility: lessons from migration in confined spaces. Nat Rev Cancer. Nature Publishing Group; 2017; 17: 131–40. doi: 10.1038/nrc.2016.123.

285. Yankaskas CL, Thompson KN, Paul CD, Vitolo MI, Mistriotis P, Mahendra A, Bajpai VK, Shea DJ, Manto KM, Chai AC, Varadarajan N, Kontrogianni-Konstantopoulos A, Martin SS, et al. A microfluidic assay for the quantification of the metastatic propensity of breast cancer specimens. Nat Biomed Eng. Springer US; 2019; 3: 452–65. doi: 10.1038/s41551-019-0400-9.

286. Sarrats A, Saldova R, Pla E, Fort E, Harvey DJ, Struwe WB, de Llorens R, Rudd PM, Peracaula R. Glycosylation of liver acute-phase proteins in pancreatic cancer and chronic pancreatitis. PROTEOMICS - Clin Appl. 2010; 4: 432–48. doi: 10.1002/prca.200900150.

287. De Bolós C, Garrido M, Real FX. MUC6 apomucin shows a distinct normal tissue distribution that correlates with Lewis antigen expression in the human stomach. Gastroenterology. 1995; 109: 723–34. doi: 10.1016/0016-5085(95)90379-8.

288. Balzer EM, Tong Z, Paul CD, Hung W, Stroka KM, Boggs AE, Martin SS, Konstantopoulos K. Physical confinement alters tumor cell adhesion and migration phenotypes. FASEB J. 2012; 26: 4045–56. doi: 10.1096/fj.12-211441.

289. Tong Z, Balzer EM, Dallas MR, Hung W-C, Stebe KJ, Konstantopoulos K.

Chemotaxis of Cell Populations through Confined Spaces at Single-Cell Resolution. Rao C V., editor. PLoS One. 2012; 7: e29211. doi: 10.1371/journal.pone.0029211.

290. Stroka KM, Wong BS, Shriver M, Phillip JM, Wirtz D, Kontrogianni-Konstantopoulos A, Konstantopoulos K. Loss of giant obscurins alters breast epithelial cell mechanosensing of matrix stiffness. Oncotarget. 2017; 8: 54004–20. doi: 10.18632/oncotarget.10997.

291. Balmaña M, Duran A, Gomes C, Llop E, López-Martos R, Ortiz MR, Barrabés S, Reis CA, Peracaula R. Analysis of sialyl-Lewis x on MUC5AC and MUC1 mucins in pancreatic cancer tissues. Int J Biol Macromol. Elsevier B.V.; 2018; 112: 33–45. doi: 10.1016/j.ijbiomac.2018.01.148.

292. Munkley J. The glycosylation landscape of pancreatic cancer (Review). Oncol Lett. 2019; 17: 2569–75. doi: 10.3892/ol.2019.9885.

293. Ricardo S, Marcos-Silva L, Valente C, Coelho R, Gomes R, David L. Mucins MUC16 and MUC1 are major carriers of SLea and SLex in borderline and malignant serous ovarian tumors. Virchows Arch. 2016; 468: 715–22. doi: 10.1007/s00428-016-1929-6.

294. Garrochamba K. Análisis por inmunohistoquímica de potenciales biomarcadores para el cáncer de páncreas.

295. Kyrochristos ID, Ziogas DE, Glantzounis GK, Roukos DH. Prediction of pancreatic cancer risk and therapeutic response with next-generation sequencing. Biomark Med. 2018; 12: 5–8. doi: 10.2217/bmm-2017-0315.

296. Canto MI, Harinck F, Hruban RH, Offerhaus GJ, Poley J-W, Kamel I, Nio Y, Schulick RS, Bassi C, Kluijt I, Levy MJ, Chak A, Fockens P, et al. International Cancer of the Pancreas Screening (CAPS) Consortium summit on the management of patients with increased risk for familial pancreatic cancer. Gut. 2013; 62: 339–47. doi: 10.1136/gutjnl-2012-303108.

297. Hashim OH, Jayapalan JJ, Lee CS. Lectins: An effective tool for screening of potential cancer biomarkers. PeerJ. 2017; 2017: e3784. doi: 10.7717/peerj.3784.

298. Llop E, Guerrero PE, Duran A, Barrabés S, Massaguer A, Ferri MJ, Albiol-Quer M,

Llorens R de, Peracaula R. Glycoprotein biomarkers for the detection of pancreatic ductal adenocarcinoma. World J Gastroenterol. 2018; 24: 2537–54. doi: 10.3748/wjg.v24.i24.2537.

299. Kuzmanov U, Kosanam H, Diamandis EP. The sweet and sour of serological glycoprotein tumor biomarker quantification. BMC Med. 2013; 11: 31. doi: 10.1186/1741-7015-11-31.

300. Llop E, Ferrer-Batallé M, Barrabés S, Guerrero PE, Ramírez M, Saldova R, Rudd PM, Aleixandre RN, Comet J, de Llorens R, Peracaula R. Improvement of Prostate Cancer Diagnosis by Detecting PSA Glycosylation-Specific Changes. Theranostics. 2016; 6: 1190–204. doi: 10.7150/thno.15226.

301. Ferrer-Batallé M, Llop E, Ramírez M, Aleixandre R, Saez M, Comet J, de Llorens R, Peracaula R. Comparative Study of Blood-Based Biomarkers, α2,3-Sialic Acid PSA and PHI, for High-Risk Prostate Cancer Detection. Int J Mol Sci. 2017; 18: 845. doi: 10.3390/ijms18040845.

302. Li F, Ding J. Sialylation is involved in cell fate decision during development, reprogramming and cancer progression. Protein Cell. Higher Education Press; 2019; 10: 550–65. doi: 10.1007/s13238-018-0597-5.

303. Satomura Y, Sawabu N, Takemori Y, Ohta H, Watanabe H, Okai T, Watanabe K, Matsuno H, Konishi F. Expression of Various Sialylated Carbohydrate Antigens in Malignant and Nonmalignant Pancreatic Tissues. Pancreas. 1991; 6: 448–58. doi: 10.1097/00006676-199107000-00012.

304. Bassagañas S, Allende H, Cobler L, Ortiz MR, Llop E, de Bolós C, Peracaula R. Inflammatory cytokines regulate the expression of glycosyltransferases involved in the biosynthesis of tumor-associated sialylated glycans in pancreatic cancer cell lines. Cytokine. 2015; 75: 197–206. doi: 10.1016/j.cyto.2015.04.006.

305. Balmaña M, Sarrats A, Llop E, Barrabés S, Saldova R, Ferri MJ, Figueras J, Fort E, de Llorens R, Rudd PM, Peracaula R. Identification of potential pancreatic cancer serum markers: Increased sialyl-Lewis X on ceruloplasmin. Clin Chim Acta. Elsevier B.V.; 2015; 442: 56–62. doi: 10.1016/j.cca.2015.01.007.

306. Peixoto A, Relvas-Santos M, Azevedo R, Santos LL, Ferreira JA. Protein

Glycosylation and Tumor Microenvironment Alterations Driving Cancer Hallmarks. Front Oncol. 2019; 9: 1–24. doi: 10.3389/fonc.2019.00380.

307. Pilecki B, Holm AT, Schlosser A, Moeller JB, Wohl AP, Zuk A V., Heumüller SE, Wallis R, Moestrup SK, Sengle G, Holmskov U, Sorensen GL. Characterization of Microfibrillar-associated Protein 4 (MFAP4) as a Tropoelastin- and Fibrillin-binding Protein Involved in Elastic Fiber Formation. J Biol Chem. 2016; 291: 1103–14. doi: 10.1074/jbc.M115.681775.

308. Ruoslahti E. RGD AND OTHER RECOGNITION SEQUENCES FOR INTEGRINS. Annu Rev Cell Dev Biol. 1996; 12: 697–715. doi: 10.1146/annurev.cellbio.12.1.697.

309. Lausen M, Lynch N, Schlosser A, Tornøe I, Sækmose SG, Teisner B, Willis AC, Crouch E, Schwaeble W, Holmskov U. Microfibril-associated Protein 4 Is Present in Lung Washings and Binds to the Collagen Region of Lung Surfactant Protein D. J Biol Chem. 1999; 274: 32234–40. doi: 10.1074/jbc.274.45.32234.

310. Wulf-Johansson H, Lock Johansson S, Schlosser A, Trommelholt Holm A, Melholt Rasmussen L, Mickley H, Diederichsen ACP, Munkholm H, Poulsen TS, Tornøe I, Nielsen V, Marcussen N, Vestbo J, et al. Localization of Microfibrillar-Associated Protein 4 (MFAP4) in Human Tissues: Clinical Evaluation of Serum MFAP4 and Its Association with Various Cardiovascular Conditions. Schulz C, editor. PLoS One. 2013; 8: e82243. doi: 10.1371/journal.pone.0082243.

311. Yin (殷晓科) X, Wanga S, Fellows AL, Barallobre-Barreiro J, Lu R, Davaapil H, Franken R, Fava M, Baig F, Skroblin P, Xing Q, Koolbergen DR, Groenink M, et al. Glycoproteomic Analysis of the Aortic Extracellular Matrix in Marfan Patients. Arterioscler Thromb Vasc Biol. 2019; 39: 1859–73. doi: 10.1161/ATVBAHA.118.312175.

312. Schlosser A, Pilecki B, Hemstra LE, Kejling K, Kristmannsdottir GB, Wulf-Johansson H, Moeller JB, Füchtbauer E-M, Nielsen O, Kirketerp-Møller K, Dubey LK, Hansen PBL, Stubbe J, et al. MFAP4 Promotes Vascular Smooth Muscle Migration, Proliferation and Accelerates Neointima Formation. Arterioscler Thromb Vasc Biol. 2016; 36: 122–33. doi: 10.1161/ATVBAHA.115.306672.

313. Kasamatsu S, Hachiya A, Fujimura T, Sriwiriyanont P, Haketa K, Visscher MO,

Kitzmiller WJ, Bello A, Kitahara T, Kobinger GP, Takema Y. Essential role of microfibrillar-associated protein 4 in human cutaneous homeostasis and in its photoprotection. Sci Rep. 2011; 1: 164. doi: 10.1038/srep00164.

314. Mecham RP, Gibson MA. The microfibril-associated glycoproteins (MAGPs) and the microfibrillar niche. Matrix Biol. Elsevier B.V.; 2015; 47: 13–33. doi: 10.1016/j.matbio.2015.05.003.

315. Sækmose SG, Mössner B, Christensen PB, Lindvig K, Schlosser A, Holst R, Barington T, Holmskov U, Sorensen GL. Microfibrillar-Associated Protein 4: A Potential Biomarker for Screening for Liver Fibrosis in a Mixed Patient Cohort. Avila MA, editor. PLoS One. 2015; 10: e0140418. doi: 10.1371/journal.pone.0140418.

316. Mölleken C, Sitek B, Henkel C, Poschmann G, Sipos B, Wiese S, Warscheid B, Broelsch C, Reiser M, Friedman SL, Tornøe I, Schlosser A, Klöppel G, et al. Detection of novel biomarkers of liver cirrhosis by proteomic analysis. Hepatology. 2009; 49: 1257–66. doi: 10.1002/hep.22764.

317. Bracht T, Mölleken C, Ahrens M, Poschmann G, Schlosser A, Eisenacher M, Stühler K, Meyer HE, Schmiegel WH, Holmskov U, Sorensen GL, Sitek B. Evaluation of the biomarker candidate MFAP4 for non-invasive assessment of hepatic fibrosis in hepatitis C patients. J Transl Med. 2016; 14: 201. doi: 10.1186/s12967-016-0952-3.

318. Johansson SL, Roberts NB, Schlosser A, Andersen CB, Carlsen J, Wulf-Johansson H, Sækmose SG, Titlestad IL, Tornoe I, Miller B, Tal-Singer R, Holmskov U, Vestbo J, et al. Microfibrillar-associated protein 4: A potential biomarker of chronic obstructive pulmonary disease. Respir Med. Elsevier Ltd; 2014; 108: 1336–44. doi: 10.1016/j.rmed.2014.06.003.

319. Blindbæk SL, Schlosser A, Green A, Holmskov U, Sorensen GL, Grauslund J. Association between microfibrillar-associated protein 4 (MFAP4) and micro- and macrovascular complications in long-term type 1 diabetes mellitus. Acta Diabetol. Springer Milan; 2017; 54: 367–72. doi: 10.1007/s00592-016-0953-y.

320. Choi J, Cho BH, Kim H-J, Kim Y, Jang J. Identification of new genes of pleomorphic adenoma. Medicine (Baltimore). 2019; 98: e18468. doi:

10.1097/MD.0000000000018468.

321. Tian Y, Bova GS, Zhang H. Quantitative Glycoproteomic Analysis of Optimal Cutting Temperature-Embedded Frozen Tissues Identifying Glycoproteins Associated with Aggressive Prostate Cancer. Anal Chem. 2011; 83: 7013–9. doi: 10.1021/ac200815q.

322. Davalieva K, Kostovska IM, Kiprijanovska S, Markoska K, Kubelka-Sabit K, Filipovski V, Stavridis S, Stankov O, Komina S, Petrusevska G, Polenakovic M. Proteomics analysis of malignant and benign prostate tissue by 2D DIGE/MS reveals new insights into proteins involved in prostate cancer. Prostate. 2015; 75: 1586–600. doi: 10.1002/pros.23034.

323. Feng Y-Y, Liu C-H, Xue Y, Chen Y-Y, Wang Y-L, Wu X-Z. MicroRNA-147b promotes lung adenocarcinoma cell aggressiveness through negatively regulating microfibril-associated glycoprotein 4 (MFAP4) and affects prognosis of lung adenocarcinoma patients. Gene. Elsevier; 2020; 730: 144316. doi: 10.1016/j.gene.2019.144316.

324. Muraoka S, Kume H, Watanabe S, Adachi J, Kuwano M, Sato M, Kawasaki N, Kodera Y, Ishitobi M, Inaji H, Miyamoto Y, Kato K, Tomonaga T. Strategy for SRM-based Verification of Biomarker Candidates Discovered by iTRAQ Method in Limited Breast Cancer Tissue Samples. J Proteome Res. 2012; 11: 4201–10. doi: 10.1021/pr300322q.

325. Yang J, Song H, Chen L, Cao K, Zhang Y, Li Y, Hao X. Integrated analysis of microfibrillar-associated proteins reveals MFAP4 as a novel biomarker in human cancers. Epigenomics. 2019; 11: 5–21. doi: 10.2217/epi-2018-0080.

326. Uhlén M, Fagerberg L, Hallström BM, Lindskog C, Oksvold P, Mardinoglu A, Sivertsson Å, Kampf C, Sjöstedt E, Asplund A, Olsson IM, Edlund K, Lundberg E, et al. Tissue-based map of the human proteome. Science (80-). 2015; . doi: 10.1126/science.1260419.

327. Chen R, Jiang X, Sun D, Han G, Wang F, Ye M, Wang L, Zou H. Glycoproteomics Analysis of Human Liver Tissue by Combination of Multiple Enzyme Digestion and Hydrazide Chemistry. J Proteome Res. 2009; 8: 651–61. doi: 10.1021/pr8008012.

328. Liu T, Qian W-J, Gritsenko MA, Camp DG, Monroe ME, Moore RJ, Smith RD. Human Plasma N -Glycoproteome Analysis by Immunoaffinity Subtraction, Hydrazide Chemistry, and Mass Spectrometry. J Proteome Res. 2005; 4: 2070–80. doi: 10.1021/pr0502065.

329. Spivey K, Banyard J. A prognostic gene signature in advanced ovarian cancer reveals a microfibril-associated protein (MAGP2) as a promoter of tumor cell survival and angiogenesis. Cell Adh Migr. 2010; 4: 169–71. doi: 10.4161/cam.4.2.11716.

330. Senthebane DA, Rowe A, Thomford NE, Shipanga H, Munro D, Mazeedi MAM Al, Almazyadi HAM, Kallmeyer K, Dandara C, Pepper MS, Parker MI, Dzobo K. The Role of Tumor Microenvironment in Chemoresistance: To Survive, Keep Your Enemies Closer. Int J Mol Sci. 2017; 18: 1586. doi: 10.3390/ijms18071586.

331. Grzesiak JJ, Bouvet M. The α2β1 integrin mediates the malignant phenotype on type I collagen in pancreatic cancer cell lines. Br J Cancer. 2006; 94: 1311–9. doi: 10.1038/sj.bjc.6603088.

332. Grzesiak JJ, Ho JC, Moossa AR, Bouvet M. The Integrin-Extracellular Matrix Axis in Pancreatic Cancer. Pancreas. 2007; 35: 293–301. doi: 10.1097/mpa.0b013e31811f4526.

333. Li J, Wang Y, Xie Y, Xu Z, Yang J, Wang F, Qu X, Norihiro K, Tang W, Zhong W, Cui S. Altered mRNA expressions of sialyltransferases in human gastric cancer tissues. Med Oncol. 2012; 29: 84–90. doi: 10.1007/s12032-010-9771-1.

334. Gupta R, Leon F, Thompson CM, Nimmakayala R, Karmakar S, Nallasamy P, Chugh S, Prajapati DR, Rachagani S, Kumar S, Ponnusamy MP. Global analysis of human glycosyltransferases reveals novel targets for pancreatic cancer pathogenesis. Br J Cancer. Springer US; 2020; : 1–12. doi: 10.1038/s41416-020-0772-3.

335. Holst S, Belo AI, Giovannetti E, Van Die I, Wuhrer M. Profiling of different pancreatic cancer cells used as models for metastatic behaviour shows large variation in their N-glycosylation. Sci Rep. Springer US; 2017; 7: 1–15. doi: 10.1038/s41598-017-16811-6.

336. Gupta R, Matta KL, Neelamegham S. A systematic analysis of acceptor specificity and reaction kinetics of five human α(2,3)sialyltransferases: Product inhibition studies illustrate reaction mechanism for ST3Gal-I. Biochem Biophys Res Commun. Elsevier Ltd; 2016; 469: 606–12. doi: 10.1016/j.bbrc.2015.11.130.

337. Shen L, Luo Z, Wu J, Qiu L, Luo M, Ke Q, Dong X. Enhanced expression of α2,3-linked sialic acids promotes gastric cancer cell metastasis and correlates with poor prognosis. Int J Oncol. 2017; 50: 1201–10. doi: 10.3892/ijo.2017.3882.

338. St. Hill CA, Krieser K, Farooqui M. Neutrophil interactions with sialyl Lewis X on human nonsmall cell lung carcinoma cells regulate invasive behavior. Cancer. 2011; 117: 4493–505. doi: 10.1002/cncr.26059.

339. Radhakrishnan P, Chachadi V, Lin M-F, Singh R, Kannagi R, Cheng P-W. TNFα enhances the motility and invasiveness of prostatic cancer cells by stimulating the expression of selective glycosyl- and sulfotransferase genes involved in the synthesis of selectin ligands. Biochem Biophys Res Commun. 2011; 409: 436–41. doi: 10.1016/j.bbrc.2011.05.019.

340. Yoshihama N, Yamaguchi K, Chigita S, Mine M, Abe M, Ishii K, Kobayashi Y, Akimoto N, Mori Y, Sugiura T. A novel function of CD82/KAI1 in sialyl Lewis antigen-mediated adhesion of cancer cells: Evidence for an anti-metastasis effect by down-regulation of sialyl Lewis antigens. PLoS One. 2015; 10. doi: 10.1371/journal.pone.0124743.

341. Wang X, Zhang Y, Lin H, Liu Y, Tan Y, Lin J, Gao F, Lin S. Alpha2,3-sialyltransferase III knockdown sensitized ovarian cancer cells to cisplatin-induced apoptosis. Biochem Biophys Res Commun. Elsevier Ltd; 2017; 482: 758–63. doi: 10.1016/j.bbrc.2016.11.107.

342. Zhang X, Yang X, Chen M, Zheng S, Li J, Lin S, Wang X. ST3Gal3 confers paclitaxel-mediated chemoresistance in ovarian cancer cells by attenuating caspase-8/3 signaling. Mol Med Rep. 2019; 20: 4499–506. doi: 10.3892/mmr.2019.10712.

343. Sakuma K, Aoki M, Kannagi R. Transcription factors c-Myc and CDX2 mediate E-selectin ligand expression in colon cancer cells undergoing EGF/bFGF-induced

epithelial-mesenchymal transition. Proc Natl Acad Sci. 2012; 109: 7776–81. doi: 10.1073/pnas.1111135109.

344. Büll C, Boltje TJ, Balneger N, Weischer SM, Wassink M, Van Gemst JJ, Bloemendal VR, Boon L, Van Der Vlag J, Heise T, Den Brok MH, Adema GJ. Sialic acid blockade suppresses tumor growth by enhancing t-cell-mediated tumor immunity. Cancer Res. 2018; 78: 3574–88. doi: 10.1158/0008-5472.CAN-17-3376.

345. Wen KC, Sung PL, Hsieh SL, Chou YT, Lee OKS, Wu CW, Wang PH. α2,3-sialyltransferase type I regulates migration and peritoneal dissemination of ovarian cancer cells. Oncotarget. 2017; 8: 29013–27. doi: 10.18632/oncotarget.15994.